Biomechanical Analysis of Lumbar Disc Degeneration Before and After Spinal Fusion

Maria Inês Vieira Godinho

Thesis to obtain the Master of Science Degree in

Biomedical Engineering

Supervisors: Prof. André Paulo Galvão de Castro
Prof. Paulo Rui Alves Fernandes

Examination Committee:

Chairperson: Prof. João Orlando Marques Gameiro Folgado

Supervisor: Prof. André Paulo Galvão de Castro

Members of the Committee: Prof. Luís Alberto Gonçalves de Sousa
Dr. Manuel José Tavares de Matos

December 2020

Preface

The work presented in this thesis was performed at the Department of Mechanical Engineering of Instituto Superior Técnico (Lisboa, Portugal), during the period February-December 2020, under the supervision of Prof. André Castro and Prof. Paulo Fernandes.

Declaration

I declare that this document is an original work of my own authorship and that it fulfils all the requirements of the Code of Conduct and Good Practices of the Universidade de Lisboa.

Agradecimentos

Porque este (de uma forma ou de outra) foi um trabalho de equipa, gostaria de deixar aqui expresso o meu obrigada a todas as pessoas, partes integrantes e fundamentais do meu percurso, que ajudaram a moldar o meu trabalho e a pessoa que sou hoje. Sem vocês tudo teria sido mais complicado.

Aos meus orientadores, Prof. André e Prof. Paulo, agradeço todo o apoio e reconhecimento que sempre me deram. Ao Prof. André, agradeço em especial o voto de confiança, a palavra amiga e paciente nos momentos mais frustrantes, e o acompanhamento constante. Foi uma ajuda imprescindível, e deixo o meu sincero obrigada por isso.

Deixo também um agradecimento especial ao Dr. Tavares de Matos, que me proporcionou a oportunidade única de assistir a uma cirurgia à coluna, e sempre se mostrou disponível para esclarecer todas as minhas questões.

Ao grupo, Mariana, Leonor, Tiago, Jorge, e Miguel, um obrigada por todo o feedback e discussão construtiva que se foi proporcionando ao longo destes meses. Foram sem dúvida meses estranhos e diferentes, meses que nos impediram de partilhar a mesma sala e companhia física, mas não a partilha de problemas e soluções para um trabalho final mais sólido e consistente.

Quero também agradecer aos meus pais, que me ensinaram a dar sempre o meu melhor e a nunca desistir dos meus objetivos, por serem exemplo de força e resiliência, de honestidade e amor, por fazerem o possível e o impossível para que consiga alcançar os meus sonhos, pelo apoio incondicional.

Às minhas irmãs, minhas pequenas catatuas, por estarem sempre do meu lado, mesmo rezingonas e com o seu jeito mal disposto de vez em quando! Obrigada por serem como são, por me inspirarem a ser melhor e a ver o mundo de uma outra perspetiva.

Aos de sempre, obrigada por todos os momentos de descompressão, companhia, e puro riso que me proporcionam, por me ajudarem a manter a minha sanidade mental, por seguirmos sempre juntos.

A ti Nuno, por teres aturado todos os meus fritanços desde o primeiro dia, por nunca me teres deixado ir abaixo, e por me teres dado sempre o carinho e o incentivo de que precisava (e por continuares a fazê-lo). Às vezes faz mesmo falta parar, respirar, e procurar a nossa luzinha.

Estou muito orgulhosa e feliz com este trabalho, com estes últimos cinco anos de curso e de vida, e sou muito grata por vos levar comigo. Ou então para voltar um dia.

“Se o que encontraste é feito de matéria pura, jamais apodrecerá. E poderás voltar um dia.”

Paulo Coelho, in *O Alquimista*

Abstract

Advancing age and degeneration frequently lead to low back pain (LBP), which is the most prevalent musculoskeletal disorder worldwide. Changes in the ligamentous structures and intervertebral discs (IVD) are typically amongst the sources of instability. Spinal fusion techniques are therefore at the core of treatment options to remove the affected IVD and relieve LBP.

The aim of this work was three-fold: (i) to understand how ligament degeneration links with LBP by determining the role of each ligament per movement, (ii) to evaluate the impact of IVD height reduction in degenerative changes, and (iii) to assess the more advantageous type of posterior fixation in interbody fusion to support clinical practice, particularly regarding adjacent disc degeneration (ADD). For that, two L3-L5 finite element models with different IVD heights were used. Different degrees of ligament and IVD degeneration were tested, and the Oblique Lumbar Interbody Fusion (OLIF) procedure was simulated with different fixation constructs.

Facet capsular ligament and anterior longitudinal ligament were identified as the most influential ligaments for spinal stability, being this influence enhanced with degeneration and IVD height reduction. After spinal fusion, these ligaments became obsolete. The OLIF procedure contributed more to ADD than IVD degeneration of the pre-instrumented level, with bilateral fixation being the best option to achieve stability and lessen ADD risk. Between models with unilateral constructs, right unilateral fixation was the most suited to reduce IVD stress. Clinical practice will benefit from the outcomes of this study and from its future extension to a wider patient database.

Keywords: Lumbar Spine, Ligaments, Degeneration, Interbody Fusion, Biomechanics, Finite Element Modelling

Resumo

O avanço da idade e degeneração levam frequentemente à lombalgia, que é o distúrbio musculoesquelético mais prevalente a nível mundial. Alterações nas estruturas ligamentares e discos intervertebrais (DIV) encontram-se entre as fontes de instabilidade. Técnicas de fusão estão no centro das opções de tratamento, para remover o DIV afetado e aliviar a lombalgia.

O objetivo deste trabalho foi triplo: (i) compreender a relação entre degeneração ligamentar e lombalgia, determinando o papel de cada ligamento no movimento, (ii) avaliar o impacto da redução de altura do DIV nas alterações degenerativas, e (iii) determinar a fixação posterior mais vantajosa na fusão intersomática, particularmente a respeito da degeneração do disco adjacente (DDA). Para tal, foram utilizados dois modelos de elementos finitos L3-L5 com alturas de DIV diferentes. Graus distintos de degeneração foram testados, e o procedimento de fusão intersomática lombar oblíqua (OLIF) foi simulado com diferentes tipos de fixação.

Os ligamentos capsular facetário e longitudinal anterior foram identificados como os mais influentes na estabilidade da coluna, sendo essa influência aumentada com a degeneração e redução de altura do disco. Após fusão, a presença dos ligamentos tornou-se irrelevante. O procedimento OLIF apresentou uma maior contribuição para DDA do que a degeneração do DIV, sendo a fixação bilateral a melhor opção para obter estabilidade e diminuir o risco de DDA. Entre modelos com fixação unilateral, a fixação direita mostrou-se a mais adequada para reduzir o stress no DIV. A prática clínica beneficiará destes resultados e da sua extensão a um conjunto mais amplo de pacientes.

Palavras-chave: Coluna Lombar, Ligamentos, Degeneração, Fusão Intersomática, Biomecânica, Modelação de Elementos Finitos

Contents

List of Figures

List of Tables

Acronyms

ADD	Adjacent Disc Degeneration
AF	Annulus Fibrosus
ALIF	Anterior Lumbar Interbody Fusion
ALL	Anterior Longitudinal Ligament
AR	Axial Rotation
BC	Boundary Condition
BPF	Bilateral Posterior Fixation
CT	Computer-Tomography
DDD	Degenerative Disc Disease
E	Extension
F	Flexion
FCL	Facet Capsular Ligament
FE	Finite Element
FEA	Finite Element Analysis
FSU	Functional Spinal Unit
ICR	Instantaneous Centre of Rotation
IDP	Intradiscal Pressure
ISL	Interspinous Ligament
ITL	Intertransverse Ligament
IVD	Intervertebral Disc
LAR	Left Axial Rotation
LB	Lateral Bending
LBP	Low Back Pain
LLB	Left Lateral Bending
LF	Ligamentum Flavum
LT	Long-Term
LUPF	Left Unilateral Posterior Fixation
NP	Nucleus Pulposus
OLIF	Oblique Lumbar Interbody Fusion
PEEK	Polyetheretherketone
PG	Proteoglycan
PLIF	Posterior Lumbar Interbody Fusion
PLL	Posterior Longitudinal Ligament
RAR	Right Axial Rotation
RLB	Right Lateral Bending
ROM	Range of Motion
RUPF	Right Unilateral Posterior Fixation
SA	Stand-Alone
SSL	Supraspinous Ligament
ST	Short-Term
TDR	Total Disc Replacement
TLIF	Transforaminal Lumbar Interbody Fusion
VB	Vertebral Body
WMD	With Morphological Degeneration
WOMD	Without Morphological Degeneration
XLIF	Extreme Lateral Interbody Fusion

Nomenclature

E	Young's Modulus
v	Poisson's Ratio
C_{10}, D_1, k_1, k_2, $kappa$	Constitutive Parameters for the Holzapfel Model
U	Strain Energy per unit of Reference Volume
I_1, I_2	Deviatoric Strain Invariants
J^{el}	Elastic Volume Ratio
C_{10}, C_{01}, D_1	Constitutive Parameters for the Mooney-Rivlin Model
k	Spring's Constant
A	Cross-sectional Area
L	Ligament Length

Chapter 1

Introduction

1.1 Motivation

With advancing age and degeneration, several changes are induced in the spine. These can possibly lead to different pathological conditions and ultimately culminate in low back pain (LBP), which is the most prevalent musculoskeletal disorder and a major source of disability worldwide [1]. Changes in the ligamentous structures or the intervertebral discs (IVDs) are common causes of LBP and they can be interconnected, hence leading to further damage [2], [3]. Therefore, it is important to understand the processes of degeneration of ligaments and IVDs, as well as their contribution to spine kinematics.

For the disorders originating from degeneration, several treatment options are available, ranging from medication, physical and massage therapy, and surgical procedures in cases of severe and debilitating pathology [4]. Spinal fusion techniques are typical surgical procedures with the intent of eliminating LBP. The focus of the present work was interbody fusion, in which the degenerated IVD is removed and a cage is inserted in its place, with additional bone graft to promote fusion [5]. There are several approaches for cage introduction, but in the current work the Oblique Lumbar Interbody Fusion (OLIF) procedure was simulated, as it is widely used and provides good clinical results. In spinal fusion, posterior fixation may or may not be supplemented and its use has been widely researched over the years. However, there is still some debate about whether bilateral fixation systems are required to stabilise the spinal segment or if unilateral constructs are enough to maintain the cage in place and promote bone fusion [6]. Moreover, there is no significant evidence to support the choice between left or right unilateral fixation systems.

To evaluate the biomechanics of the spine and devise solutions for this type of questions, three different methods are available: *in vivo*, *in vitro,* and *in silico* methods. *In silico* analysis resorts to the finite element (FE) method and it is a very useful tool to ensure reproducibility of results without destroying the test samples. With FE analysis (FEA) it is possible to compare healthy and pathological conditions of the spine, evaluating the impact of referred conditions in the natural movement and trying to determine their origin. Moreover, it also allows the study of surgical procedures and instrumented models of the spine to better understand their benefits and setbacks, in the long or short term, when trying to return the spine to its natural healthy condition.

1.2 Objectives

Although there have been several studies evaluating the mechanical properties of healthy spinal ligaments and IVD degeneration [7]–[12], the process of ligament degeneration and its effects on spinal kinematics are still unclear. To the author's knowledge, there are no FE studies focused on ligament

changes with degeneration. Moreover, regarding ligament removal and morphological degeneration (namely IVD height reduction), it is also important to further understand their impact on the stability of a degenerated spine, as well as the changes induced in adjacent levels. From the degenerated spine, treatment decisions can benefit from in-depth FE simulations of different scenarios to support clinical practice with enhanced data. With this in mind, the aim of this work was three-fold:

i. to explore the role of each ligament per movement and determine the effects of ligament degeneration on spine kinematics. A previously developed L3-L5 FE model was modified to include ligament changes and a full biomechanical analysis was performed.
ii. to evaluate the impact of IVD height reduction in degenerative changes. A new L3-L5 FE model with reduced IVD height was devised and outcomes such as range of motion (ROM) and supported loads were compared between both models with and without morphological degeneration.
iii. to assess the more advantageous type of posterior fixation in interbody fusion to support clinical practice, with focus on adjacent disc degeneration (ADD). The OLIF procedure was simulated in the new L3-L5 FE model and different types of fixation were introduced. Relevant parameters such as stability and loads supported by the adjacent IVD were evaluated, both in short and long-term simulations. The role of ligaments during this procedure was also important to be evaluated since these structures contribute to spinal stabilisation.

1.3 Thesis Outline

The present work is structured in six chapters.

The first chapter, *Introduction*, explains the relevance of this work, including a brief introduction to the topic, motivation, and the main objectives.

The second chapter, *Anatomy of the Spine*, presents a brief description of the human spine and its main functional units (vertebrae, IVDs, and ligaments), with focus on the lumbar segments. The goal is to provide to the reader the basic concepts and functions of spinal structures so they become familiarised with the subject and fully understand the developed work and obtained results. A subsection about spinal diseases and common treatment options is also included.

The third chapter, *State of the Art*, presents the evolution of knowledge that has occurred in this field over the years, including the development of interbody fusion devices, and intact and instrumented FE models of the lumbar spine. Moreover, literature review regarding ligament and IVD degeneration is also presented since degeneration in these structures is the focus of the current work.

The remaining chapters are related with the simulations and analyses conducted in the present work. These are divided into two different parts, each related to a different FE model and with their specific purposes. The first part, corresponding to chapter 4, *Part I – Ligament modelling*, takes advantage of a previously developed FE model to study ligament removal and degeneration and to assess their impact in spinal stability. This chapter includes all the associated Methodology, Results and Discussion. Chapter 5 comprises the second part of this work, *Part II – Morphological Degeneration and Spinal Fusion*, in which a new FE model was developed to assess changes with morphological

degeneration (i.e. IVD height reduction) and simulate the process of interbody fusion. In this chapter are presented the methodology for the FE model construction, the steps for its validation, and a complete analysis of the results of the performed simulations.

Finally, the sixth and last chapter, *Conclusions and Future Work*, includes the main conclusions of this study, limitations, and suggestions for future work.

Chapter 2

Anatomy of the Spine

The spinal column, also called spine, backbone, or vertebral column, is one of the main support structures of the human body. It is composed of a set of small irregular bones, known as vertebrae, interleaved with fibrocartilaginous deformable structures, the IVDs. The main functions of the spine are weight-bearing and head support, spinal cord protection, and allowing motion between the upper torso and pelvis. Additionally, it serves as an attachment point for back muscles and ligaments, the ribs, and the pelvic girdle [13]. The typical adult human spine consists of 24 movable vertebrae, which can be further divided into three different portions: cervical spine (C1 to C7), thoracic spine (T1 to T12), and lumbar spine (L1 to L5) [13]–[15]. The sacral and coccygeal regions are the distal portion of the spine, formed as a result of fusion of 5 and 4 vertebrae, respectively. Figure 2.1 shows a complete human spine divided into its five regions (including the sacrum and the coccyx). On the right, it is illustrated the characteristic S-shaped anatomy of the spine when viewed in the sagittal plane, with its four characteristic bends.

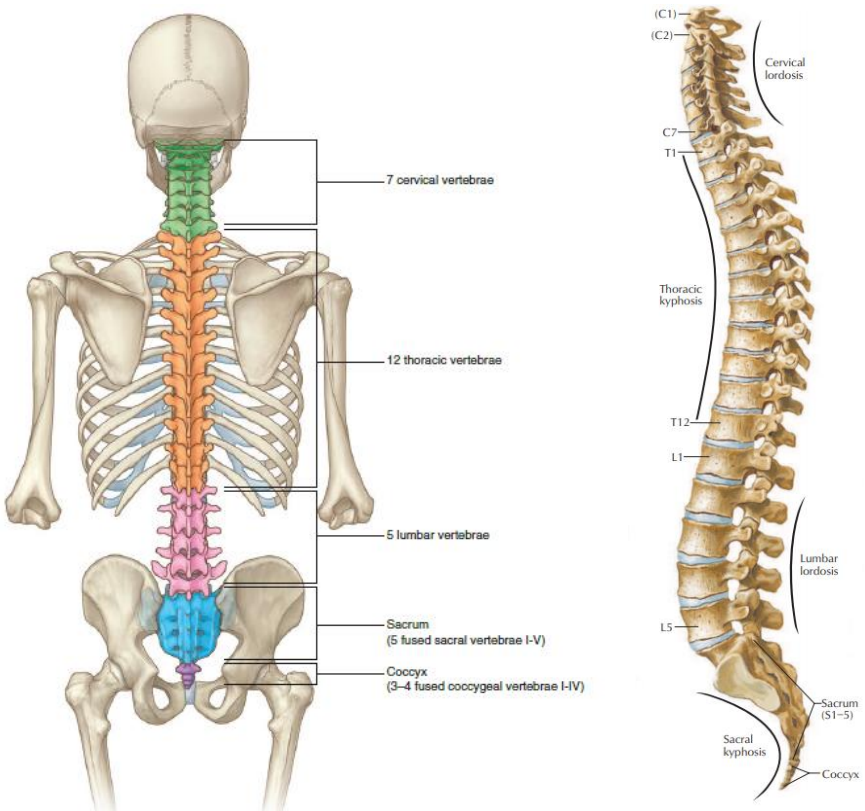

Figure 2.1: Complete human spine with its different regions highlighted (left). Adapted from [13]. S-shaped anatomy of the human spine (right). Adapted from [14].

Between the 24 vertebrae, there are 23 IVDs that separate one vertebra from the adjacent one, starting from C2. Each set of two vertebrae and one IVD constitute one motion segment, which is the functional unit of the spine (or functional spinal unit – FSU) [16]. Anchored to the vertebrae are ligaments and muscles, with the purpose of maintaining the spine aligned and stabilised.

The lumbar region is typically the most studied one given that it is subjected to the highest loads and rotational movements that allow the performance of daily activities. Therefore, the size and density of the vertebrae increase from C1 to the last lumbar vertebra, in order to support the increasing compressive loads [17].

2.1 Vertebrae

Although the vertebrae vary in terms of size and shape according to the region of the spine where they are located, their basic features are the same. Each vertebra is composed by a *vertebral body* (VB) and a *neural arch* (also known as vertebral arch), which are the most anterior and posterior segments of the vertebra, respectively. When these two segments are joined together, a hole is created between them, known as *foramen*, through which the spinal cord runs. Furthermore, when all vertebrae are stacked one on top of the other, a gap occurs between adjacent vertebrae (one on each side), that allows the passage of a single spinal nerve. This opening is called *intervertebral foramen* [13]. Figure 2.2 illustrates the basic features of a vertebra.

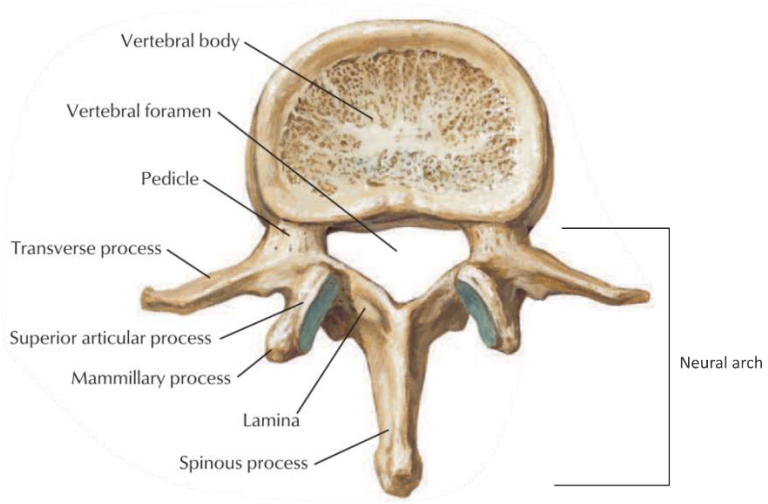

Figure 2.2: Superior view of L2 illustrating the basic features of a vertebra. Adapted from [14].

The vertebral body is a disc-shaped portion of trabecular bone with an outer cortical bone shell and it is responsible for the support of the major loads imposed in the spinal column. Its top and bottom surfaces are slightly concave and covered with hyaline cartilage, called *vertebral endplates*. The neural arch extends backwards from this segment. The most anterior structures of the neural arch are the *pedicles*, that start from the VB (one on each side) and project backwards, where they are joined together and unite with the *laminae*. The laminae are the flat portions of the arch, which end in a sharp

thin projection that forms the *spinous process*. From the point of junction of the laminae with the pedicles, two *transverse processes* are projected laterally (one on each side of the neural arch). These processes, in combination with the spinous one, serve as attachment points for muscles. Finally, four processes allow communication between the different vertebrae: two for the articulation between one vertebra and the one immediately above; and two for the articulation between one vertebra and the one immediately below. These are called *superior* and *inferior articular processes*, respectively, and are projected upwards or downwards accordingly. The surfaces of these processes, known as *facets*, are covered with hyaline cartilage, allowing a smooth articulation between vertebrae [13], [15], [17]. The facet joint enables load transfer from vertebra to vertebra and plays a role in limiting axial rotation (AR) and stabilising flexion/extension [18].

2.2 Intervertebral Discs

The IVD is a fibrocartilaginous structure that is located between two adjacent vertebral bodies, from C2 to the sacrum. The main function of the IVD is serving as a shock absorber. Nevertheless, it also works as a mobility and junction point, maintaining the vertebrae in place and preventing excessive motion [19]. Similarly to the VB, the IVD is disc-shaped, and it consists of three different regions:

- an outer ring, called *annulus fibrosus* (AF), mainly composed by concentric layers of collagen fibres, resulting in a lamellar structure.
- an inner gelatinous region, the *nucleus pulposus* (NP), mainly composed by water and proteoglycans (PGs), primarily responsible for supporting compressive and shear stresses.
- and the semi-permeable vertebral endplates, that articulate with the vertebral bodies and allow the supply of nutrients to the IVD (since it is an avascular structure).

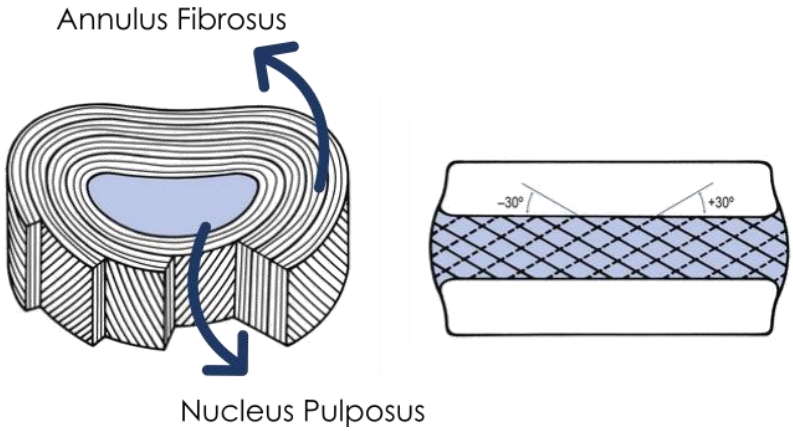

Figure 2.3: Schematic of the different regions of the IVD and its structure. Adapted from [20].

PGs are highly negatively charged molecules. Therefore, the high quantity of PGs present in the NP allows the nucleus to retain water, maintaining its swelling pressure. On the other hand, the lamellar architecture of the AF is useful for maintaining the tensile properties of the IVD, while providing structural support for PG synthesis [19]. There is no physical separation between the AF and the NP, establishing

the IVD as a continuous biphasic medium, with an increasing amount of fibres towards the outer AF. Within each lamella of the AF, the fibres are oriented at an average of 30 degrees in relation to the transverse plane (Figure 2.3). When considering two adjacent lamellae, the fibres run in opposite directions – fibres of two adjacent lamellae form an angle of around 120 degrees between them. This configuration confers additional resistance to rotation forces [18], [20].

In the lumbar region, IVDs are the largest to support the loads of daily activities [15]. For this reason, the lumbar spine is the most common area for IVD degeneration since nutrient diffusion is much more difficult and takes longer to occur.

2.3 Ligaments

Ligaments are critical in preventing hypermobility and excessive IVD bulging, therefore being fundamental for the stability of the spine. These structures are composed by connective tissue (i.e. parallel collagen fibres), typically connecting two or more bones together. In the case of the spine, they are responsible for holding the different vertebrae in place and protecting the IVDs whilst limiting their ROM. Due to ligament elasticity, they allow the spine to return to its neutral position after a movement in a given direction, being only active in tension [17], [20]. In combination with ligaments, spinal muscles contribute to the stability and support of the spine [20]. There are seven major ligaments in the lumbar spine [17], presented next and illustrated in Figure 2.4:

- Anterior longitudinal ligament (ALL) – a continuous band attached to the anterior portion of the vertebral bodies and IVDs.
- Posterior longitudinal ligament (PLL) – similar to ALL, but located in the posterior portion of the vertebrae and IVDs.
- Ligamentum flavum (LF) – a continuous band of fibres located on the anterior portion of the laminae. It plays a role in connecting the vertebrae and limiting flexion.
- Interspinous ligament (ISL) – a thin band of fibres that connect two adjacent spinous processes.
- Intertransverse ligament (ITL) – connects two adjacent transverse processes.
- Supraspinous ligament (SSL) – connects two adjacent spinous processes.
- Facet capsular ligament (FCL) – a small band of fibres that form a ring around the facet joint, preventing the facets from sliding relative to each other.

2.4 Spinal Diseases and Treatment

Lumbar spine disorders are a major source of disability worldwide. Most of them are based on degenerative processes of spinal structures, namely IVDs and facet joints, being age progression a major causal factor. However, the origin of degeneration of the spine is still unknown, and the degeneration of one structure will most likely induce degeneration in another, exacerbating the pathological condition even further [2], [3]. Therefore, the complete elimination of the disease is extremely difficult and the focus is placed on symptoms relief instead.

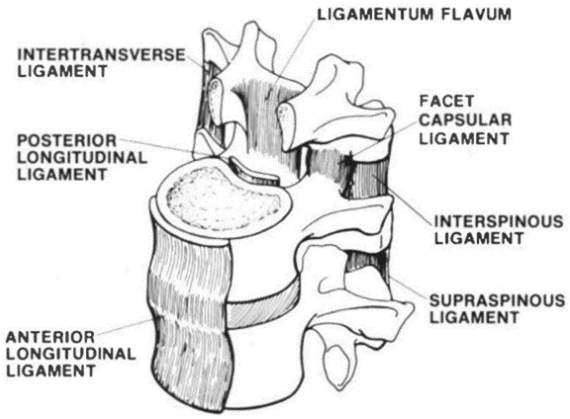

Figure 2.4: Schematic view of all the seven ligaments of the lumbar spine. Retrieved from [20].

The process of IVD degeneration begins with a loss of hydration by the IVD and calcification of the vertebral endplates, which leads to increased stiffness. This is a problem for nutrient diffusion and removal of waste products, as their only pathway across the IVD is through the endplates [19]. As a consequence, it becomes impossible to maintain healthy chondrocytes in the IVD and degeneration is increased even further. As the NP becomes stiffer, there is a gradual loss of PGs, which in turn lose their water-binding capacity as a result of increased cross-linking of collagen fibres [21]. Due to this phenomenon, there is a further hydration loss and reduction in IVD height. The load supported by the annular fibres decreases and their laxity increases, which allows a larger ROM. At a certain point, the increase in stiffness prevails over fibre laxity, directly hampering joint motion [22].

Another possible cause of spinal diseases is ligament degeneration. With advancing age, there is a loss of elasticity due to the cross-linking of collagen fibres and, therefore, ligament stiffness increases [18]. This compromises the stability of the spine and can lead to spondylolisthesis. Spondylolisthesis is one lumbar spine disorder that occurs when a VB slips forward relative to the adjacent one. Other disorders include degenerative disc disease (wear and tear of IVDs), spinal stenosis (nerve root narrowing), osteoarthritis (stiffening of facet joints due to cartilage wear), and scoliosis (twist of the spine to the side in the frontal plane) [23].

Low back pain is a typical and severe consequence of spine disorders, affecting many people worldwide, in different age groups. Recent studies suggest that 60-80% of adults will experience LBP at some point in their life and that 30% of all teenagers experience at least one episode of this disorder [24]. This condition is the lead cause of activity limitation. It is responsible for high treatment costs, work absent days, and one of the main reasons people seek health care services, imposing a high economic burden on individuals and society [1]. In this way, treatment options must be considered.

One specific disorder that can lead to LBP is degenerative disc disease (DDD), which is the focus of the present work. As the IVDs start degenerating, they can bulge or protrude through weak points, possibly leading to herniation and compression of the nerve roots in extreme cases, which results in acute pain. Spinal canal stenosis can also be originated due to facet joint hypertrophy, as a result of hypermobility and instability from IVD degeneration [25].

Since IVDs are composed by cartilage, their regeneration is highly unlikely. Therefore, non-surgical treatments, such as medication and physical therapy, are mainly focused on addressing the symptoms, minimising pain, and improving mobility, rather than acting on the source of problems [20]. To recover functionality of the spine in cases of debilitating disease, surgical approaches are the most suitable option. Spinal fusion – or arthrodesis – is the most common procedure used to address DDD. During a spinal fusion surgery, two adjacent vertebrae are merged together over time, leading to the stabilisation of the spine, recovery of natural movement, and pain relief. This can be achieved by replacing the degenerated IVD with an implantable cage (i.e. interbody fusion) or simply by placing bone graft in the lateral regions of the spine [26]. A spinal fusion procedure may have different approaches (Figure 2.5) [27]:

- Posterolateral Gutter Spine Fusion – bone graft is placed in the posterolateral portion of the spine, between transverse processes, to promote fusion.
- Posterior Lumbar Interbody Fusion (PLIF) – disc space is approached posteriorly from the lower back. It requires a laminectomy and retraction of nerve roots, with risk of nerve damages.
- Anterior Lumbar Interbody Fusion (ALIF) – disc space is approached anteriorly from the abdomen, retracting the abdominal muscles, peritoneum, and the great vessels, with risk of vascular injuries.
- Transforaminal Lumbar Interbody Fusion (TLIF) – disc space is approached from the back with the cage being introduced unilaterally through the intervertebral foramen.
- Extreme Lateral Interbody Fusion (XLIF) – disc space is approached from the side, not disrupting major back muscles or ligaments, with the exception of a slight disruption in the psoas muscle.
- Oblique Lumbar Interbody Fusion (OLIF) – disc space is approached laterally, avoiding direct exposure of anterior vessels and posterior nervous and bony structures. It differs from XLIF as the incision is done more anteriorly, lowering the risk of lumbar plexus and psoas injury.

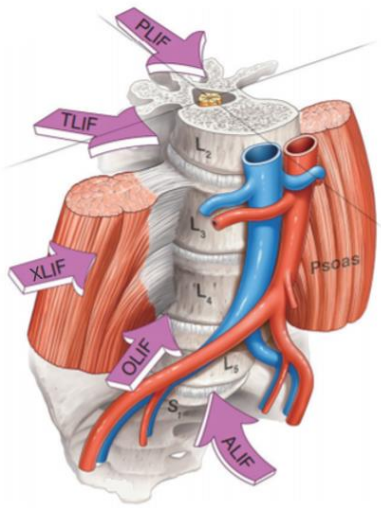

Figure 2.5: Different approaches for spinal interbody fusion surgery. Adapted from [27].

However, one downside of spinal fusion technique is that, due to the fusion process, the movement of the implanted segment cannot be recovered. Artificial disc replacement – or total disc replacement (TDR) – is a different possibility for DDD treatment that allows to maintain the movement in the implanted spinal unit by replacing the damaged IVD with a prosthetic implant. Nonetheless, this approach is limited to some types of IVD pathology [28].

Chapter 3

State of the Art

The focus of this work is the evaluation of changes in lumbar spine kinematics with advancing degeneration, before and after interbody fusion. In this way, it is relevant to understand the progress made in this field over the years. In this chapter are highlighted the main advances and the most significant models available in the literature.

3.1 Interbody Fusion and Instrumentation

Interbody fusion surgery, using cage technology, is nowadays one of the most common procedures for spinal fusion [29]. Its main goal is to restore stability and maintain the natural balance of the spine, eliminating LBP.

Since the introduction of the spinal fusion concept by Hibbs [30] and Albee [31] in 1911, the clinical outcomes of this technique have been proven extremely beneficial when treating numerous spine disorders, such as DDD, spondylolisthesis, and spinal stenosis [5]. In the late 1940s, King [32] adapted Hibbs' technique by adding vertebral screw fixation, being this the first use of a rigid fixation system. This system was later improved by the use of longer screws placed more medially in the pedicles [33], as well as the addition of a rod in combination with the pedicle screws [34]. This led to an increase in stability and higher fusion rates. Through a load distribution between cage and posterior fixation, it is easier to attain stability of the spine and better clinical results, with minimal cage migration [29]. However, rigid fixation systems have been associated with some drawbacks, such as pedicle screw loosening or failure, and the imposition of high stresses on adjacent segments, increasing the probability of adjacent degeneration [35]. Therefore, dynamic fixation systems have been presented as an alternative to tackle rigid fixation drawbacks, as they ensure maintenance of mobility in the intervened segment. Nonetheless, there is still some debate about whether or not the use of dynamic systems should be advised [36].

In 1988, the first cage design was proposed by Bagby to be used in horses. It consisted of a stainless-steel fenestrated cylinder with an autograft inside to help fusion. This model was later adapted to be used in humans [29]. Nowadays, cages may have numerous different designs, which vary mostly according to the surgical procedure that is adopted for cage insertion. However, the choice of design must be carefully weighted as the fusion efficacy depends on several design parameters, such as shape, material, and size [5]. Very large cages can damage the surrounding structures, whereas those that are very small can lead to instability [37]. On the other hand, cages with increased height may lead to endplate trauma and increased probability of adjacent disc degeneration, but those that are too low may migrate and result in fusion failure [38]. Figure 3.1 shows an example of an interbody fusion cage, introduced via OLIF and requiring posterior fixation.

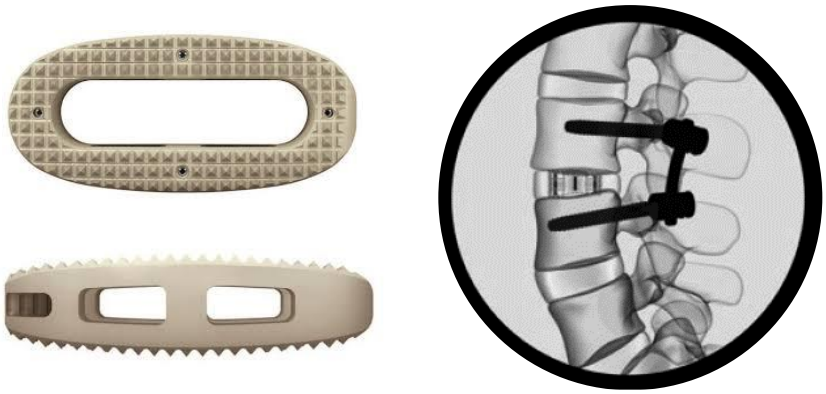

Figure 3.1: Example of an OLIF cage (Oracle®, left) and respective posterior fixation (right). Adapted from [39].

The ideal material for an interbody fusion device is one that is stiff enough to maintain stability, but with Young's modulus similar to bone to prevent subsidence and stress-shielding. Usually, these devices are made of titanium alloys or polyetheretherketone (PEEK), but both have some advantages and disadvantages. Titanium alloys present higher durability and strength, being biocompatible and resistant to corrosion. Moreover, they promote high fusion rates due to their osteoconductive potential. However, their elastic modulus is relatively high compared to bone, often leading to cage subsidence and stress-shielding. On the other hand, PEEK has an elastic modulus comparable to bone, but its potential for osseointegration is limited [5], [40].

In addition to traditional instrumentation, the focus on personalized medicine has increased in recent years. Patient-specific rods and the development of a tool to determine optimal placement and size for TDR are some examples within spine surgery. Regarding promotion of osseointegration, current research focuses on tissue-engineered bone grafts, bio-actively coated screws, and surface engineering technology, since different cage surface properties are thought to stimulate osteogenesis [29], [41].

3.2 FE models

FE analysis is an approach that allows to determine the mechanical behaviour of a motion segment without the need for destroying a cadaveric or animal sample. This method consists of dividing a certain domain into a set of subdomains (the "finite elements"), that maintain the original properties, and then determining their interpolating functions. The degree of complexity of the problem is hence reduced by the individual analysis of each subdomain. Moreover, FE modelling allows the alteration of several parameters, such as geometry, material properties (e.g. ligament stiffness), and external load, and to understand the impact of these changes on kinematics.

3.2.1 Intact Models

The first use of FEA was reported back in the 1950s in the aircraft industry [42], but the first model in biomechanics was only developed in 1972 by Brekelmans et al. [43]. In this study, a two-dimensional model of a femur was constructed, and a mathematical model based on FE method was developed for the prediction of the mechanical behaviour of the model. It could then be generalized and applied to any

given skeletal component. The femur was subjected to different loading conditions and it was concluded that the complex geometry of the model, as well as the variety of load situations, did not pose any problems to the determination of mechanical behaviour by this method.

In 1974, Belytschko et al. [44] devised the first model of a functional spinal unit with one IVD and two adjacent vertebral bodies. The posterior processes were not included assuming that little to no load is supported outside of the vertebral bodies during small axial deformations. For simplification, the model was considered axisymmetric with respect to a vertical centreline, and also symmetric relative to a horizontal plane passing through the middle of the IVD. In view of these symmetries, Figure 3.2 shows the final model used.

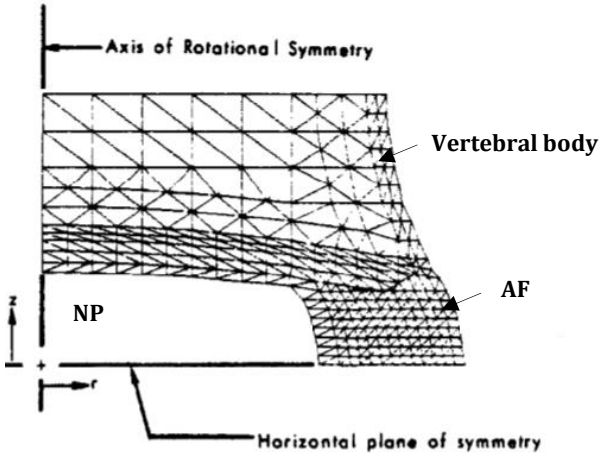

Figure 3.2: Final FE model of a functional spinal unit developed by Belytschko et al.. Adapted from [44].

The vertebrae were divided into cortical and trabecular bone and modelled as linear elastic isotropic materials. The NP was assumed to be incompressible and in a hydrostatic state of stress, whereas AF was modelled with linear orthotropic material properties. This model was later improved by modelling the annulus with non-linear orthotropic properties, obtained by comparison with experimental results. In this work, degeneration by annular tears and desiccated nucleus were also studied [45].

In 1978, Hakim and King [46] developed one 3D model of a lumbar vertebra (Figure 3.3), being the first ones to include facet joints in their study. The anatomical details were represented by direct measurement, and the model was assumed to be bilaterally symmetric since the load was applied in the sagittal plane only. Later, the IVD was introduced and modelled by linear axial elements. However, when comparing the results with experimental data, some inconsistencies were found due to the complexity of the problem and uncertainties in representing the geometry and material properties properly [47].

Another possibility for the development of skeletal models is through medical image reconstruction. Bozic et al. [48] constructed a three-dimensional model of a cervical human vertebra based on computer tomography (CT) scans to investigate the mechanism of burst fractures. The adjacent IVDs were modelled as spring elements. The advantage of this approach was that the Young's Modulus of each element could be derived from the apparent bone density of the pixels in the CT image.

Years later, models with more developed material properties started arising. For example, in 1984, Shirazi-Adl et al. designed a L2-L3 FE model based on *in vitro* measurements to determine which components are most susceptible to failure under compressive loads. The model took into account geometric nonlinearities and the composite structure of the AF, therefore modelling it as a fibre-reinforced material with collagen fibres – represented by axial elements with non-linear properties – embedded in the ground matrix in a criss-cross pattern, as represented in Figure 3.4. The NP was modelled as an incompressible inviscid fluid. It was shown that, for a healthy IVD, the most vulnerable components under compression were the trabecular bone and endplates. Degenerated IVDs were also studied by removing the NP and, in these cases, the AF bulk material was also found to be susceptible to failure whilst the annular fibres maintained their integrity.

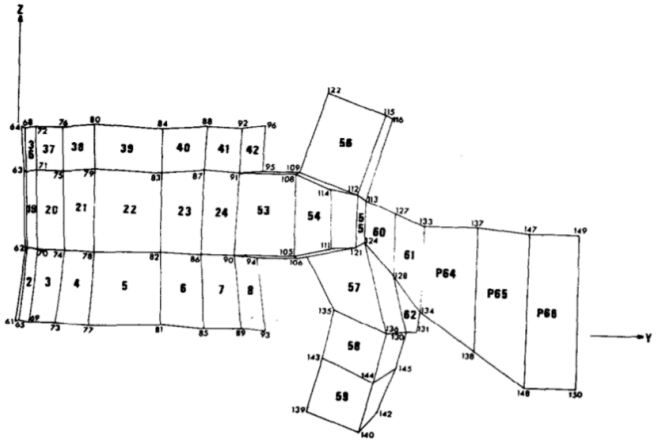

Figure 3.3: Sagittal view of the model of the lumbar vertebra developed by Hakim and King. Adapted from [46].

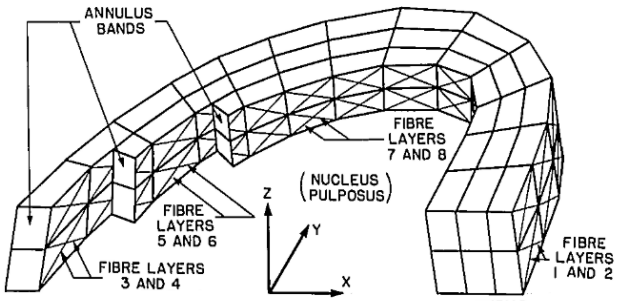

Figure 3.4: Representation of annulus bands and fibre orientation in the FE model developed by Shirazi-Adl et al.. Adapted from [49].

In 1985, Simon et al. [50] reported probably the first poroelastic FE model of an IVD, with creep and steady-state responses matching experimental observations. In 1993, this model was further extended by Laible et al. [51] to include the swelling process caused by osmotic pressure. A few years later, in 1997, the time-dependent response of a lumbar IVD was considered by Wang et al. [52] with the development of a nonlinear viscoelastic FE model of a lumbar segment (L2-L3). The aim of this

study was to quantify the model´s mechanical responses to time-varying loads, and a good agreement was found between the outcomes and experimental observations.

Breau et al. were the first group to develop a complete model of the lumbar spine, from L1 to S1, based on CT image reconstruction [53]. The AF and NP were modelled as Shirazi-Adl et al. considered in their work [49]. However, in this case, ligaments were also included, being represented as axial elements and their points of insertion selected using direct observations and anatomical data.

Over the years, the representation of ligaments in FE models has also evolved. Spinal ligaments have been modelled with linear [54], [55], bilinear, and nonlinear material properties [56]–[59], being these last ones the most appropriate solution to simulate the complex nature of ligaments. The nonlinear behaviour is typically represented through stress-strain curves [56], by defining different material properties at different strains [57], [60].

3.2.2 Degenerated Models

3.2.2.1 IVDs

Apart from the study and modelling of the intact spine, IVD degeneration has been the subject of several studies throughout the years. Multiple papers have reported the differences, in terms of intersegmental motion, intradiscal pressure (IDP), etc., between healthy and degenerated IVDs, with different degrees of degeneration being evaluated [7]–[9]. For example, Rohlmann et al. [9] used a L3-L4 FE model to study different degeneration stages, and their results showed an increase in intersegmental rotation for mild degeneration. This mobility then decreased as degeneration became more pronounced. Furthermore, IDP was found to be lower in the degenerated model, while stress in AF and facet forces were higher when compared with the healthy model.

Degeneration can be simulated by simply altering IVD material properties, or, in addition, by morphological changes, such as IVD height reduction or endplate calcification. In fact, clinical scenarios including more than one degenerative change are common. Galbusera et al. [61] investigated the mechanical response of the lumbar spine when subjected to a combination of IVD degenerative changes. They used a poroelastic FE model of the healthy L4-L5 segment and from this model 30 different ones were created through a combination of different degenerative changes and degrees of degeneration. The evaluated degenerative changes were water loss, calcification and thickness reduction of endplate cartilage, IVD height reduction, osteophyte formation, and diffuse sclerosis. They found that there was an increase in stiffness and IDP with progressive degeneration and that all degenerative changes had a significant impact on spine kinematics. Ruberté et al. [60] also studied IVD degeneration by modelling degeneration with changes in geometry and material properties. Geometry changes included IVD height and NP area reduction in a FE model of the complete lumbar spine (L1-S1). The aim of this work was to evaluate the contribution of degeneration of the L4-L5 segment to the degeneration of the adjacent levels. Their results showed a decrease in stiffness, accompanied by an increase in ROM, in the early degeneration stages. However, as degeneration progressed, the stiffness increased, ROM decreased, and there was a shift in the load transmission from NP to AF. Finally, it was proven that single-level degeneration can increase the degeneration risk at the adjacent levels.

3.2.2.2 Ligaments

Ligaments are critical structures in preventing hypermobility and excessive IVD bulging, being fundamental for the stability of the spine. They are responsible for holding the different vertebrae in place and protecting the IVDs whilst limiting their range of motion [13], [17], [19]. Nevertheless, ligament disruption may occur, which is inevitable with advancing age and degeneration.

There are few studies focused on the degeneration of ligaments and its effects on lumbar spine biomechanics. For example, to determine changes in ligament properties with ageing, Nachemson and Evans [62] performed mechanical tests in LF, while Neuman et al. [63] did the same for ALL. In the case of ISL, the correlation between ligament degeneration and ageing was performed by Keorochana et al. based on the observation of MR images [64]. Other studies focused on histological changes of ligaments [65] or on their chemical content [66] to evaluate the respective evolution with age and determine their effects. However, none of these studies evaluated the impact of age-related changes and the role of ligaments in spine kinematics and stability, as opposed to the following. Gunzburg et al. [67] performed cadaveric experiments to determine the role of FCL in axial rotation and determined that this movement is in fact limited by this ligament. On the other hand, Adams and Hutton [68] loaded intervertebral joints in torsion and compression and showed SSL, ISL and FCL not to play a significant role in AR.

As opposed to IVD degeneration, the use of FE simulations for the evaluation of different ligament properties has been very limited. Sharma et al. [69] developed a FE model of an L3-L4 motion segment (Figure 3.5) to evaluate the effects of posterior ligaments and facet removal. They found ISL/SSL and LF to provide the strongest resistance to flexion, and FCL in the case of extension. Gudavalli and Triano [70] used an L4-L5 model to explore forces and strains on ligaments, as well as the effect of ligament transection. Their results indicated that SSL is the ligament subjected to the highest load and strain. Moreover, with ligament transection, there was an increase in flexibility of the joint and the loads and strains carried by the remaining ligaments were also increased.

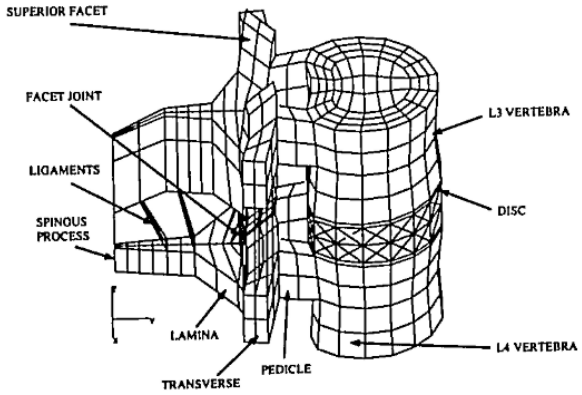

Figure 3.5: FE model developed by Sharma et al. to evaluate the effects of posterior ligaments and facet removal. Retrieved from [69].

The possibility of ligament failure with advancing age should also be considered. For this purpose, some studies have already performed stepwise anatomy reductions, in which ligaments are removed

sequentially and their impact is assessed. This is a way of determining the influence of each ligament in each movement and it may be useful when deciding whether a transected ligament should be repaired or not, or which movements to avoid if there is no possible repair. In addition, when replacing a degenerated IVD with a cage, it allows for the separation between implant insertion and ligament changes effects. Heuer et al. [11] performed *in vitro* tests in eight spinal segments and determined SSL to resist slightly in extension, ALL slightly in AR and strongly in extension, and FCL in axial rotation. Adams et al. [71] also focused on cadaveric experiments, during flexion, and found out that FCL and IVD were the structures that offered more resistance during this movement. Naserkhaki et al. [72] evaluated the effects of eight different ligament property datasets on an L4-L5 FE model. Changes in ligament properties were found to only affect sagittal movements (extension/flexion) in a significant way. Moreover, SSL was determined to be the dominant ligament in flexion, and ALL crucial in resisting extension, while PLL was negligible in this movement. Alapan et al. [73] developed an L4-L5 FE model to evaluate the effects of ligament failure on the instantaneous centre of rotation (ICR), as well as on ligament load-sharing. As ligaments were removed, there was a consistent increase in ROM and a shift in ICR. Finally, Zander et al. [12] evaluated the effects of ligament removal on intersegmental motion and ligament forces of a healthy L3-L4 FE model, showing the most active ligament in each movement.

However, since these studies only included one motion segment, the effects on adjacent levels were neglected. Conversely, Ellingson et al. [10] developed a FE model of the lumbar spine from L3 to the sacrum, to explore the effects of IVD degeneration and also to define the role of each ligament in functional mechanics. Their results showed an increase in ROM and decrease in stiffness with incremental ligament removal, being lateral bending (LB) the least affected motion.

3.2.3 Instrumented Models

Nowadays, several studies intend to evaluate the biomechanics of the spine when subjected to different types of instrumentation. One of the main goals is to understand the differences in relation to a healthy spine, especially in the segments adjacent to the cage insertion level, since there are indications that these segments may become more susceptible to degeneration [36]. For example, Jiang et al. [74] developed an L3-L5 FE model, and introduced a cage in L4-L5 through a PLIF approach, with the aim of identifying changes in the proximal adjacent level when subjected to different degrees of degeneration (Figure 3.6). The results of this work showed that, after PLIF, ROM and IDP values increased in the adjacent segment. However, as degeneration progressed, intersegmental motion decreased, whereas IDP in the AF and NP continued to increase.

A very similar study to the one of Jiang et al. was conducted by Tang et al. [75], but this time regarding an ALIF procedure. The obtained results were identical, with the only exception that, with advancing degeneration, ROM values increased in flexion/extension.

Also in the scope of instrumentation, FE studies are often conducted to test new cage or fixation designs, as well as the introduction of new materials and their impact on load-sharing. In 2012, Galbusera et al. [76] developed a new cage design for lumbar interbody fusion to limit the risk of cage subsidence and to promote fusion. The aim of the study was to explore different values for the design

variables (namely, cage stiffness, thickness of cage layers, and rod material properties), and evaluate their biomechanical effects in order to optimise cage performance.

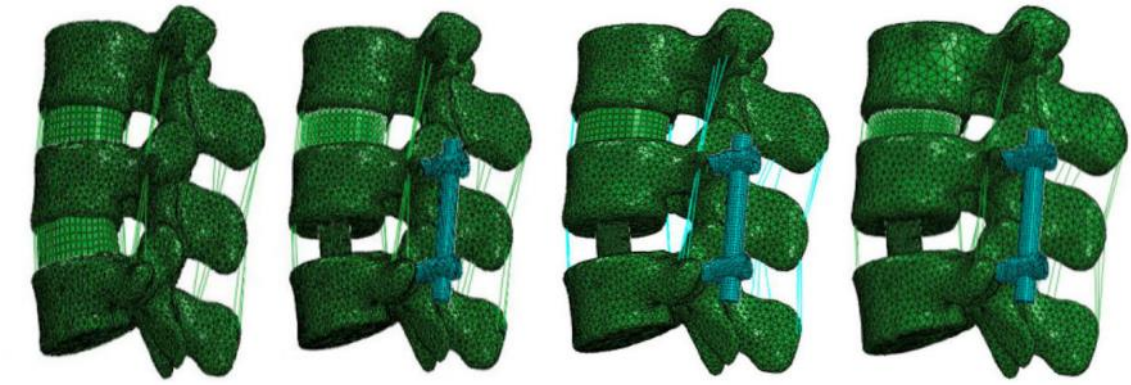

Figure 3.6: FE models of the L3-L5 lumbar spine, developed by Jiang et al., from the healthy intact model to models with PLIF and progressive degeneration (from left to right). Adapted from [74].

The effects of different surgical procedures and correct placement of instrumentation are also the focus of some studies. For example, Loenen et al. [77] recently conducted a study that showed that misaligned posterior fixation may induce high internal forces and result in clinical complications. Guo et al. [78] studied the OLIF procedure and investigated the stability of different fixation constructs, including stand-alone cages, lateral rod-screws, facet screws, and uni- and bilateral pedicle screw systems. Comparing ROM and stress values between models, it was concluded that the bilateral pedicle screw device provided the best biomechanical stability, being associated with the minimum ROM and cage and screw stresses. On the other hand, the stand-alone cage could not provide sufficient stability. The stress exerted on internal fixation was the highest for the lateral rod-screw device with contralateral translaminar facet screw. Figure 3.7 shows the FE models developed by Guo et al. with different types of fixation.

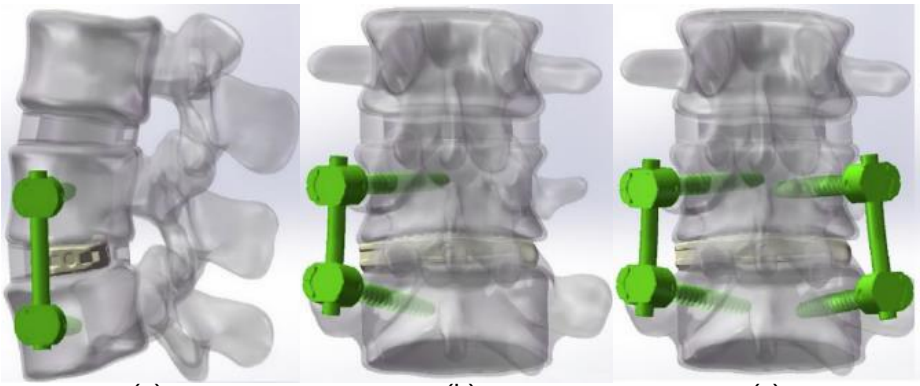

Figure 3.7: OLIF FE models developed by Guo et al. with different types of fixation: (a) lateral rod-screw, (b) unilateral pedicle screw, and (c) bilateral pedicle screw. Adapted from [78].

Chen et al. [79] investigated the influence of bilateral versus unilateral posterior fixation in the kinematics of the full lumbar spine, using FE models subjected to a TLIF approach in L4-L5 level (Figure 3.8). An additional aim of this work was to determine the effects of different cage positioning in the TLIF models. Their results indicated that models with unilateral fixation are subjected to a higher motion and have increased AF and screw stresses, as compared with models with bilateral fixation. Amongst all the TLIF cage models, the diagonal cage was the one for which the outcome increases were more pronounced. However, if a contralateral facet screw was inserted, the outcome values decreased and became very close to the ones of bilateral models. Therefore, the use of unilateral posterior fixation in TLIF surgery is only advised if accompanied by a contralateral facet screw. Moreover, cage geometry did not affect the model behaviour if used together with appropriate posterior fixation.

More recently, Chen et al. [80] concluded that, from a clinical point of view, unilateral fixation constructs can achieve the same efficiency as bilateral constructs in TLIF procedures, but unilateral models having the benefits of less surgical injuries and cost.

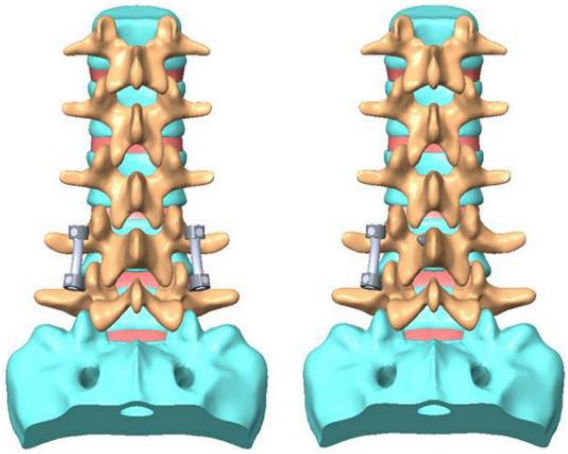

Figure 3.8: FE model of the lumbar spine with bilateral (left) and unilateral (right) posterior fixation developed by Chen et al.. Adapted from [79].

The differences between mono- and bisegmental fixation have also been previously studied by Zander et al. [81]. Using a FE model with bone graft insertion in L2-L3 – and also in L3-L4 in the case of bisegmental fixation –, they demonstrated that there are no significant differences in the mechanical behaviour of the lumbar spine after mono- or bisegmental stabilisation.

Many studies regarding instrumentation have been performed to determine the mechanical effects of posterior fixation, and whether or not it is essential in spinal fusion surgeries. Within these studies, some focus on the comparison between rigid and dynamic fixators. Rohlmann et al. [36] compared a dynamic fixation device with a rigid fixator, evaluating the effects on intersegmental motion, IDP, and facet and implant forces. They used a FE model of the complete lumbar spine (L1-L5), with bilateral fixation in L3-L4, and determined a ROM decrease at the implant level, but a slight increase at the adjacent level, particularly in flexion. IDP decreased in extension for healthy IVDs, and facet forces also decreased at implant level. All these effects were found to be more pronounced for rigid fixation.

However, Rohlmann et al. concluded that the difference in the mechanical effects between a posterior dynamic or rigid implant was smaller than often expected.

Similarly, Oktenoglu et al. [35] explored the effects of a novel pedicle-screw dynamic fixator on the stabilisation of the lumbar spine and compared the obtained results with equivalent rigid and semi-rigid systems. For that purpose, *in vitro* testing and FEA were performed, using L2-S1 segments. Their results showed a significant decrease in intersegmental motion for rigid and semi-rigid systems, whereas the dynamic system was able to maintain ROM values similar to the intact spine. Regarding load-sharing, the dynamic fixator allowed lower stresses at the bone-implant interface when compared with equivalent rigid and semi-rigid systems. The lower peak stresses in the screws of the dynamic fixator are also an indicator of reduced probability of screw loosening.

Chapter 4

Part I – Ligament Degeneration

The first part of this work consists in the assessment of the impact of degenerative changes due to advancing age in a healthy FE model of the lumbar spine, namely the impact of ligament changes. To this end, changes in material properties were applied in a standard healthy model developed in previous work [82] to reflect degeneration. Multiple combinations of IVD and ligament degeneration were tested. Furthermore, simulations were performed with the removal of ligaments in order to understand the role of each ligament in each natural movement of the spine and further explore their effects on the adjacent level and stability. This chapter presents the Methodology, Results, and Discussion of these simulations.

4.1 Materials and Methods

To evaluate the role of ligaments in the stabilisation of the lumbar spine a series of FE simulations was performed. First, all ligaments were removed from a previously validated L3-L5 model in the healthy state [82]. Secondly, the same process was repeated for different stages of the degenerated spine. Finally, from the intact model, the degeneration process of ligaments was evaluated.

4.1.1 FE Model

The model used in the first part of this work was developed in a previous study [82], based on CT scans from a healthy 40-year-old woman (Figure 4.1). It included three vertebrae (L3 to L5), two IVDs, and the seven major ligaments of the lumbar spine: ALL, PLL, FCL, LF, ISL, ITL and SSL.

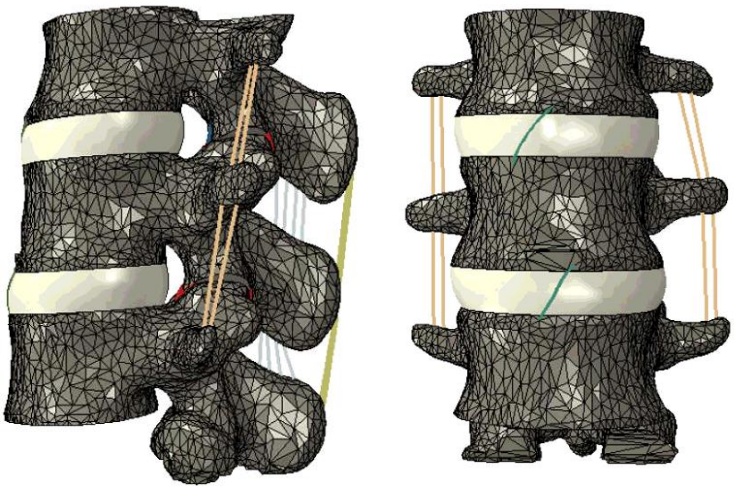

Figure 4.1: Sagittal (left) and frontal (right) views of the FE model used in the first part of this work.

Material properties of the model components were taken from the literature [10], [11], [83], [84] (Table 4.1). Bone was modelled as linear elastic; AF was defined as hyperelastic anisotropic, following the Holzapfel formulation (Equations 4.1 and 4.2); and the behaviour of NP was represented as hyperelastic isotropic, following the Mooney-Rivlin formulation (Equation 4.3). In equations 4.1 to 4.3, U is the strain energy per unit of reference volume; *N* is the number of fibres; J^{el} is the elastic volume ratio; C_{10}, C_{01}, D_1, k_1, k_2 and *kappa* are constitutive parameters; I_1 and I_2 are the first and second invariants, respectively; and E_α is defined by equation 4.2 with $I_{4(\alpha\alpha)}$ as a pseudo-invariant. Ligaments were modelled as linear elastic tension-only spring elements.

$$U = C_{10}(I_1 - 3) + \frac{1}{D_1}\left(\frac{(J^{el})^2 - 1}{2} - \ln(J^{el})\right) + \frac{k_1}{2 \times k_2}\sum_{\alpha=1}^{N}\{exp[k_2\langle E_\alpha\rangle^2] - 1\} \quad (4.1)$$

$$E_\alpha = kappa(I_1 - 3) + (1 - 3\,kappa)(I_{4(\alpha\alpha)} - 1) \quad (4.2)$$

$$U = C_{10}(I_1 - 3) + C_{01}(I_2 - 3) + \frac{1}{D_1}(J^{el} - 1)^2 \quad (4.3)$$

In all cases, a pre-load of 100 N [7], [85] and a moment of 7.5 Nm were applied, with boundary conditions (BCs) completely restraining the movement of L5. The main outcome of the simulations was the range of motion, namely the relative ROM changes. Since ligament stiffness can yield a wide range of values and it is unknown in most cases for a given patient, the relative changes induced by ligament removal are much more relevant than absolute values [12].

4.1.2 Ligament Removal

For ligament removal, a four-phase process was established, adapted from the work of Ellingson et al. [10]: (i) removal of superficial ligaments (ISL, ITL, SSL, LF), (ii) FCL removal, (iii) PLL removal, and (iv) ALL removal. Ligaments were removed sequentially from posterior to anterior locations from the whole/intact model, with different degrees of IVD degeneration.

The removal process was conducted twice for each model: (1) removing ligaments only in L4-L5, given that this is usually the segment most affected by degeneration [86], and (2) removing all ligaments in both L3-L4 and L4-L5 levels. These will be referred to as cases 1 and 2, respectively. Having in mind the sequential removal of ligaments, the previous removal stage was used as benchmark (in the first stage, the whole model was taken as reference).

Ligament removal was simulated in a model with healthy IVDs to understand the impact of ligaments in each spinal movement. However, one important aspect to consider is that ligaments are only removed in clinical practice for the introduction of spinal cages in cases of unhealthy and unstable spines, in which the IVDs are degenerated or collapsed and need to be replaced. In this way, besides the healthy model that was used as benchmark, different cases of degeneration of IVDs were considered by assigning different material properties to each IVD. This allows to individualise ligament removal effects from the posterior effects of cage introduction.

Table 4.1: Material properties assigned to each model component.

Material	Formulation	Parameters	Reference
Cortical Bone	Linear Elastic	E = 1200 MPa v = 0.3	[72]
Trabecular Bone	Linear Elastic	E = 200 MPa v = 0.315	[72]
Nucleus Pulposus	Hyperelastic Isotropic (Mooney-Rivlin)	C_{10} = 0.120 MPa C_{01} = 0.030 MPa D_1 = 0.667 MPa^{-1}	[72]
Annulus Fibrosus	Hyperelastic Anisotropic (Holzapfel)	C_{10} = 0.315 MPa D_1 = 0.254 MPa^{-1} k_1 = 12 MPa k_2 = 300 *kappa* = 0.1	[87]
ALL	Linear Elastic	E = 20.0 MPa A = 75.9 mm^2	[10] [83]
PLL	Linear Elastic	E = 10.0 MPa A = 1.6 mm^2	[10] [84]
FCL	Linear Elastic	E = 7.5 MPa A = 19.0 mm^2	[10] [84]
LF	Linear Elastic	E = 13.0 MPa A = 39.0 mm^2	[10] [84]
ITL	Linear Elastic	E = 12.0 MPa A = 1.8 mm^2	[10] [84]
ISL	Linear Elastic	E = 9.8 MPa A = 12.0 mm^2	[10] [84]
SSL	Linear Elastic	E = 8.8 MPa A = 6.0 mm^2	[10] [84]

A – cross-sectional area; E – Young's Modulus; v – Poisson's ratio; C_{10}, C_{01}, D_1, k_1, k_2 and kappa are the constitutive parameters defined in equations 1 and 2

The process of IVD degeneration begins, as previously mentioned, with a loss of hydration by the IVD, leading to increased stiffness. Consequently, there is a decrease in the load supported by the annular fibres and an increase in their laxity, which allows a larger ROM. At a certain point, the increase in stiffness prevails over fibre laxity, directly hampering joint motion [22], [82]. These changes can be reflected in alterations of IVD material properties. Geometrical parameters, such as IVD height, were not altered in this case. Three degenerated cases were created by combining two different degeneration

IVD stages (mild and moderate) with the healthy state, taking into account that L4-L5 level is usually the most affected by degeneration. The model with both IVDs moderately degenerated was excluded as this study is focused on analysing degeneration cases with predominance of L4-L5 degeneration. Hence, L3-L4 is considered to be mildly degenerated at most. Table 4.2 presents all simulated cases with the different degeneration combinations. Material properties for each degeneration stage were adopted from previous work [82], based on the evolution of degeneration presented in the literature [22], [60], [87]. Table 4.3 shows the material properties assigned to the IVD components with increasing degeneration.

Table 4.2: Summary of all simulated cases with different degeneration degrees.

	L3-L4 IVD	L4-L5 IVD		
Model A	Healthy	Healthy	→	H-H
Model B	Healthy	Mild	→	H-Mild
Model C	Mild	Mild	→	Mild-Mild
Model D	Mild	Moderate	→	Mild-Mod

Table 4.3: Material properties assigned to each IVD component in different degeneration stages.

Degeneration Stage	Annulus Fibrosus	Nucleus Pulposus
Healthy	C_{10} = 0.315 MPa D_1 = 0.254 MPa^{-1} k_1 = 12 MPa k_2 = 300	C_{10} = 0.120 MPa C_{01} = 0.030 MPa D_1 = 0.667 MPa^{-1}
Mild	C_{10} = 0.500 MPa D_1 = 0.320 MPa^{-1} k_1 = 1.74 MPa k_2 = 43.5	C_{10} = 0.168 MPa C_{01} = 0.042 MPa D_1 = 0.476 MPa^{-1}
Moderate	C_{10} = 1.130 MPa D_1 = 0.140 MPa^{-1} k_1 = 0.435 MPa k_2 = 8.7	C_{10} = 0.221 MPa C_{01} = 0.055 MPa D_1 = 0.723 MPa^{-1}

4.1.3 Ligament Degeneration

Regarding ligament degeneration and its impact on spine biomechanics, one of the approaches to evaluate this process is to change the mechanical properties of ligaments, namely their stiffness. First, it is important to consider that the degeneration process may have different origins, and also occur in different stages. In this particular case, the focus is on age-related ligament degeneration and, based

on available literature [62], [65], [88], [89], the following two-stage ligament degeneration process was developed, assuming that IVD degeneration occurs first [90]:

i. Ligament relaxation (i.e. stiffness decrease) due to reduced mobility of the IVDs
ii. Increase in ligament stiffness due to collagen cross-linking

In summary, as IVD degeneration progresses with calcification and reduced mobility, ligaments start losing function and, consequently, they start to relax, following the reduction in IVD height in some cases. Then, in later stages, there is a loss of elasticity due to the cross-linking of collagen fibres and loss of elastin [18], [91], leading to an increase in stiffness and ligament shortening. For the purpose of this work, it was considered that ligament stiffness is first decreased and then increased, to study the effects of degeneration in the first and second stages of this process, respectively.

For the first stage, given that degeneration should be more advanced – or equal – in IVDs than in ligaments, Model C was considered, in which both IVDs presented a mild degeneration. Considering ligaments as linear elastic spring elements, their behaviour can be represented using the relationship between a spring's constant and Young's modulus (Equation 4.4) [92]:

$$k = E\frac{A}{L} \tag{4.4}$$

where k is the spring's constant, E is the Young's modulus, A is the cross-sectional area, and L is the ligament length. Therefore, the reduced ligament stiffness is translated into a reduced Young's modulus since the length and area of the ligament remain the same – assuming that ligaments will not break. For the first simulations, E was reduced in 25%, mimicking mild ligament degeneration. For the second stage, in order to simulate more advanced ligament degeneration, it was also necessary to increase IVD degeneration. Thus, Model D was considered for this situation, with L3-L4 IVD and L4-L5 IVD mildly and moderately degenerated, respectively. For ligament degeneration, two options were evaluated: Mild-Mild, as in the first stage, in which the ligaments in the L4-L5 level had not yet followed the degeneration of the IVD, and then Mild-Moderate (Mild-Mod), in this case with an increase in stiffness (i.e. in E) of 25% compared to the original value in L4-L5 FSU ligaments. In L3-L4 level, ligaments remained with a mild degeneration as the IVD was also mildly degenerated. In posterior simulations, degenerations of 50% and 75% were also tested.

For simplicity purposes, not all ligaments were degenerated in the current simulations, being this analysis mainly focused on the ligaments intervening on spine movement; otherwise, degeneration would have no significant impact. Therefore, only ALL and FCL were degenerated, given that, from the results obtained in this work[1], these are the ligaments that showed the most significant impact on movement – FCL in flexion and AR, and ALL in extension. In LB, there were no ligaments with significant impact. Nonetheless, this may be a limitation since ligament degeneration is unlikely to be an isolated event and not influencing degeneration of other ligaments. Considering this aspect, further simulations were performed in which all ligaments were degenerated in the same proportion, since there is no information about which ligaments degenerate together and in which way. However, this remains an

[1] Results to be presented in further sections of this thesis (section 4.2.1).

approximation as it is also not very likely for all ligaments to degenerate exactly at the same time and in the same proportion.

4.2 Results and Discussion

The results of the simulations are reported in two levels of analysis. First, ligament removal outcomes are presented for the healthy and degenerated models. Second, the biomechanical behaviour of the lumbar spine with degenerated ligaments is presented. For both cases, the main outcome of the simulations was ROM evolution, namely ROM relative changes. The numerical prediction of ROM variation was performed to evaluate the instability of the spine and the influence of each ligament in the movement. The higher the ROM variation, the greater the movement restriction imposed by the ligament that was removed or degenerated. For ligament removal simulations, the stress in the ligaments was also evaluated in the intact healthy model, i.e. before removal, to understand the extent of influence of ligaments regarding load support.

4.2.1 Ligament Removal

4.2.1.1 Healthy IVDs

Table 4.4 presents the outcomes for a model with healthy IVDs and removed ligaments. In terms of AR, all ligaments presented a very low influence in the movement (almost zero influence for all cases), keeping ROM values approximately constant with sequential ligament removal. Nonetheless, FCL stood out as the ligament with the greatest impact. Regarding load-sharing, FCL was the ligament that supported the highest load, followed by PLL. The loads supported by the remaining ligaments were negligible. Figure 4.2 shows the load distribution between ligaments for the healthy intact model as a function of direction of movement.

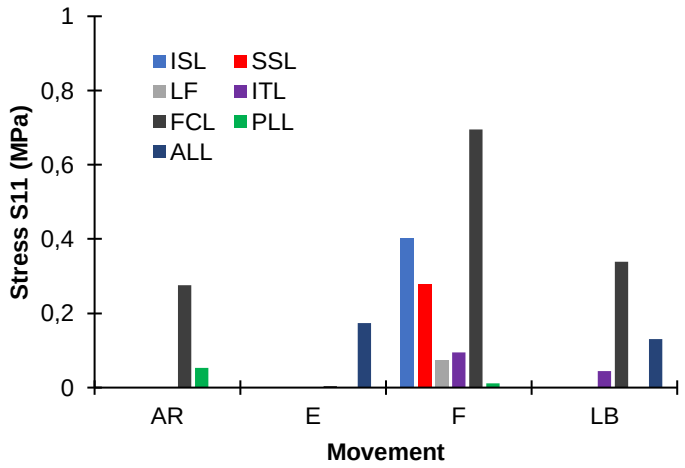

Figure 4.2: Load distribution between ligaments for the intact healthy model as a function of movement.

In the case of flexion, FCL was the ligament that influenced this movement the most, with an increase in ROM of 19.42% in case 1 and 10.91% in case 2. The remaining ligaments had a low to zero influence in the case of superficial ligaments and ALL/PLL, respectively. Due to its anatomical position, one might expect a more significant influence of PLL in flexion. However, since it might be more restricted by the vertebrae, its influence was not visible. Besides inducing the largest ROM variation upon removal, FCL was also the ligament subjected to the highest load, followed by ISL and SSL.

Table 4.4: Segmental ROM relative changes (%) measured on L3-L4 and L4-L5 levels with ligament removal as a function of movement.

			Superficial ligaments	**FCL**	**PLL**	**ALL**
AR	Case 1	L3-L4	0.00	0.63	0.05	-0.01
		L4-L5	0.00	0.45	0.00	0.00
	Case 2	L3-L4	0.00	2.34	0.03	0.00
		L4-L5	0.00	0.54	0.02	0.00
F	Case 1	L3-L4	0.11	-1.84	0.00	0.00
		L4-L5	4.86	19.42	0.00	0.00
	Case 2	L3-L4	12.85	36.26	0.58	0.00
		L4-L5	2.36	10.91	-0.14	0.00
E	Case 1	L3-L4	0.00	0.00	0.00	-0.53
		L4-L5	0.00	0.00	0.00	14.12
	Case 2	L3-L4	0.00	0.00	0.00	6.58
		L4-L5	0.00	0.00	0.00	13.78
LB	Case 1	L3-L4	0.00	0.10	0.00	-0.30
		L4-L5	0.00	2.67	0.00	9.72
	Case 2	L3-L4	0.16	6.44	0.01	7.42
		L4-L5	-0.02	1.70	0.00	9.23

Regarding extension, the only influential ligament was ALL (ROM change of 14.12% and 13.78% in cases 1 and 2, respectively). This was also the ligament subjected to the highest load before its removal, with the remaining ligaments presenting a non-significant contribution to load-sharing.

In LB, ALL was again the most restrictive ligament, with an increase in ROM of 9.72% and 9.23% upon its removal in cases 1 and 2, respectively. PLL and the superficial ligaments had no influence in the movement, and the impact of FCL was also very low. In terms of load distribution, FCL supported the highest load, followed by ALL and ITL.

In general, the relative ROM changes in case 2 were higher than analogous changes in case 1. This was expected given that the removal of ligaments in both segments (case 2) allows the movement to be less restricted. Nevertheless, there were some exceptions, which were only considered relevant if the absolute ROM difference between cases 1 and 2 was higher than 0.1 degrees. Since ROM was in the range of 0-5 degrees, a variation of 0.1 degrees was taken as a very small and negligible movement. Thus, the exceptions which were considered relevant were FCL and superficial ligaments in flexion, and

FCL and ALL in LB. What happened in these cases was that the relative ROM changes in L4-L5 level decreased when ligaments were removed from both FSUs in relation to when they were removed only from L4-L5. This was due to a compensation mechanism, in which the top motion segment (L3-L4) was not restricted by ligaments anymore and was then able to move freely, whereas the L4-L5 segment was constrained by the applied boundary conditions. Furthermore, ROM in L3-L4 level was expected to be higher due to the proximity to the point of application of the load (on the top surface of L3). In this way, it is justified, for instance, in the case of FCL in flexion, the decrease of ROM variation from 19.42% in case 1 to 10.91% in case 2, since there was a compensation in L3-L4 with an increase from -1.84% to 36.26%.

When the two levels were unrestricted, larger ROM changes in L3-L4 were evident in most cases (when compared with L4-L5), once again for the reasons presented above, mainly the constraining boundary conditions in L5. Therefore, in certain cases, the presence of the ligaments ends up having a greater influence on the restriction of movement when analysing the L3-L4 segment, compared to what was expected with an analysis focused on L4-L5. This was verified for instance for the superficial ligaments in flexion (ROM change of 12.85% in L3-L4 compared with 2.36% in L4-L5), and also for FCL in LB (ROM change of 6.44% in L3-L4 compared with 1.70% in L4-L5).

The abovementioned results are aligned with the literature. Heuer et al. [11] performed cadaveric experiments in eight L4-L5 segments and determined SSL to resist slightly in extension, ALL slightly in AR and strongly in extension, and FCL in axial rotation. In flexion, removal of SSL, ISL, and LF also resulted in a slight motion increase, but PLL was the main responsible for changes in this loading direction. In current simulations, it was confirmed the role of ALL in extension and FCL in AR. Regarding flexion, there was also an increase in ROM when superficial ligaments were transected, which is compatible with the motion increase due to SSL, ISL, and LF removal referred by Heuer et al. as ITL was not included in this study. However, the influence of PLL in flexion was not shown in the present work, as opposed to what was found by Heuer et al.. This was possibly due to the fact that, in the work by Heuer et al., PLL was removed after the transection of vertebral arches. These structures limit the motion carried by the ligament, thus enhancing the role of PLL during flexion if they are absent. Finally, the slight influences of SSL in extension and ALL in AR were also not determined in current simulations, possibly because they represent small variations that are inherent to these particular cadaveric samples and not reproducible. Moreover, the absence of ITL may also justify the referred differences.

Ellingson et al. [10] developed a FE model of the lumbar spine, from L3 to the sacrum, to determine the effects of IVD degeneration and define the role of each ligament in the movement. In this work, ligaments were removed in sets and not individually. FCL was determined the most active ligament in flexion, and ALL/PLL in extension, followed by FCL. Lateral bending was only restrained by ALL/PLL, whereas AR was primarily affected by FCL removal. Current outcomes are aligned with these findings, but were less pronounced possibly due to differences in modelling.

Finally, Zander et al. [12] explored the effects of ligament transection on intersegmental motion based on a healthy L3-L4 FE model. The strongest influence on ROM during extension and LB was exerted by ALL, and by FCL on AR, which is aligned with current results. ISL had the highest influence in flexion. Conversely, in the present work, it was FCL that led to the greatest variations in ROM in this

movement. The referred difference might be a result of distinct ligament removal processes. In the work by Zander et al., each ligament was transected separately with all others left intact, whereas in current simulations ligament transection was sequential. Therefore, the order of ligament removal may influence the outcomes as the remaining ligaments may induce different effects. Nonetheless, differences in modelling may have also contributed to outcome changes.

4.2.1.2 Degenerated IVDs

For the degenerated models, the instability of the spine will be due, not only to the removal of ligaments as in the previous case, but also to the degeneration of IVDs. In general, there was an increase in ROM in the early stages of degeneration as the effect of fibre laxity prevailed. With more advanced stages of degeneration, ROM decreased due to increased IVD stiffness. Extension was the movement in which ROM absolute values suffered the least changes with degeneration due to a larger influence of facet joints which restrict the movement. The comparison of ROM evolution between the degenerated models and the healthy case is presented next, being highlighted the main differences between them. The segmental percentages of ROM variation with ligament removal for each degenerated model are presented in detail in Appendix I for synthesis of the results.

4.2.1.2.1 Model B (H-Mild)

Model B represented the softest degenerated model, with only the IVD between L4 and L5 being mildly degenerated and L3-L4 IVD remaining in a healthy condition. Regarding this model, the main differences in relation to the healthy one (Model A) occurred in AR and flexion (Figure 4.3). In the first movement, all ligaments presented a very low influence, as in Model A, except FCL, which had a higher impact in AR, with a ROM change of 10.43% and 10.18%, in cases 1 and 2, respectively, compared with a ROM change of 0.45% and 0.54% in the healthy model.

In terms of flexion, the trend for Model B in case 2 was significantly different from the one of Model A, as the ligament that previously presented the highest influence (FCL), with a ROM change of 10.91%, had a low impact on the movement, with a ROM change of only 3.01%. However, if the focus is turned to an L3-L4 ROM analysis, ROM changes were similar in both Models A and B, indicating that this loss of influence of FCL in flexion for Model B was most likely due to the degeneration of the L4-L5 FSU. In fact, the loads supported by the remaining ligaments increased from an average of 2.52^{-12} MPa in the healthy model to 4.23^{-11} MPa in the degenerated model in the case of ALL, and from 1.19^{-12} MPa to 3.66^{-2} MPa for PLL. This may lead to an increase in ligament resistance and consequent motion restriction despite FCL removal. Considering case 1, in which ligaments were only removed from L4-L5 level, the trend for flexion was very similar to the healthy case, with FCL being the most active ligament (ROM change of 20.99%, compared with 19.42% in Model A). This was possibly because L3-L4 FSU was restricted and, therefore, only the L4-L5 segment could move freely, despite the degeneration restrictions. In the previous case (case 2), L3-L4 FSU was also able to move, and, consequently, the degeneration effects restricting L4-L5 were more evident. The compensation mechanism between L3-L4 and L4-L5 levels was still present for the removal of superficial ligaments and FCL.

Regarding extension, the trend was similar for both models in both cases 1 and 2. All ligaments presented no influence in the movement except for ALL, which was the most active ligament in extension. Nevertheless, the variation in ROM was lower in Model B (9.04% and 8.84% for cases 1 and 2 in L4-L5, respectively) when compared with Model A (14.12% and 13.78%, for cases 1 and 2 in L4-L5, respectively). In Model B, the L4-L5 IVD was degenerated and, consequently, there was less impact with ligament removal in this particular movement. Furthermore, this decrease in influence of ALL in extension was also felt in L3-L4 level. Although in this particular model L3-L4 IVD remained healthy, there was a decrease in ROM change from 6.58% to 1.95% from the healthy to the degenerated model, indicating a possible influence of the adjacent degenerated level in motion restriction.

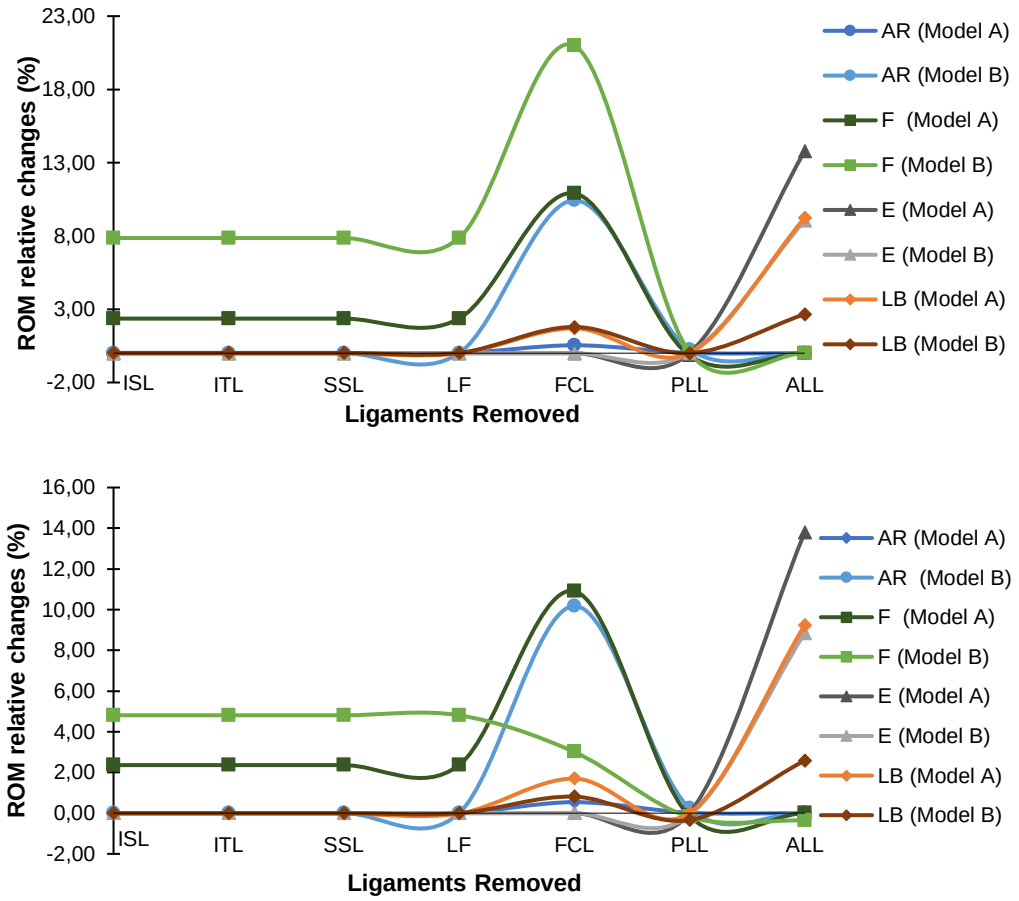

Figure 4.3: Evolution of relative ROM changes with sequential ligament removal, for cases 1 (top), and 2 (bottom). Comparison between models A and B as a function of movement.

As for lateral bending, the trend for both models was very similar, with ALL being the most active ligament. However, the relative ROM changes for ALL removal in Model B were not significant, meaning that the impact of this ligament in LB was reduced from the healthy to the degenerated model. There was a decrease in ROM change from 9.72% and 9.23%, to 2.66% and 2.58%, for cases 1 and 2, respectively. In terms of L3-L4 analysis, there was an increase in ROM change for FCL and PLL removal relative to Model A, possibly indicating a compensation mechanism for the decrease in L4-L5 segment.

This phenomenon was also verified for FCL and superficial ligaments in flexion, as already happened in the healthy model.

4.2.1.2.2 Model C (Mild-Mild)

In Model C, both IVDs were mildly degenerated, being the stage of degeneration of L4-L5 IVD the same as in the previous model. Therefore, the evolution of ROM with ligament removal was very similar for both models B and C when considering removal only at L4-L5 level (case 1), since ROM is highly influenced by IVD degeneration. As before in Model B, ALL was the most active ligament in extension (ROM change of 9.15%), but with a lower impact when compared with the healthy model. FCL was the most active ligament in AR and flexion (ROM change of 9.72% and 19.82%, respectively), and in LB there was no significant influence from any ligament.

Regarding case 2, ligament removal occurred in both levels, thus inducing larger ROM variations relative to the healthy model as the effects of L3-L4 IVD degeneration were also felt. Similar to Model B, FCL played an active role in AR (ROM change of 8.12%), being this one of the main differences from the healthy model. Nonetheless, in Model C, the variations of ROM induced in L3-L4 level when FCL was removed were also significant (ROM change of 17.68%), which did not happen in the previous degenerated model in which L3-L4 IVD was healthy.

The main difference of this model in relation to the previous degenerated model occurred for the flexion movement. In this case, FCL was still the most active ligament in flexion, but the variation of ROM that was induced in L4-L5 upon FCL's removal was negative, meaning that, when FCL was removed, ROM decreased in relation to the previous removal stage. Due to the multifactorial nature of IVD degeneration and ligament removal, the remaining ligaments were subjected to higher loads. Consequently, their resistance may have increased, restricting the movement when FCL was removed, similarly to what has occurred in Model B. The load supported by ALL increased from an average of 2.52^{-12} MPa in the healthy model to 4.60^{-11} MPa in the degenerated model. Similarly, the load supported by PLL increased from 1.19^{-12} MPa to 3.31^{-2} MPa. Although the loads acting on ALL and PLL were similar to the previous degenerated model, the motion restriction with FCL removal was much more pronounced, possibly indicating an influence of L3-L4 degeneration on the adjacent level, as this was the only difference between the two models. In L3-L4 FSU, there was a compensation mechanism with a ROM increase of 31.20%. This compensation mechanism was also felt with the removal of superficial ligaments as before. In this case, the motion accumulated in L3-L4 was higher (ROM change of 17.30% compared with 13.19% in Model B), since the motion carried by L4-L5 FSU decreased with advanced degeneration.

In terms of extension, ALL remained the ligament with the most influence, with a ROM change of 8.97% similar to Model B. In LB, ROM variations were comparable to the previous degenerated model.

Finally, it was possible to conclude that the mild degeneration of L3-L4 IVD did not have a great impact on ROM evolution as the outcomes were very similar – with the exception of FCL's influence in flexion – to the previous model with healthy L3-L4 IVD and L4-L5 IVD mildly degenerated. Figure 4.4 illustrates the evolution of ROM change with ligament removal, for both models A and C, as a function of movement.

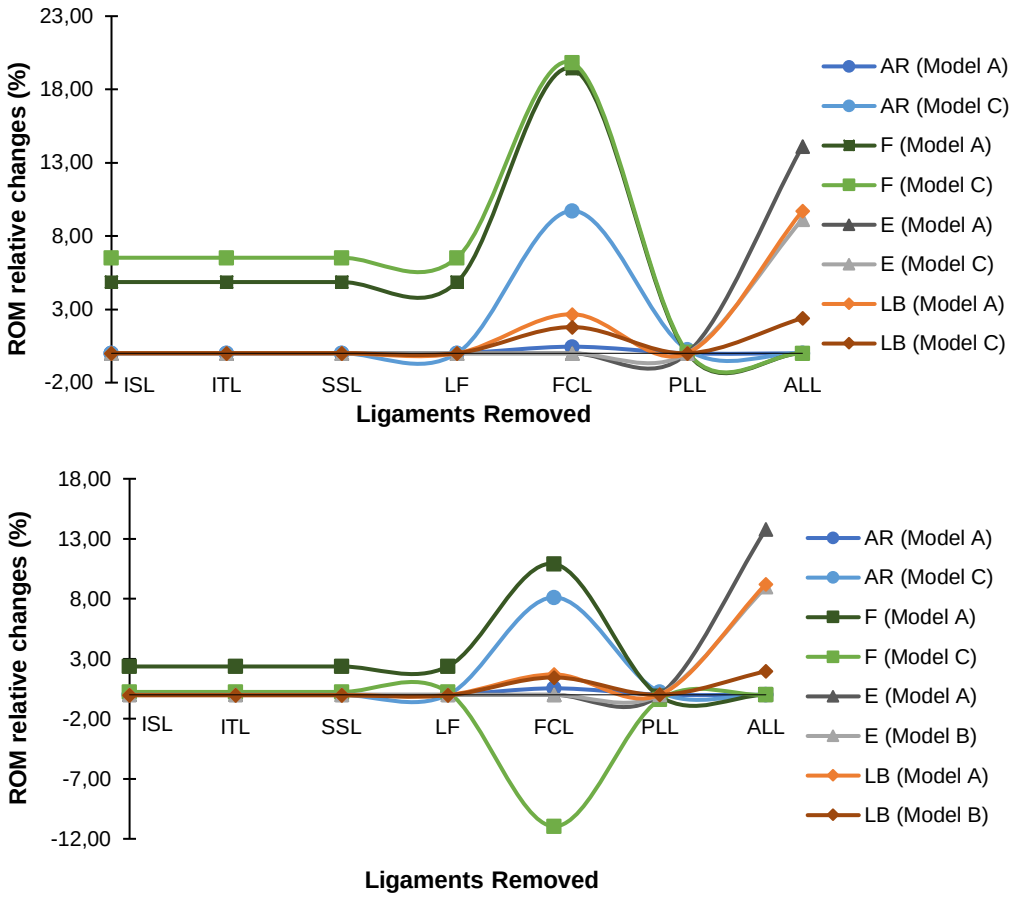

Figure 4.4: Evolution of relative ROM changes with sequential ligament removal, for cases 1 (top), and 2 (bottom). Comparison between models A and C as a function of movement.

4.2.1.2.3 Model D (Mild-Mod)

Model D represented the highest degenerated model, with L4-L5 IVD moderately degenerated and L3-L4 IVD in a mild stage of degeneration. Although this was the only model with advanced degeneration at L4-L5 level, the evolution of ROM was similar to previous models. Regarding AR and flexion, FCL remained the ligament that most affected the movement, with ROM change of 8.67% and 7.51% in AR, and 16.84% and -11.80 % in flexion, for cases 1 and 2, respectively. However, in terms of flexion in case 2, similarly to what occurred in Model C, the induced variation was negative, leading to a decrease in L4-L5 ROM when FCL was removed and a compensation mechanism in L3-L4 (ROM change of 44.44%). Also for AR, the compensation mechanism was maintained. Regarding extension, ALL remained the most active ligament in this movement in both cases 1 and 2. Finally, in terms of LB, all ligaments presented a low influence on the movement. Nonetheless, there was a slight increase in ROM when ALL was removed compared with the previous model (ROM change of 4.01% and 3.65%, in cases 1 and 2, respectively).

Figure 4.5. illustrates the evolution of ROM change with ligament removal, for comparison between models A and D as a function of movement.

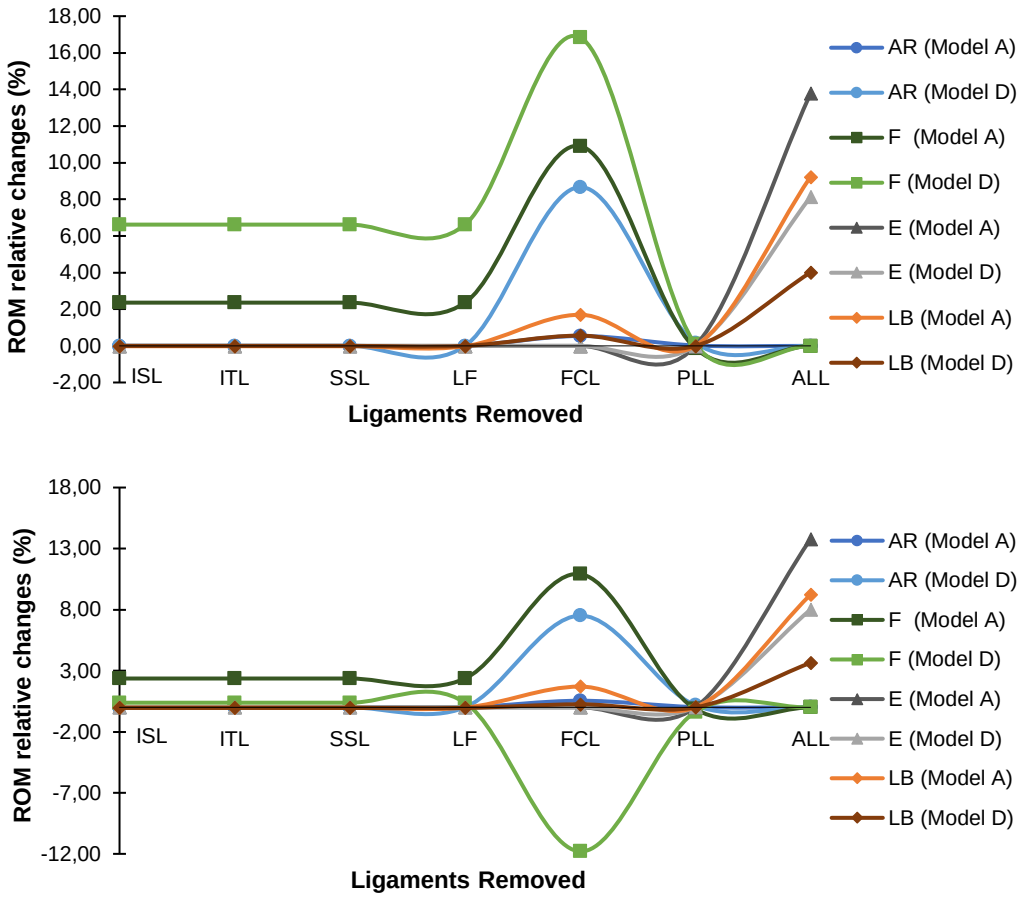

Figure 4.5: Evolution of relative ROM changes with sequential ligament removal, for cases 1 (top), and 2 (bottom). Comparison between models A and D as a function of movement.

4.2.2 Ligament Degeneration

Besides ligament removal, ligament degeneration must be considered when evaluating spine stability. Regarding the first ligament degeneration stage (Mild-Mild), it was verified a slight increase in ROM for flexion and AR movements when only FCL was degenerated (ROM change of 3.58% and 2.38%, respectively). Since the stiffness of this ligament was reduced by 25%, a slight increase in mobility in the referred directions was expectable, considering that, in previous simulations, FCL removal led to significant positive ROM variations in these directions. When it comes to extension, considering previous simulations, ALL should be the ligament to have the most impact in the movement, and this was in fact verified (Table 4.5). When FCL and ALL were degenerated simultaneously (FCL + ALL), what was verified was that, for each movement, the ROM value was equal to the case in which only the ligament with greater influence in that particular movement was degenerated. In other words, in flexion and AR, ROM was equal to the case in which FCL was degenerated and, in extension, ROM was the same as in the case where ALL suffered degeneration. This occurred for every degeneration stage and validates the finding that FCL did not have any influence in extension, and the same for ALL in the case of flexion and AR. Furthermore, it is an indicator that, although FCL and ALL were degenerated in the

same stage, there was no relation between them, i.e. the movement of one did not restrict or facilitate the movement of the other.

Table 4.5: Global ROM values (in deg) with 25% mild ligament degeneration as a function of movement. Between brackets are the per cent changes in relation to the healthy model.

	Healthy	FCL	ALL	FCL + ALL	All
E	4.22	4.22 (0.00%)	4.24 (0.56%)	4.24 (0.56%)	4.24 (0.56%)
F	3.31	3.43 (3.58%)	3.31 (0.00%)	3.43 (3.58%)	3.53 (6.47%)
AR	6.10	6.24 (2.38%)	6.10 (0.00%)	6.24 (2.38%)	6.24 (2.42%)

Finally, when comparing the results from the simulations in which FCL and ALL were degenerated as a set with the ones from the simulations in which all ligaments were degenerated simultaneously, it was interesting to notice that ROM variations were very similar, validating the conclusions of ALL and FCL being the only ligaments with significant impact in the movement. Nonetheless, in terms of flexion, comparing the outcomes of FCL degeneration (ROM change of 3.58%) with the ones of overall degeneration (ROM change of 6.47%), the difference between them was significantly higher than for other movements. This is an indicator that, for this particular motion, – besides FCL that is the dominant ligament – the remaining ligaments also have small contributions that become significant when added. This situation became even more evident as the percentage of ligament degeneration was increased, given that every ligament was less stiff and more prone to move.

When considering the same ligament degeneration stage (Mild-Mild, with decreased stiffness), but in a model with advanced IVD degeneration in L4-L5 level (Mild-Moderate), the same trends were verified, with FCL and ALL being the most active ligaments in flexion and AR, and extension, respectively. For most cases, it was verified that ROM relative changes were slightly higher for this model than for the one with mildly degenerated IVD, considering L4-L5 level. This indicates that IVD degeneration influenced the degeneration of ligaments, reinforcing the idea that the IVDs degenerate first and most likely lead to later ligament degeneration. Regarding L3-L4 FSU, ROM variation was approximately the same as the one in the model with both IVDs mildly degenerated given that the stage of IVD degeneration at this level remained the same.

Regarding the second degeneration stage (Mild-Moderate), the analysis was focused on L4-L5 level in which ligament stiffness was increased. In this case, FCL and ALL remained the ligaments with greatest influence in the movement, but this time inducing negative ROM changes since there was more restriction to the movement due to ligament stiffening. This effect was more evident for FCL degeneration, as the influence of this ligament in the movement was always the highest. In L3-L4 level, the outcomes were in general very similar to the previous case, since IVD and ligament degeneration in this level were the same as before. However, there were some cases in which ROM variation slightly increased from the model with mildly degenerated ligaments, highlighting the effect of L4-L5 ligament degeneration on the adjacent level. This effect was more pronounced for higher percentages of ligament degeneration. Table 4.6 presents the ROM values for the second stage of ligament degeneration as a function of movement.

Table 4.6: L4-L5 ROM values (in deg) with 25% moderate ligament degeneration as a function of movement. Between brackets are the per cent changes in relation to the healthy model.

	Healthy	FCL	ALL	FCL + ALL	All
E	2.34	2.34 (0.00%)	2.32 (-0.70%)	2.32 (-0.70%)	2.32 (-0.70%)
F	0.73	0.70 (-3.71%)	0.73 (0.00%)	0.70 (-3.71%)	0.69 (-5.96%)
AR	2.59	2.56 (-1.49%)	2.60 (0.00%)	2.56 (-1.49%)	2.56 (-1.51%)

As degeneration became more pronounced, i.e. the variation in ligament stiffness increased, there was a general increase in ROM relative changes in the first stage of degeneration, when compared to the model with no ligament degeneration. This means that, as degeneration became more evident, there was a higher range of motion allowed due to lower ligament restriction. Table 4.7 presents the ROM values of the model with 50 and 75% mild ligament degeneration. With a 75% reduction in stiffness, degeneration was obviously more marked than with a 50% reduction, so the increase in ROM was greater.

Table 4.7: Global ROM values (in deg) with 50% and 75% mild ligament degeneration as a function of movement. Between brackets are the per cent changes in relation to the healthy model.

Degeneration	Movement	Healthy	FCL	ALL	All
50%	E	4.22	4.22 (0.00%)	4.28 (1.44%)	4.28 (1.44%)
	F	3.31	3.57 (7.80%)	3.31 (0.00%)	3.82 (15.25%)
	AR	6.10	6.41 (5.21%)	6.70 (0.00%)	6.42 (5.39%)
75%	E	4.22	4.22 (0.00%)	4.34 (2.98%)	4.34 (2.98%)
	F	3.31	3.74 (12.81%)	3.31 (0.00%)	4.23 (27.61%)
	AR	6.10	6.62 (8.57%)	6.70 (0.00%)	6.64 (8.99%)

Nevertheless, there was an exception that occurred for the flexion movement in L4-L5 level when all ligaments were degenerated. What happened in this case was that ROM variation decreased as degeneration increased, even becoming negative with a 75% degeneration, indicating that there was a strong restriction of movement in this level (Table 4.8). When only FCL was degenerated, the first-mentioned observations were maintained, in which the decreased stiffness in the ligament enabled a looser movement. However, if the remaining ligaments were degenerated at the same time, they possibly exerted force in the opposite direction so that the movement was more restricted in the end. As so, a compensation mechanism occurred at L3-L4 level with a considerable increase in ROM when compared to an analogous situation with no IVD or ligament degeneration.

In the second degeneration stage, there was again an increase in ROM relative changes as the percentage of ligament degeneration progressed. However, in this case, ROM relative changes became more negative, with an analysis focused on L4-L5, since ligament stiffness was increased and, consequently, a higher restriction of motion was verified (Table 4.9). Regarding L3-L4 level, the effects of adjacent ligament degeneration were also felt, as previously mentioned, with a slight increase in ROM relative changes in relation to the previous stage. Regarding active ligaments, the same trends were

verified as in the 25% degeneration case for both stages, with ALL and FCL being those with greatest influence.

Table 4.8: L4-L5 ROM values (in deg) with 75% mild ligament degeneration as a function of movement. Between brackets are the per cent changes in relation to the healthy model.

	Healthy	FCL	ALL	All
E	2.31	2.31 (0.00%)	2.41 (4.05%)	2.41 (4.05%)
F	1.03	1.04 (0.68%)	1.03 (0.00%)	1.00 (-2.62%)
AR	2.76	2.92 (5.61%)	2.76 (0.00%)	2.92 (5.66%)

Table 4.9: L4-L5 ROM values (in deg) with 50% and 75% moderate ligament degeneration as a function of movement. Between brackets are the per cent changes in relation to the healthy model.

Degeneration	Movement	Healthy	FCL	ALL	All
50%	E	2.34	2.34 (0.00%)	2.31 (-1.23%)	2.31 (-1.23%)
	F	0.73	0.67 (-7.45%)	0.73 (0.00%)	0.64 (-12.25%)
	AR	2.59	2.52 (-2.26%)	2.59 (0.00%)	2.52 (-2.79%)
75%	E	2.34	2.34 (0.00%)	2.30 (-1.66%)	2.21 (-5.44%)
	F	0.73	0.64 (-11.31%)	0.73 (0.00%)	0.58 (-19.53%)
	AR	2.59	2.49 (-3.85%)	2.59 (0.00%)	2.49 (-3.89%)

4.3 Discussion Summary

This first part of the current study investigated the individual biomechanical effects of sequential ligament removal combined with IVD degeneration, as well as the impact ligament degeneration in each movement. This is extremely useful to understand if a given biomechanical response is triggered by ligament removal/degeneration or implant insertion.

In terms of AR, all ligaments presented almost zero influence in the movement, whereas in flexion FCL was the ligament responsible for the highest ROM change. This is in agreement with Ellingson et al. [10] and other studies that reported FCL as one of the main active ligaments in flexion [73], [93]. ALL was the ligament that influenced extension the most, whereas PLL and the remaining ligaments had no impact on this movement. This is in line with Heuer et al. [11] that reported a lack of influence of PLL in extension, and other studies that highlight the significant mechanical role of ALL in extension [2], [12], [72]. Similarly to AR, in terms of LB, all ligaments presented a low influence in movement restriction, with the exception of ALL.

When comparing the outcomes between cases 1 and 2, ROM changes in case 2 were higher than analogous changes in case 1, which is justified by less restricted movement occurring when ligaments are removed from all levels (case 2). However, there were a few exceptions in which the opposite occurred, i.e. in which ROM changes in L4-L5 decreased from case 1 to case 2. This was due to the boundary conditions applied in L5, which limited the motion of L4-L5. Therefore, when the two levels were unrestricted, L3-L4 FSU could move freely and accumulated the movement that L4-L5 could

not perform. This suggests a compensation mechanism between both segments and justifies the larger ROM changes in L3-L4 relatively to analogous changes in L4-L5.

Considering IVD degeneration, the outcomes were slightly different relatively to the healthy model. In general, there was an increase in ROM in the early stages of degeneration, as the effect of fibre laxity prevailed. With more advanced stages of degeneration, ROM decreased due to increased IVD stiffness. In AR, FCL presented in this case a significant impact in the movement, with a ROM change of around 10% in the degenerated models compared with less than 1% in the healthy model. In extension, ALL remained the most active ligament. However, its influence was decreased with progressive degeneration since there was a decrease in mobility and less impact with ligament removal. Regarding LB, similarly to extension, ALL remained the ligament with most impact, but in the degenerated models there was a decrease in its influence. Since ROM was already increased due to IVD degeneration, the increase due to ligament removal could not be as pronounced to prevent excessive motion. ROM absolute values in the ALL removal stage were very similar across the various degenerated models, which suggests that these work in fact like an upper limit to the movement. Therefore, in cases of mild degeneration, in which the increase in ROM due to fibre laxity was higher, the increase due to ALL removal was lower. In cases with more advanced degeneration, since IVD stiffness led to a decrease in ROM, removing ALL increased ROM change. Finally, when it comes to flexion, this was the movement that led to the most different outcomes across degenerated models, but with FCL as the most restrictive ligament in every case. Comparing the multiple degenerated models, it was also possible to verify that IVD degeneration and motion restriction may be highly influenced by adjacent levels.

Ligament degeneration is also an intricate process that alters spine stability, and the selected approach in this study was to implement changes in ligament stiffness. Ligament degeneration was assumed to follow IVD degeneration and considered a process composed of two stages, first with a decrease and then with an increase in stiffness. In the first stage, there was a slight increase in ROM, for flexion and AR when FCL was degenerated, and for extension when ALL was degenerated. When all ligaments were degenerated, ROM variations were very similar to the previous simulations, confirming that ALL and FCL were ruling the movement. If higher percentages of degeneration were considered, an increase in ROM relative changes was verified due to lower ligament restriction. In the second stage, FCL and ALL remained the most active ligaments in flexion and AR, and extension, respectively, but this time inducing negative ROM changes since ligament stiffness increased and the motion was hampered. These negative ROM changes became more pronounced as the percentage of ligament degeneration was increased. In L3-L4 FSU, the outcomes were very similar throughout every simulation given that the stage of IVD degeneration in this level was always the same. However, when degeneration in L4-L5 IVD was more advanced, ROM changes slightly increased, highlighting the influence of adjacent degeneration.

When comparing the outcomes between models with different IVD degeneration, it was verified that ROM relative changes with mild ligament degeneration were slightly higher in the model with the most advanced stage of IVD degeneration. This indicates that ligament degeneration is influenced by IVD degeneration.

Chapter 5

Part II – Morphological Degeneration and Spinal Fusion

In the second part of this work, and based on the knowledge obtained in the previous part, the intention was to apply the variations of IVD and ligament degeneration in a new FE model with degeneration also at a morphological level, namely IVD height reduction. The goal was to assess the impact of geometric changes in the results. Moreover, simulations were performed with the introduction of OLIF instrumentation to determine the more advantageous type of posterior fixation and the role of ligaments in the intervened level, as these results can benefit the clinical practice. Finally, changes at the adjacent level were evaluated to identify, between instrument placement and degeneration of the pre-instrumented level, which is the major contributing factor for adjacent IVD degeneration.

This chapter includes the Methodology, Model Validation, Results, and Discussion regarding the numerical simulations abovementioned.

5.1 Materials and Methods

This section describes the construction details of the new L3-L5 model with morphological degeneration, as well as the reasoning behind some modelling decisions undertaken in this work. It also includes the description of the degenerated and instrumented models.

5.1.1 Intact Model

The intact model was constructed based on CT scans from a 78-year-old woman, available on the xVertSeg Database from the Laboratory of Imaging Technologies (University of Ljubljana, Faculty of Electrical Engineering, Slovenia) [94]. This particular set of images was chosen due to the reduced IVD height presented by this subject, as well as the significantly reduced level of lordosis. These are good indicators of IVD degeneration and, therefore, of an unhealthy spine that may benefit from the introduction of spinal cages.

Proceeding with model construction, the three vertebrae from L3 to L5 were reconstructed through image segmentation using ITK-SNAP® [95]. Since in CT scans the IVDs are not visible, these had to be posteriorly introduced in SolidWorks® (Dassault Systèmes SolidWorks Corp., USA), having as reference the space that appears between adjacent vertebrae in the CT images. This model was exported in .stl format and imported in MeshLab® [96] for decimation, as the ITK-SNAP® generated mesh was too complex to be properly supported by SolidWorks®. A 20% decimation was applied and again a 3D model in .stl format was obtained. The next step was the import of the model in SolidWorks® as a .stl solid body. In this software, the original body was decomposed into three separate vertebrae,

mimicking the facet joint between the inferior and superior articular processes through the introduction of a 1 mm gap. In the literature, this gap ranges between 0.1 - 0.5 mm [7], [9], [10], [72]. However, the thin layer of articular cartilage that covers the joint should also be considered, leading to a higher distance between the two processes. Since in this model, as an approximation, the articular cartilage was not considered, a higher gap value was used. Figure 5.1 illustrates the workflow for the development of the FE model.

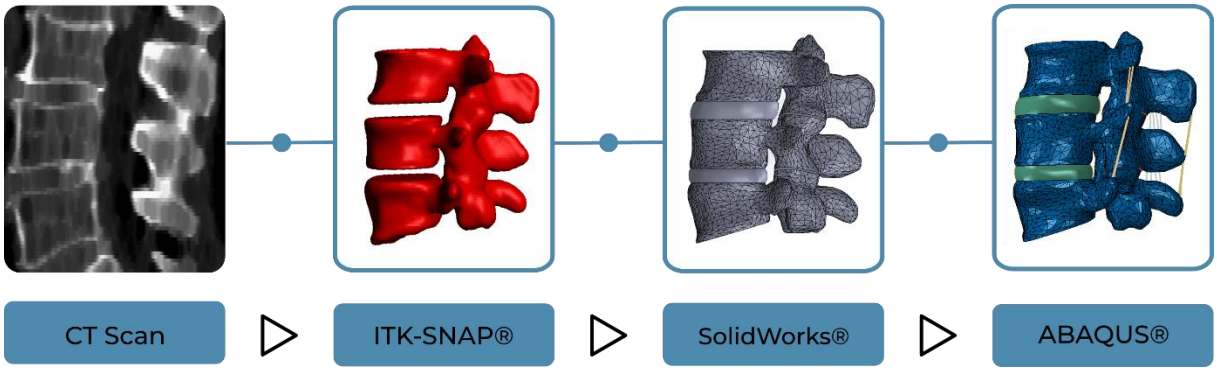

Figure 5.1: Flowchart illustrating the process of FE model construction.

As previously mentioned, the IVDs were also introduced in SolidWorks®. For the IVD between L3 and L4, this was achieved by copying the outline of the bottom surface of L3 and the top surface of L4 onto a transverse plane immediately below the bottom of L3 and above the top of L4, respectively. Then, a loft was created between the two sketches, with 3D guide curves to define the lateral bulging profile of the IVD. Finally, with the split tool, the IVD was divided into AF and NP, each representing 70% and 30% of the whole structure, respectively. The same process was then applied to the IVD between L4 and L5. An example of an IVD and a vertebra is presented in Figure 5.2.

Figure 5.2: Sagittal view of two parts of the 3D L3-L5 model: L5 vertebra (left) and L3-L4 IVD (right).

The separation between cortical and trabecular bone was also performed in SolidWorks®. The first step was the estimation of the average thickness of cortical bone of each vertebra from the CT scans. Then, in SolidWorks®, three new parts were created, corresponding to the core of trabecular bone of each vertebra. These were created, similarly to the IVDs, by copying the outline of the top and bottom surfaces of the vertebra to transversal planes immediately above and below the vertebra,

respectively. From these sketches, an offset equal to the average thickness of cortical bone was applied, representing the cortical bone of each vertebra. Then, a loft was created between the top and bottom sketches with 3D guide curves to define the profile of the VB. In the end, a cavity operation was performed to subtract the newly created vertebral bodies of trabecular bone to the vertebrae in order to create a cortical shell for each one.

The final model was composed of three vertebra (separated in trabecular and cortical bone) and two IVDs. The dimensions of every part are reported in Tables 5.1 and 5.2. The model was then imported as *Parasolid* to ABAQUS® (Dassault Systèmes Simulia Corp., USA) for FE analysis (Figure 5.3).

Table 5.1: Dimensions of the vertebral bodies.

Vertebra	Lateral diameter (mm)	Sagittal diameter (mm)	Anterior height (mm)	Posterior height (mm)
L3	51.51	35.18	23.64	23.64
L4	54.32	37.48	22.87	22.87
L5	59.01	33.83	27.98	18.09

Table 5.2: Dimensions of the two IVDs.

Level	Anterior height (mm)	Posterior height (mm)	Total Area (mm^2)	NP's Area (mm^2)
L3-L4	8.44	8.44	1212.31	594.61
L4-L5	6.64	6.64	1309.08	524.39

In ABAQUS®, the same material properties as in Part I were assigned to each model component based on previous work [82]. The model was considered rigidly bonded using the merge tool, retaining intersecting boundaries. The next step was the orientation of AF fibres, which was established through the definition of a material orientation of type *discrete* for each AF. Fibres were oriented at 35 or 145 degrees in consecutive layers relative to the transverse plane through the definition of multiple referential systems throughout the AF. The *y-axis* was perpendicular to the top surface of the structure pointing upwards, and the *x-axis* was tangent to the outer edge of the AF pointing to the right side.

For the analysis, two steps were defined with minimum increment of 1^{-5} and maximum increment and increment size of 1. In the first step, a pre-load of 100 N [7], [85] was applied (with the option "follow nodal rotation"), and in the second step moments of 7.5 Nm were applied in different directions in order to simulate natural movements of flexion, extension, AR and LB. The loads were applied in a reference point on the top surface of L3 with a coupling interaction between point and surface for an even distribution of load. In the bottom surface of L5, a boundary condition of type *encastre* was defined.

Regarding interactions, to prevent intersection, a surface-to-surface contact was defined between facet joints, choosing a soft normal contact with exponential pressure-overclosure option. The contact parameters to fit the exponential curve were pressure of 50 N/mm^2 and clearance of 1 mm [97]. This

means that, when the distance between facet joints is lower than 1 mm, a contact pressure arises, increasing exponentially as distance decreases, and reaching 50 N/mm^2 when the distance is zero.

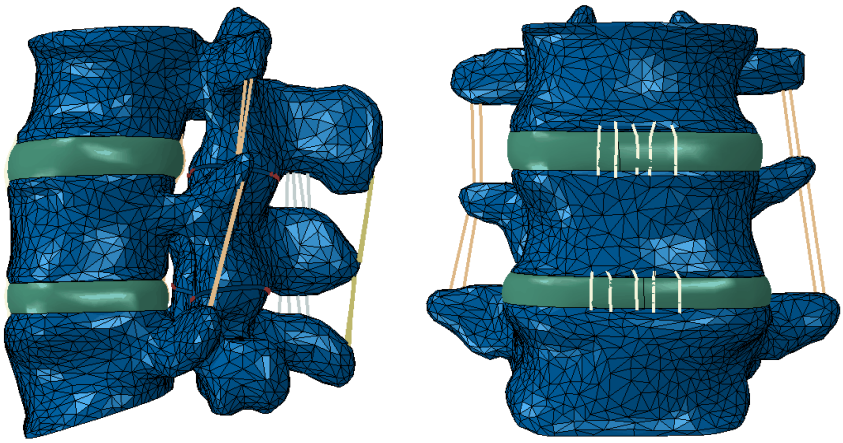

Figure 5.3: Sagittal (left) and frontal (right) views of the intact L3-L5 FE model.

For the mesh generation, the first step was the selection of the *virtual topology* option, with default parameters, to eliminate small edges and faces that would result in non-uniform mesh elements. Then, to take into account abrupt transitions of stiffness in the model, the mesh of the IVDs was refined, whereas, in the region of trabecular bone inside the model, the mesh could be less refined. Thus, a general *global seed* size of 2.2 mm was defined, and then seed edges of 1.5 mm on IVDs and 3 mm on the trabecular bone were added. These size values were chosen according to a convergence analysis presented later in section 5.2. The final mesh consisted of 230 051 elements of type C3D10 and 334 481 nodes. The element type chosen was quadratic tetrahedral, as this is the typical element type for models based on medical images.

The final step of model construction was the introduction of ligaments. The model included the seven major ligaments of the lumbar spine: ALL, PLL, LF, ISL, ITL, SSL, and FCL, modelled as tension-only linear elastic wires between two nodes. The design of these structures, as well as the choice of their insertion points, were based on the literature [98]. Table 5.3 shows the ligament design, namely the number of elements for each ligament.

Table 5.3: Ligament design with number of elements per ligament.

Ligament	Design
ALL	5 parallel wires, each with 7 in series
PLL	3 parallel wires, each with 7 in series
FCL	8 parallel wires (on each side)
LF	3 parallel wires
ISL	4 parallel wires
ITL	2 parallel wires (on each side)
SSL	3 parallel wires

In order to enforce an attachment between ligaments and the L3-L5 segments and avoid loosened or deformed structures, coupling interactions were defined at the insertion points with an influence radius of 2. This also ensures that forces are evenly distributed on the surface, as occurs in a real human spine. Finally, these elements were meshed as truss elements of type T3D2, with an element size that ensures that only one element per ligament is created. The final model was then composed of 230 051 C3D10 elements and 172 T3D2 elements.

5.1.2 Degenerated Models

To include degenerative changes apart from the intrinsic IVD height reduction, the intact model presented in the previous section was modified. In a first analysis, only IVDs were degenerated, following the same principles used in Part I, described in section 4.1.2. Material properties of AF and NP were altered, creating four models with different combinations of IVD degeneration (apart from the healthy one). L3-L4 IVD was mildly degenerated at most due to the height difference in relation to L4-L5 IVD. It is worth noticing that, for the present FE model, it is not clinically significant to have both IVDs in a healthy condition (H-H model). In reality, due to the geometry of the model and evident height reduction in L4-L5 FSU, at least this particular IVD must be degenerated. Nonetheless, this model is still interesting from a numerical point of view, and to be used as benchmark.

For ligament degeneration, the same methodology described in section 4.1.3 was applied. However, in this case, only the Mild-Mod model was used to study both stages of ligament degeneration as it is clear that, due to the differences in IVD height, L4-L5 IVD must have a higher degree of degeneration than the one of L3-L4 IVD.

Table 5.4 summarises the degenerated models that were developed to study the impact of different degenerative changes.

Table 5.4: Summary of all FE models used to study the effects of degeneration.

Degeneration	**Models**				
IVD Degeneration	Healthy – Healthy (H-H)	Healthy – Mild (H-Mild)	Mild – Mild	Healthy – Mod (H-Mod)	Mild - Mod
Ligament Degeneration	×	×	×	×	✓

5.1.3 Instrumented Models

From the intact model, four instrumented models were constructed to simulate the OLIF procedure and evaluate the influence of posterior fixation: stand-alone cage model (SA), model with left unilateral posterior fixation (LUPF), model with right unilateral posterior fixation (RUPF), and model with bilateral posterior fixation (BPF). The OLIF approach was chosen as it is widely used in clinical practice and provides good clinical results. For that, the L4-L5 IVD was removed in SolidWorks® – as this was the most degenerated IVD – and a CLYDESDALE® cage system (CLYDESDALE Spinal System;

Medtronic Sofamor Danek USA, Inc., Memphis, Tennessee, USA) was introduced in its place, virtually mimicking the OLIF surgical procedure [99]. This represents the cage-only instrumented model, without posterior fixation, i.e. the SA model. For the models with posterior fixation, additional screws were added through the right and/or left pedicles with a rod connecting them, simulating unilateral or bilateral fixations (Figure 5.4).

The models of the cage, rod, and screws were adapted from previous work [100]. The height, width, and length of the OLIF cage were 8 mm, 22 mm, and 50 mm, respectively. The length and diameter of the pedicle screws were 55 mm and 5.5 mm, respectively. The diameter of the rod was the same as the screws [99].

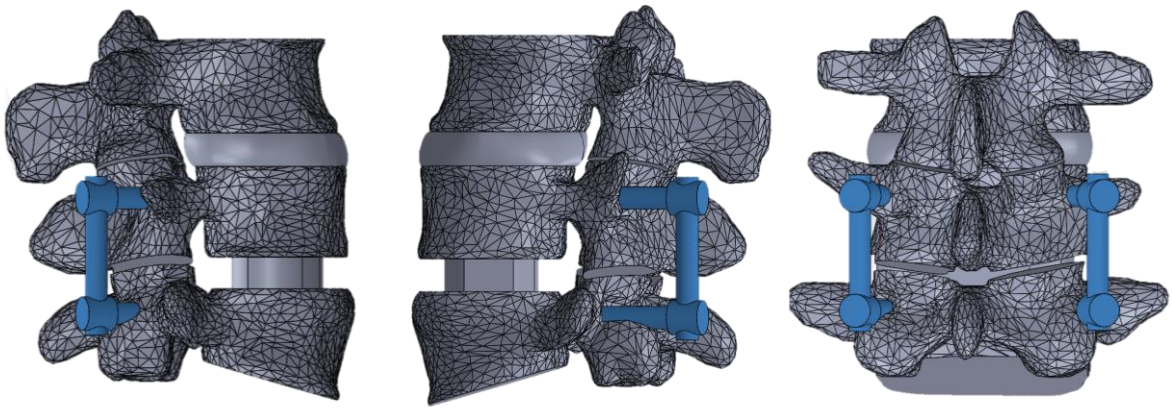

(a) (b) (c)

Figure 5.4: Instrumented models with different posterior fixation systems: (a) right unilateral pedicle screw, (b) left unilateral pedicle screw, and (c) bilateral pedicle screw.

The instrumented models were then imported to ABAQUS® and the same process as in the intact model was followed, with the exception that this time two different analyses were required to evaluate the biomechanical impact of the cage: short-term and long-term analyses. These led to differences in the interaction between cage and vertebrae. In the short term, bone-screw interactions were modelled as being fully bonded with a *tie* constraint, while cage-bone interactions were defined as surface-to-surface contact with a friction coefficient of 0.8, selecting the option *penalty* in the friction formulation of tangential behaviour. The definition of this high friction coefficient allows the simulation of the serrated surface of the cage, which was not included in the SolidWorks® model as an approximation, to simplify the model and reduce simulation times and critical stress points [55]. In the long term, cage and posterior fixation are completely osseointegrated in the spine and there is no relative motion between them. As such, all model components were assumed to be rigidly bonded using the merge tool, mimicking the bone ingrowth and vertebral fusion that occurs.

Material properties were also assigned to each instrumentation component, being the cage composed of PEEK and the rod and screws of a titanium alloy. Table 5.5 summarises the material properties of these components. Degeneration was also included in the instrumented models by altering the material properties of the L3-L4 IVD, similarly to what occurred in the intact degenerated models (in

section 5.1.2). Since L3-L4 IVD does not have evident reduced height (compared with L4-L5 IVD), it was considered only mildly degenerated.

Two additional variations of the RUPF model were also constructed to test the influence of ligaments in the stabilisation of the instrumented spine: (i) with ligament removal only on the intervened L4-L5 level, and (ii) with ligament removal on both levels. These simulations have an academic-only purpose since the removal of all ligaments simultaneously is not performed in clinical practice. Nonetheless, it may lead to interesting conclusions to support the surgical approach.

Table 5.5: Material properties assigned to the instrumentation components.

Material	**Formulation**	**Parameters** [100]
PEEK	Linear Elastic	E = 3600 MPa v = 0.38
Titanium	Linear Elastic	E = 105 000 MPa v = 0.34

5.2 Validation

5.2.1 Convergence Analysis

One important aspect that must be considered before running any simulation is the choice of an appropriate element mesh size. This ensures that the final solution does not depend on the number of mesh elements, and also that the computational power is not excessively high by choosing an element size lower than the necessary. Therefore, to decide the most adequate element mesh size, a convergence analysis was performed in which different mesh sizes were tested under a compressive force of 100 N. For each mesh, the Von Mises stress was evaluated on a node on the top surface of L3. Figure 5.5 illustrates the evolution of stress as a function of the number of mesh elements, which in turn relate to the mesh size.

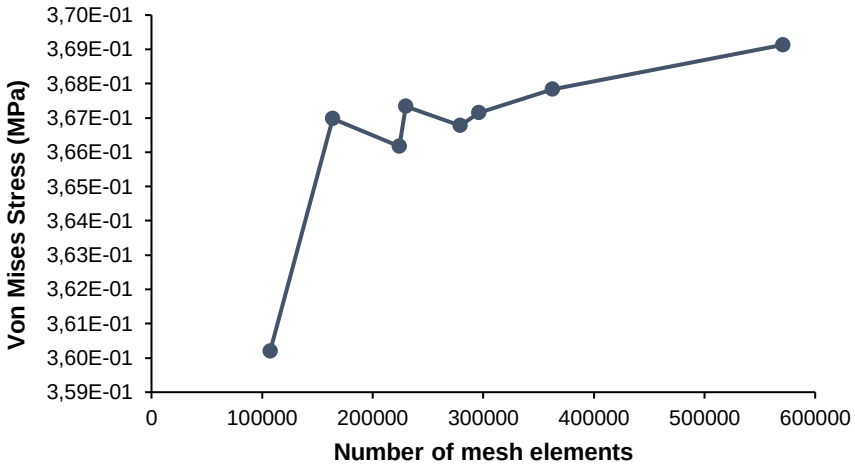

Figure 5.5: Von Mises stress on a node on the top surface of L3 as a function of the number of mesh elements.

Through the observation of the plot in Figure 5.5, it is possible to verify that stress values become more stable from a mesh size of around 300 000 elements. Nevertheless, a plateau is never reached and, therefore, the solution does not appear to converge. However, if one focuses instead on the stress variations between different meshes, it is then possible to conclude that, from a mesh size of 2.5 mm, changes between one mesh and the next are negligible (changes equal or lower than 0.35%). In this case, convergence can be accepted. Table 5.6 presents the stress values for each mesh size, as well as the respective per cent change (p.c.) between a given mesh and the following. The meshes 1.5 IVDs and 1.2 IVDs represent meshes with a *global seed size* of 2.2 mm and a refinement of 1.5 mm and 1.2 mm in the IVDs, respectively.

Table 5.6: Von Mises stress and respective per cent change as a function of the number of mesh elements.

Mesh Size	No. of Elements	Von Mises Stress (MPa)	p.c. (%)
3	107 307	3.60E-01	1.88
2.5	164 028	3.67E-01	-0.22
2.2	223 880	3.66E-01	0.32
1.5 IVDs	230 051	3.67E-01	-0.16
2	278 884	3.67E-01	0.10
1.2 IVDs	298 937	3.67E-01	0.19
1.8	362 328	3.68E-01	0.35
1.5	570 627	3.69E-01	-----

To ensure computational efficiency and quality of results, the mesh 1.5 IVDs, with 230 051 elements, was the one chosen. This was the mesh used for all models in this work, including degenerated and instrumented models.

5.2.2 Intact Model Validation

Model validation is especially useful to verify if material properties have been well assigned and if the model behaves as expected when subjected to different moments. However, it is particularly difficult to validate an unhealthy model since there are multiple cases of degeneration and each case will translate into different spine behaviours. Moreover, the effects of degeneration are often patient-specific. In this way, a healthy sample was chosen as reference for validation, remembering that there should be differences to some extent between the results.

The model was validated against the work presented by Heuer et al. [11]. In this work, eight L4-L5 spinal segments were used for *in vitro* testing, in which a stepwise anatomy reduction was performed with the aim of evaluating the biomechanical effects of each component under different loading conditions. It should be taken into account that the samples used in this study included only one spinal segment and a low degree of degeneration. Table 5.7 presents the minimum and maximum ROM values found in the work of Heuer et al. in comparison with the ROM values of the current study.

Comparing the results found in the literature [11] with the ones of the current study, it was possible to verify that the current model followed the same ROM trends as in [11], with an increase in ROM as

moment increased. However, all ROM values of the current intact model were below the minimum ROM value in the work of Heuer et al., with the exception of the values in axial rotation. This can be justified since the degenerated model with decreased IVD height suffers a loss of hydration by the NP, therefore increasing IVD stiffness [101]. In this way, the degenerated model will have a hampered motion when compared with a healthy model or with one with a lower degree of degeneration, which is the case in the work of Heuer et al.. The fact that axial rotation is the only movement within the ROM range of the literature, for all applied loads, is probably an indicator that this particular movement is less affected by an extended morphological degeneration, i.e. rotation movement is not significantly altered due to IVD height reduction.

Table 5.7: Minimum and maximum ROM values found in the literature [11] in comparison with the ROM values obtained in the current study for the intact model.

		Heuer et al. [11]		**Current study**
Movement	Moment (Nm)	Minimum ROM (deg)	Maximum ROM (deg)	ROM of the current model (deg)
E	1	0.33	1.67	0.14
	2.5	1.08	2.83	0.28
	5	2.50	4.08	0.47
	7.5	3.17	4.92	0.64
	10	3.83	5.75	0.80
F	1	0.42	1.49	0.38
	2.5	1.66	4.48	0.97
	5	3.32	6.80	2.07
	7.5	4.15	8.13	3.25
	10	4.90	9.46	4.45
LB	1	0.74	1.74	0.28
	2.5	2.05	3.78	0.64
	5	3.29	5.52	1.16
	7.5	3.97	6.51	1.62
	10	4.52	7.13	2.04
AR	1	0.12	0.74	0.43
	2.5	0.31	1.79	0.98
	5	0.74	2.84	1.73
	7.5	1.17	3.70	2.35
	10	1.54	4.32	2.88

5.3 Results and Discussion

In this section are presented the results of the simulations conducted in this part of the study, divided into four levels of analysis. First, are presented the results relative to the degenerated intact models, including IVD and ligament degeneration. Second, outcomes of the simulations of the instrumented models mimicking the OLIF procedure are also presented, so that the more beneficial type of posterior fixation is determined. IVD degeneration was also replicated in the instrumented models and the results of these simulations are included in subsection 5.3.3. Finally, in the last subsection, it is

discussed, based on previously presented results, whether ADD is more promoted by degeneration or spinal fusion.

5.3.1 Degenerated Intact Models

The main outcomes of the simulations with IVD degeneration were ROM values and stress in the IVDs, to evaluate the stability of the spine and the influence of morphological changes. For that, five different nodes of the models were selected to evaluate the stress in different regions of the AF and NP: anterior (AF A), posterior (AF P), lateral left (AF LL), and lateral right (AF LR) regions in the AF, and in the centre of NP. In the case of ligament degeneration, the main outcomes were ROM relative changes.

The analyses of the simulations of the degenerated models are presented next, divided into two sections according to the structure that suffered degeneration: IVD or ligaments.

5.3.1.1 IVD Degeneration

To understand the effects of IVD degeneration on the biomechanics of the lumbar spine in combination with morphological degeneration (WMD), different combinations of degenerated IVDs were considered and five different models were tested, as previously mentioned in section 5.1.2. ROM values were determined in L4-L5 and L3-L4 levels to evaluate spinal stability and the effects on the adjacent level (Figure 5.6).

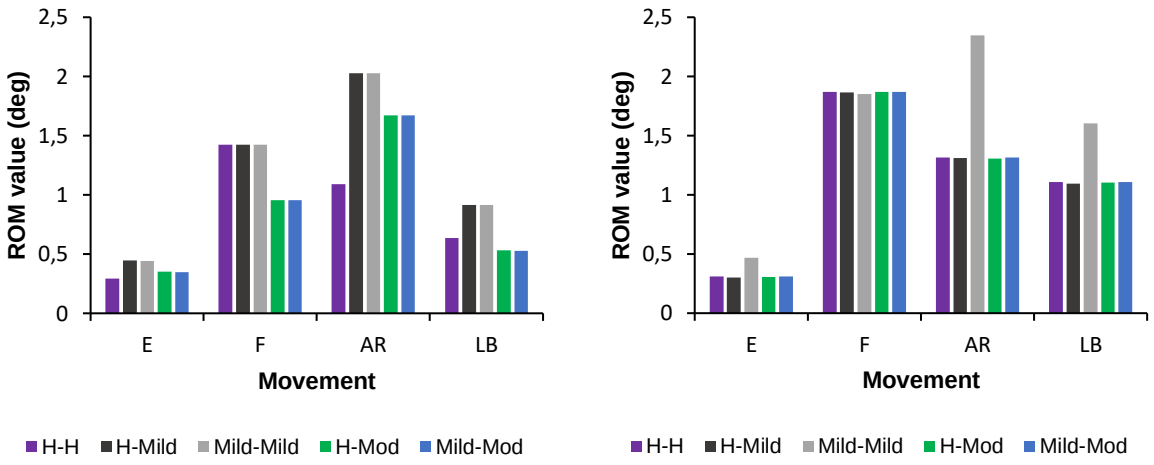

Figure 5.6: ROM evolution of the L3-L5 FE model with progressive IVD degeneration for different movements at L4-L5 (left) and L3-L4 levels (right).

Assuming an increasing degenerative state from H-H to Mild-Mod model, global ROM values increased in the first stages of degeneration, until the state with both discs mildly degenerated, and then started decreasing as degeneration became more pronounced. This is in agreement with the process of IVD degeneration and previously obtained results, even for the model without morphological degeneration [9], [82]. In the first stages of degeneration, with mildly degenerated IVDs, there was an increase in fibre laxity, which resulted in increased mobility and instability. The greatest increase in

ROM, of around 40%, occurred for AR from the healthy to the H-Mild model. As degeneration progressed, including IVDs with moderate degeneration, IVD stiffness prevailed over fibre laxity and the motion became more restricted. It is interesting to notice that, although the Mild-Mod model is in a more advanced state of degeneration than the H-Mod model, the ROM of the first was higher than the one of the latter. This occurred due to the mildly degenerated L3-L4 IVD of the first model, which contributed to widen the ROM as a result of the increased fibre laxity. Nonetheless, in all cases, the motion was still higher than the one of the healthy model, except for lateral bending.

When compared with the previous model in Part I, without morphological degeneration (WOMD), absolute ROM values were generally lower in the model WMD for all loading directions, since the decreased IVD height is associated with a loss of hydration by the NP, therefore increasing IVD stiffness and restricting motion.

The abovementioned observations apply to all movements, except flexion. The main difference of this movement in relation to the others occurred for the early stages of degeneration, in which ROM remained the same as in the healthy model and did not increase. This situation could possibly be a result of the model's morphological changes. Since there was a decrease in IVD height, there was a lower ROM allowed before the bone was reached. Therefore, there was an upper limit to the movement that prevented ROM from further increase. With advancing degeneration, ROM values decreased as before.

If the analysis is focused on L4-L5 level, the same trends of the global level were verified, with ROM increasing from the healthy model to models with IVD mildly degenerated, and then decreasing as the IVD advanced to a moderate stage of degeneration. When degeneration increased at L3-L4 level, ROM values at L4-L5 remained approximately the same in most cases. However, there were situations in which ROM slightly decreased, as it was the case of extension from H-Mod to Mild-Mod model, with a decrease in ROM of around 1.38%. This demonstrates the influence of adjacent degeneration in the L4-L5 level. This effect was even more pronounced if the analysis was turned to the L3-L4 level. In this case, when comparing models with similar L3-L4 IVD degeneration and increasing L4-L5 IVD degeneration, the differences in ROM were even more marked, mostly because the adjacent L4-L5 IVD had a stronger degeneration. For example, from the Mild-Mild to the Mild-Mod model, there was a decrease of around 44% in ROM in AR, and 34% in extension.

In terms of supported loads, the trends were the same throughout all models given that, according to the movement that is performed, the same IVD regions will be under stress (Figure 5.7).

In the case of extension and flexion, there was more load supported by the anterior and posterior regions, respectively, which are high tension regions. For LB, the right IVD region was the most active one under tension since this was the opposite direction of the bending movement. Regarding AR, all IVD regions were under similar tension, except for the posterior region, which was subjected to lower loads. For every movement, the load supported by regions under tension was significantly higher than the one supported by the contralateral regions under compression, which was not significant. Therefore, specific points were chosen to evaluate tensile stresses for a given movement: AF A for extension, AF P for flexion, AF LL for LB, and an average of AF P, AF A, AF LL, and AF LR for AR. NP was subjected to similar compressive forces throughout every model, with the exception of extension which presented

tensile stresses. Table 5.8 presents the obtained stress results measured in these points as a function of movement and degeneration.

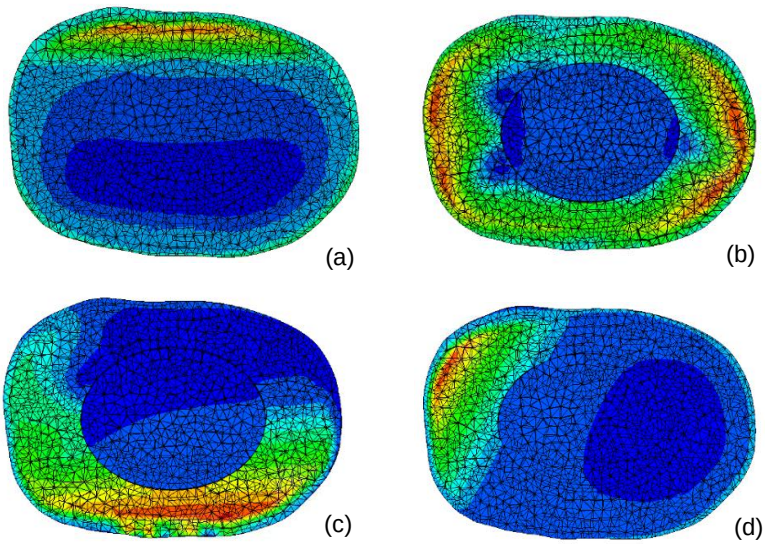

Figure 5.7: Top view of stress distribution in L3-L4 IVD of the H-H model during (a) flexion, (b) AR, (c) extension, and (d) LB. Red regions represent tensile stresses and blue regions represent compressive stresses.

Table 5.8: Stress values (in MPa) in the IVDs as a function of movement and model degeneration, for each L3-L4 and L4-L5 level.

		H-H	**H-Mild**	**Mild-Mild**	**H-Mod**	**Mild-Mod**
L3-L4	LB	0.4026	0.4019	0.3175	0.4033	0.3179
	E	0.2350	0.2324	0.1097	0.2340	0.1102
	F	0.3719	0.3705	0.1387	0.3734	0.1397
	AR	0.3320	0.3319	0.1883	0.3318	0.1882
L4-L5	LB	0.3244	0.2747	0.2732	0.3368	0.3348
	E	0.2631	0.1361	0.1350	0.1970	0.1947
	F	0.3419	0.1259	0.1254	0.2197	0.2187
	AR	0.3705	0.2028	0.2028	0.1583	0.1583

From Table 5.8, it is possible to conclude that the loads supported by L3-L4 IVD were in general higher than the ones supported by L4-L5 IVD. This was possibly due to the height reduction in L4-L5 IVD, but mainly to the closest proximity between L3-L4 IVD and the point of application of the load, on the top surface of L3, leading to a stress distribution more targeted on the top motion segment. If the analysis is focused only on one FSU at a time, the stress to which a particular IVD was subjected to remained approximately the same throughout all degenerated models if its state of degeneration also remained the same, regardless of the degeneration of the adjacent IVD. Thus, when the IVD had a mild degeneration, there was a decrease in the supported load for any movement, for both L3-L4 and L4-L5 IVDs. From the healthy to H-Mild model, there was a reduction in L4-L5 ROM of around 15%, 48%, 63%, and 45% for LB, E, F, and AR, respectively. When the degeneration increased, the load increased

due to IVD stiffening, except for AR, which is aligned with the previous findings regarding this movement. However, this was only visible for L4-L5 IVD since L3-L4 IVD was mildly degenerated at most. From Mild-Mild to H-Mod model, L4-L5 ROM increased by approximately 23%, 46%, 75% for LB, E, and F, respectively, and decreased 22% for AR. These stress trends were also verified in the model WOMD.

Although stress values in the IVDs remained approximately the same regardless of the degeneration of the adjacent level, there were still some slight variations between models with the same IVD degeneration. For example, in L3-L4 level, there was a stress decrease of 1.1% from the healthy to the H-Mild model in extension, which indicates a slight influence of degeneration on the adjacent level.

A study conducted by Rohlmann et al. [9] on the analysis of the influence of IVD degeneration on spinal motion supports the current results. They developed an L3-L4 FE model and different degeneration degrees (mild, moderate, and severe) were simulated by changing IVD height and the bulk modulus of NP. Their results showed that a mildly degenerated IVD increases intersegmental motion for all movements and that, with further degeneration, the intersegmental motion starts decreasing. This corresponds to the increase in ROM from healthy to mildly degenerated models in the current results, with subsequent ROM decrease when the transition to moderate degeneration occurs. Moreover, Rohlmann et al. concluded that the stress in AF was higher in the degenerated model in comparison with the healthy one, with LB being the movement in which the IVD was under the highest load. These results are also aligned with current simulations and *in vitro* studies [102]–[104].

Similar to Rohlmann et al., Ellingson et al. [10] developed a complete model of the lumbar spine to study the role of ligaments and influence of IVD degeneration on movement. They discovered a progressive decrease in ROM for all directions with advancing degeneration. At first, these outcomes seem to contradict the currently obtained results, since it was shown that ROM increased in the first stage of degeneration (mild degeneration) and only after it started decreasing – in the case of moderate degeneration. However, two different degeneration degrees were evaluated in the study of Ellingson et al. (moderate and severe, compared with mild and moderate in the current work), representing more advanced stages of degeneration. Therefore, it makes sense that their results only refer the ROM reduction with progressive degeneration.

With the purpose of studying the influence of degeneration on the adjacent levels, Ruberté et al. [60] modified a FE model of the lumbar spine to mimic two different degrees of degeneration at the L4-L5 level. Degeneration was simulated by reducing IVD height and nucleus area, and by altering the material properties of AF and NP, modelled as hyperelastic (following a Mooney-Rivlin formulation) and as a fluid linear elastic element, respectively. Their results suggested that single-level degeneration might increase the risk of injury at adjacent levels. At the degenerated level, it was found a progressive decrease in ROM with increasing degeneration for AR and LB. For extension and flexion, similar results to the current ones were obtained, with an increase in ROM for mild degeneration, and then a decrease in the further degenerated case. In terms of loads acting on AF, there was an increase in load for mild degeneration in all directions, but, with advancing degeneration, the load in AF decreased. Nonetheless, it was still higher than in the healthy case. In the current simulations, the opposite occurred, i.e. there was a decrease in load from the healthy to the mildly degenerated case, and then an increase in the last degeneration stage. This difference in outcomes might be due to differences in simulation and

modelling of IVD, thus making a direct comparison not possible. Moreover, the fact that Ruberté et al. based their work on a model of the full lumbar spine might also induce some differences, namely on the behaviour of the degenerated and adjacent levels. In the present study, there was a variation in global ROM with degeneration, whereas in the work of Ruberté et al. the total ROM was the same for healthy and degenerated models, since there were more adjacent levels to compensate for the changes at the degenerated IVD. Regarding changes at the top adjacent IVD, there was a decrease in ROM and increase in stress with progressive degeneration, which seems to be following the abovementioned reasoning.

5.3.1.2 Ligament Degeneration

The trends of ligament degeneration in the model with morphological changes are presented next, being highlighted the respective differences in relation to the model without morphological degeneration.

When considering the first ligament stage (Mild-Mild), in general there was an increase in ROM, as before, since ligament stiffness was decreased and the motion became less restricted. Nonetheless, it was verified a greater ROM increase for flexion and AR when FCL was degenerated in relation to the model WOMD (ROM changes of 11.10% and 5.71%, respectively, compared with 3.92% and 2.40% in the model WOMD). Similarly, in extension, ROM was higher in the case of ALL degeneration (ROM change of 1.12%, compared with 0.66% in the model WOMD). As before, it was possible to conclude that the impact of FCL in the movement was greater than the one of ALL. Table 5.9 shows the ROM values of the model WMD with 25% mild ligament degeneration.

Table 5.9: Global ROM values (in deg) with 25% mild ligament degeneration as a function of movement. Between brackets are the per cent changes in relation to the healthy model.

	Healthy	FCL	ALL	All	ISL	LF
E	0.82	0.82 (0.01%)	0.83 (1.12%)	0.83 (1.13%)		
F	2.81	3.12 (11.10%)	2.81 (0.00%)	3.35 (19.09%)	2.89 (2.70%)	2.87 (2.18%)
AR	4.02	4.25 (5.71%)	4.02 (0.02%)	4.27 (6.28%)		

Regarding the second degeneration stage (Mild-Moderate), FCL and ALL remained the ligaments with greatest impact in flexion and AR, and extension, respectively (Table 5.10). However, ROM changes at the L4-L5 level were also more enhanced relative to the model WOMD, being the motion more restricted with the same increase in ligament stiffness (ROM changes of - 6.99%, - 3.31%, and - 0.89% compared with - 3.71%, - 1.49%, and - 0.70%, for flexion, AR, and extension, respectively). In L3-L4 level, there were slight variations in the outcomes compared with the previous degeneration stage, although the ligament degeneration in this level remained the same. This already occurred for the model WOMD, highlighting the effect of L4-L5 ligament degeneration on the adjacent level, but the absolute ROM values were higher for the current model.

With progressive degeneration, i.e. with increasing percentages of variation in ligament stiffness (namely, 50% and 75%), the abovementioned outcomes were also verified, but with more pronounced ROM changes.

Table 5.10: L4-L5 ROM values (in deg) with 25% moderate ligament degeneration as a function of movement. Between brackets are the per cent changes in relation to the healthy model.

	Healthy	FCL	ALL	All	ISL	LF
E	0.35	0.35 (0.00%)	0.35 (-0.89%)	0.35 (-0.89%)		
F	0.95	0.89 (-6.99%)	0.95 (0.00%)	0.85 (-10.65%)	0.93 (-2.25%)	0.94 (-1.75%)
AR	1.67	1.62 (-3.31%)	1.67 (-0.01%)	1.61 (-3.57%)		

Comparing the results from the simulations in which ALL and FCL were degenerated as a set with the ones from the simulations in which all ligaments were degenerated simultaneously, ROM variations were very similar for extension, as in the model WOMD. The main differences in relation to this model occurred for AR and flexion. For these movements, the differences between ROM changes with FCL and overall degeneration were higher, namely in flexion. This shows that, besides FCL that was the most active ligament, the remaining ligaments also had small contributions to the movement that became significant when added. In the case of flexion, in particular, are highlighted the contributions of ISL and LF, since their impact in ROM increase was higher than the one of the remaining ligaments (although not as significant as the one of FCL). For example, in the first stage of degeneration with a reduction in ligament stiffness of 50%, ISL and LF led to an increase in ROM of around 5% each, whereas FCL degeneration increased ROM by 24.13%.

In general, the results for ligament degeneration followed the same trends verified in Part I (Chapter 4, section 4.2.2) for the FE model WOMD. However, ROM variations were more pronounced in the case WMD, leading to believe that an increased IVD degeneration, including IVD height reduction, results in an increased ligament degeneration as well. This is a good indicator that ligament degeneration follows IVD degeneration.

5.3.2 Instrumented Models

Simulation outcomes for the instrumented models were analysed in terms of ROM and stress, as it was the case for the degenerated models. However, in addition to the IVD stress analysis, the maximum stress supported by the cage and screws was also tested to evaluate load-sharing and the possibility of instrumentation failure. With these aspects into consideration, the goal was to infer if there is any type of fixation that is more beneficial for clinical practice, and to assess the impact of each construct in spine kinematics.

Simulations were performed with a long-term perspective since it is fundamental to evaluate the fixation role on osseointegration and spinal stability. Nonetheless, it is also important to study the

process through which stabilisation is achieved. Therefore, each subsection is divided into two different stages: long-term (LT) and short-term (ST) simulations.

5.3.2.1 ROM

5.3.2.1.1 Long-Term

In the long-term, the use of instrumentation led to a marked ROM decrease from the intact model for all loading directions (Figure 5.8). The greatest decrease with cage introduction occurred for AR, with a ROM value around 55% lower than in the intact model, followed by LB and flexion with a reduction in ROM of around 30%. However, given that the long-term goal with the introduction of instrumentation is spinal fusion, a decline in ROM values is expectable, especially in the intervened L4-L5 level. In fact, when analysing ROM values at this level, it is evident that the movement of the bottom FSU was practically zero in all directions (Table 5.11).

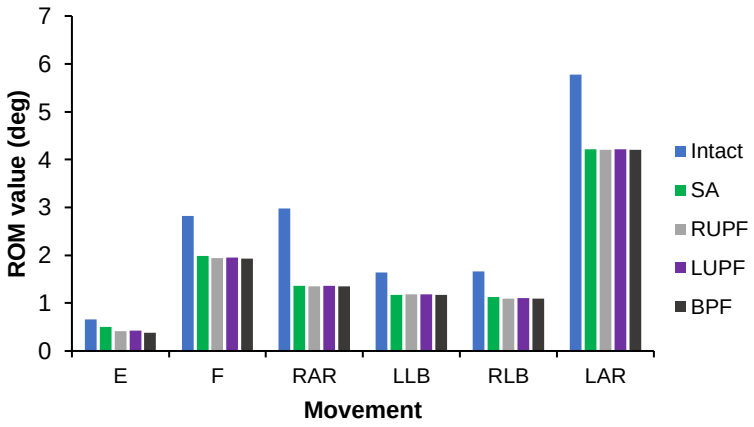

Figure 5.8: Global ROM values of the different instrumented models as a function of movement in long-term analysis.

Comparing the SA model with the models with posterior fixation, ROM decreased slightly further in the models with unilateral fixation, and even more in the BPF model, particularly for extension. Extension was the movement in which differences in fixation had the strongest impact. For the remaining movements, there were no marked differences between models with uni- or bilateral constructs, although BPF model had the lowest ROM absolute value for all directions. Between RUPF and LUPF models, the one with right unilateral fixation presented a slightly higher restriction of movement.

Table 5.11 presents the segmental ROM values of the different instrumented models as a function of movement. The mobility in the bottom FSU was null for all loading directions. If the top motion segment is considered, it was evident an increase in ROM from the intact to the SA model, possibly indicating a compensation mechanism as L4-L5 ROM decreased. This may contribute to the degeneration of the adjacent level. The greatest ROM increase occurred for extension (ROM change of 20.6%), followed by LLB with a ROM variation of around 4%. For the remaining movements, the compensation mechanism may be neglected as ROM increase was lower than 1%. ROM values remained approximately the same

across all instrumented models, with variations lower than 1%, except for extension, in which ROM decreased around 10% in the models with posterior fixation compared with the SA model.

Table 5.11: Segmental ROM values (in deg) of the different instrumented models as a function of movement, for each L3-L4 and L4-L5 level. Between brackets are the per cent changes in relation to the intact model.

		Intact	SA	RUPF	LUPF	BPF
L3-L4	E	0.31	0.37 (20.6%)	0.33 (8.58%)	0.34 (10.9%)	0.32 (4.02%)
	F	1.87	1.88 (0.77%)	1.87 (0.21%)	1.88 (0.40%)	1.87 (-0.03%)
	RAR	1.31	1.31 (0.42%)	1.32 (0.52%)	1.32 (0.65%)	1.32 (0.55%)
	LLB	1.10	1.15 (4.00%)	1.15 (4.50%)	1.15 (4.39%)	1.15 (3.88%)
	RLB	1.10	1.09 (-0.14%)	1.07 (-2.69%)	1.07 (-2.11%)	1.07 (-2.49%)
	LAR	4.17	4.17 (0.16%)	4.17 (0.11%)	4.19 (0.53%)	4.17 (0.09%)
L4-L5	E	0.35	0.13 (-63.7%)	0.08 (-77.7%)	0.09 (-76.4%)	0.06 (-83.1%)
	F	0.10	0.10 (-89.4%)	0.07 (-92.6%)	0.07 (-92.3%)	0.06 (-93.9%)
	RAR	1.67	0.04 (-97.3%)	0.04 (-97.6%)	0.04 (-97.6%)	0.04 (-97.8%)
	LLB	0.53	0.02 (-96.2%)	0.03 (-94.0%)	0.03 (-94.4%)	0.03 (-95.0%)
	RLB	0.57	0.03 (-94.0%)	0.03 (-94.8%)	0.03 (-94.2%)	0.03 (-95.4%)
	LAR	1.61	0.04 (-97.3%)	0.04 (-97.7%)	0.03 (-98.2%)	0.03 (-97.8%)

5.3.2.1.2 Short-Term

In short-term, when osseointegration is being established, ROM trends were slightly different compared with the case of complete spinal fusion. Considering global ROM values, there was a significant ROM increase from the intact to the SA model for all loading directions (Figure 5.9). The greatest increase occurred in extension, followed by RAR. For these movements, ROM was around four and three times higher in SA than in the intact model, respectively. With the introduction of posterior fixation, it was verified a decrease in mobility, especially with the introduction of a bilateral fixation system, similar to what occurred in the long term.

Between the models with unilateral fixation, ROM values were similar for movements in the sagittal plane. However, for AR and LB, ROM was higher in the RUPF or LUPF models when these movements took place towards the right or left directions, respectively – i.e. ROM values were higher if the movement occurred towards the side of the unilateral posterior fixation.

ROM values at L4-L5 level followed global trends, with a marked increase in intersegmental motion when the IVD was removed and a cage was inserted in its place. This occurred since, in short-term, there is no spinal fusion and there is more mobility in this segment. As fixation became more restrictive, the mobility in this segment decreased. If the focus is turned to L3-L4 level, ROM values were very similar across all instrumented and intact models, indicating that changes in mobility were only due to the instability in the bottom FSU.

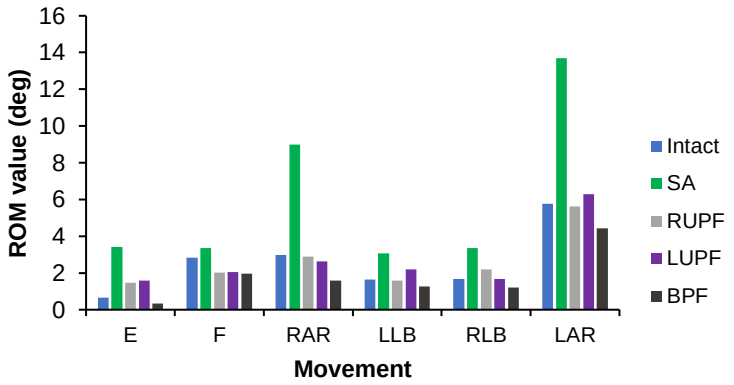

Figure 5.9: Global ROM values of the different instrumented models as a function of movement in short-term analysis.

5.3.2.2 Stress

5.3.2.2.1 Long-Term

Considering a stress analysis in the adjacent IVD, there was an increase in supported load during LB and flexion (18.5% and 10.2%, respectively), and a decrease during extension and AR (8.52% and 7.34%, respectively) from the intact to the SA model. With the introduction of posterior fixation, a reduction in IVD load should be expected due to load-sharing. However, with a focus on unilateral fixation outcomes, this situation only occurred for flexion and RLB in RUPF, and for LB in LUPF (Table 5.12). The load increase in the remaining loading directions might therefore contribute to accelerate adjacent degeneration.

Table 5.12: Stress values (in MPa) supported by L3-L4 IVD in the different instrumented models as a function of movement in long-term simulations. Between brackets are the per cent changes in relation to the SA model (or intact model in the case of SA).

	Intact	SA	RUPF	LUPF	BPF
E	0.2340	0.2141 (-8.52%)	0.2428 (13.4%)	0.2639 (23.3%)	0.2283 (6.64%)
F	0.3734	0.4116 (10.2%)	0.2670 (-35.1%)	0.4821 (17.1%)	0.3138 (-23.8%)
RAR	0.3318	0.3074 (-7.34)	0.3083 (0.28%)	0.3237 (5.30%)	0.2981 (-3.02%)
LLB	0.4033	0.4780 (18.5%)	0.5284 (10.5%)	0.4550 (-4.80%)	0.3825 (-20.0%)
RLB		0.4232	0.4177 (-1.30%)	0.4133 (-2.33%)	0.4257 (0.60%)
LAR		0.0979	0.0988 (0.94%)	0.1115 (13.9%)	0.0783 (-20.1%)

With the introduction of bilateral fixation, it was possible to remove load from the IVD, leading to a reduction in stress values from SA to BPF models for all movements, except extension. In RLB, a slight stress increase also occurred, but this was neglected as the variation was lower than 1%. The greatest decrease occurred for flexion, with a stress variation of around 24%. Between both models with unilateral constructs, LUPF presented higher stresses acting on the IVD compared with RUPF, except for LB. This may be a result of the asymmetry of cage placement. Since the cage is introduced from the left side of the body, it will be subjected to higher loads on this side, relieving the load acting on the left portion of the adjacent IVD. In fact, in the SA model, the right portion of the IVD withstood higher loads for all loading directions. The posterior fixation is thus more useful on the right side of the body, explaining the lower stress values of the IVD in the RUPF model. This could also be an indicator that the left side of the body already provides some support to interbody fusion and, therefore, left posterior fixation is not so critical. However, the current models did not include musculature and surrounding organs for this support to be verified.

Regarding instrumentation, Von Mises stress was evaluated as this relates best with the probability of a given material to yield or fracture. The stress acting on the cage was always higher in the cage-only model, comparing the four models with and without posterior fixation, which may lead to an increased risk of cage subsidence and implant migration (Table 5.13). The greatest load support occurred for movements in the sagittal plane: extension (12.67 MPa), followed by flexion (6.627 MPa). With the introduction of posterior fixation, cage stress was reduced, especially with bilateral fixation, due to an increased load-sharing between constructs. Figure 5.10 illustrates the distribution of stress acting on the cage during extension throughout the four instrumented models, with decreased magnitude from the SA to the BPF model.

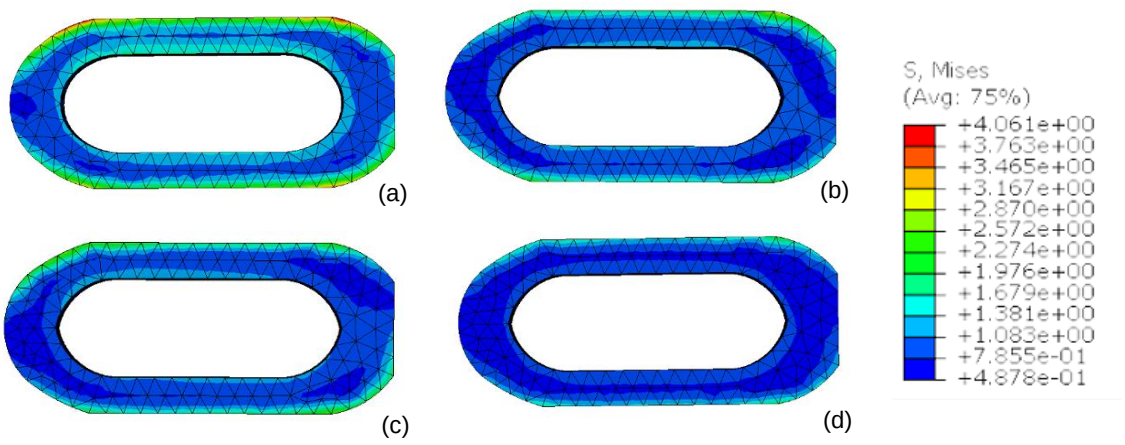

Figure 5.10: Von Mises stress in the cage throughout instrumented models during long-term extension: (a) SA, (b) RUPF, (c) LUPF, and (d) BPF models.

The greatest load decrease occurred in the BPF model for all loading directions, being more significant in extension (decrease of 68.5%), followed by flexion (decrease of 37.6%), as these were also the movements in which the cage supported the highest loads in SA model.

Table 5.13: Cage stress values (in MPa) in the different instrumented models as a function of movement in long-term simulations. Between brackets are the per cent changes in relation to the SA model.

	SA	RUPF	LUPF	BPF
E	12.67	6.520 (-48.5%)	5.792 (-54.3%)	3.992 (-68.5%)
F	6.627	5.030 (-24.1%)	5.375 (-18.9%)	4.138 (-37.6%)
RAR	4.061	3.457 (-14.9%)	3.604 (-11.3%)	3.039 (-25.2%)
LLB	5.681	5.614 (-1.18%)	4.473 (-21.3%)	4.248 (-25.2%)
RLB	5.693	4.582 (-19.5%)	5.672 (-0.37%)	4.192 (-26.4%)
LAR	4.313	3.093 (-28.3%)	3.945 (-8.53%)	2.934 (-32.0%)

Regarding RUPF and LUPF models, significant differences occurred for LB movements, depending on their direction. Results showed that the stress acting on the cage was lower if the bending movement occurred towards the side of the unilateral fixation due to the support provided by the construct. In movements towards the opposite side of fixation, the stress values were higher. This was verified in RUPF model for LLB (5.612 MPa compared to 4.582 MPa in RLB), and for RLB in LUPF model (5.672 MPa compared to 4.473 MPa in LLB). In the case of AR, stress values were always higher in the LUPF model regardless of the direction of movement. This supports the finding that unilateral fixation is more beneficial when placed on the right side of the body. Finally, regarding extension and flexion, there were also some differences between the two models, which were not expected since these are movements in the sagittal plane that should not depend on the side of fixation. In extension, stress was lower with the introduction of left unilateral constructs (LUPF model), whereas in flexion this was verified for right unilateral fixation (RUPF model). This indicates that extension and flexion were not perfectly aligned movements in the sagittal plane (possibly due to the cage asymmetry) and exerted more load over the right and left sides of the cage, respectively.

Although there were some situations in which the Von Mises stress supported by the cage was considerably high relative to other movements or models, these values are very small when compared with the ultimate tensile strength of PEEK (100 MPa [105]). Therefore, there is no risk of cage failure. Nonetheless, the risk of fixation failure must also be evaluated for the instrumentation to be considered safe. The posterior fixation stress was the highest in extension, followed by flexion. However, the supported loads were in general higher than in the cage to avoid cage subsidence. Table 5.14 shows the stress values acting on the posterior instrumentation as a function of movement.

Table 5.14: Posterior fixation stress values (in MPa) in the different instrumented models as a function of movement in long-term simulations.

	RUPF	LUPF	BPF
E	42.21	40.45	32.76
F	26.97	26.51	20.18
RAR	21.56	16.91	20.64
LLB	10.60	14.24	16.31
RLB	14.32	9.41	16.43
LAR	25.28	16.48	25.97

As before, the introduction of bilateral fixation led to the highest stress reductions. However, in this case, it was only verified for extension and flexion. For the remaining movements, stress values were lower in the model with left unilateral construct given that, due to cage asymmetry, posterior fixation on the left side was not so critical. Since the BPF model includes right unilateral fixation in addition to the left construct, and that fixation on the right side is required for support (supporting higher loads), the loads exerted on the instrumentation increased.

Comparing RUPF and LUPF models, the stress acting on the left unilateral construct was lower than the one on the right for the same reasons abovementioned, namely cage asymmetry. Moreover, the load supported by the adjacent IVD was lower in the RUPF model, thus requiring the instrumentation to support higher loads. This was true for every movement except LLB. In this case, loads were higher in the LUPF model since the instrumentation will be under increased stress if the movement occurs towards the side of fixation.

In any case, there was no risk of failure or screw loosening since even the maximum stress value (42.21 MPa) was significantly below the tensile strength of titanium alloys (500 – 1000 MPa [106]). If stress in the screws is kept at a low level, screw loosening can be prevented [35]. Therefore, every construct is safe to use in clinical practice regarding mechanical failure.

5.3.2.2.2 Short-Term

As opposed to what happened with ROM values, the trends in supported loads by the adjacent IVD and instrumentation were very similar between long and short-term simulations.

In summary, with an analysis focused on the adjacent IVD, from the intact to the SA model, the stress acting on this structure increased during LB and flexion (17.8% and 6.26%, respectively), and decreased during extension and AR (11.3% and 7.30%, respectively), as already occurred in the long term. In models with posterior fixation, there was load-sharing and stress decrease with the movement, namely in the BPF model (Table 5.15). In this case, ADD may be prevented as load reduction in the IVD was achieved in all loading directions.

Table 5.15: Stress values (in MPa) supported by L3-L4 IVD in the different instrumented models as a function of movement in short-term simulations. Between brackets are the per cent changes in relation to the SA model (or intact model in the case of SA model).

	Intact	**SA**	**RUPF**	**LUPF**	**BPF**
E	0.2340	0.2077 (-11.3%)	0.2333 (12.3%)	0.2517 (21.2%)	0.0807 (-61.1%)
F	0.3734	0.3968 (6.26%)	0.2613 (-34.2%)	0.4748 (19.7%)	0.3107 (-21.7%)
RAR	0.3318	0.3076 (-7.30%)	0.3074 (-0.06%)	0.3265 (6.16%)	0.2974 (-3.31%)
LLB	0.4033	0.4752 (17.8%)	0.5254 (10.6%)	0.4495 (-5.42%)	0.3770 (-20.7%)
RLB		0.4211	0.4113 (-2.32%)	0.4098 (-2.69%)	0.4182 (-0.68%)
LAR		0.0946	0.0993 (4.95%)	0.1104 (16.7%)	0.0785 (-17.1%)

The stresses acting on the IVD in LUPF model were in general higher than in RUPF model since more support was needed on the right side to remove load from the IVD – on the left side there is already support to some extent due to cage asymmetry, as previously mentioned. Absolute stress values

between short and long-term simulations were very similar but slightly lower in short-term (Tables 5.12 and 5.15).

As in long-term, the stress acting on the cage was always the highest in the SA model, comparing between the four models with and without posterior fixation (Table 5.16). The greatest load support occurred for LB (around 60 MPa), shifting for extension/flexion in the long-term. As unilateral fixation was introduced in the models, cage stress was reduced for all loading directions, except extension. In the case of the model with bilateral construct, stress was reduced even further, for all directions of movement. Between both models with unilateral fixation, RUPF presented the highest stresses in AR and LB, and LUPF in sagittal plane movements. Table 5.16 shows the values of stress acting on the cage for the different instrumented models as a function of movement. By comparing these values with the ones in Table 5.13, relative to long-term simulations, it is evident that the stress supported by the cage was significantly higher in short-term. This situation was also verified for posterior fixation (Tables 5.14 and 5.17).

Table 5.16: Cage stress values (in MPa) in the different instrumented models as a function of movement in short-term simulations. Between brackets are the per cent changes in relation to the SA model.

	SA	**RUPF**	**LUPF**	**BPF**
E	15.35	18.70 (21.8%)	18.78 (22.3%)	0.0019 (-99.9%)
F	19.30	7.531 (-61.0%)	7.650 (-60.4%)	4.135 (-78.6%)
RAR	9.579	7.613 (-20.5%)	6.575 (-31.4%)	7.593 (-20.7%)
LLB	54.97	25.73 (-53.2%)	25.62 (-53.4%)	11.73 (-78.7%)
RLB	60.40	28.85 (-52.2%)	26.54 (-56.1%)	5.678 (-90.6%)
LAR	13.81	5.220 (-62.2%)	3.477 (-74.8%)	3.701 (-73.2%)

The posterior fixation stress was significantly higher than the stress acting on the cage, as before in long-term, since fixation aims to reduce the stress supported by the cage and share the load. The maximum fixation stresses occurred for AR, followed by extension (Table 5.17), and the introduction of bilateral fixation led to the greatest stress reductions. Between the unilateral models, the loads supported during flexion and extension were similar in both cases. For AR and LB, the stress acting on posterior instrumentation was higher if the movement occurred towards the side of fixation.

In any case, although higher than in long-term simulations, the stress acting on the cage and instrumentation was below the maximum tensile stress of PEEK and titanium, respectively, thus making every construct safe to use regarding implant subsidence or migration.

Table 5.17: Posterior fixation stress values (in MPa) in the different instrumented models as a function of movement in short-term simulations.

	RUPF	**LUPF**	**BPF**
E	140.6	141.7	32.32
F	43.81	43.92	26.65
RAR	202.7	178.0	85.73
LLB	79.20	96.90	38.44
RLB	113.9	84.14	38.11
LAR	190.1	230.8	100.6

5.3.2.3 Role of Ligaments

Besides the introduction of instrumentation, ligaments also play an important role in the stabilisation of the spine. Therefore, it is of extreme importance to understand the extent of their influence since, in some situations, it is particularly difficult to keep all ligaments intact. Moreover, by individualising the biomechanical effects of ligaments, it is easier to separate between ligament removal and cage introduction effects. During L4-L5 OLIF procedures, all ligaments are often maintained, but this might not always be the case as each patient has a specific anatomy. Furthermore, other surgical approaches, such as ALIF or PLIF, or even OLIF procedures in other levels, may not allow the maintenance of all ligaments. In this way, determining the role of ligaments in the current instrumented models might be useful to support (and maybe guide) clinical practice. Table 5.18 shows the evolution of ROM when ligaments were removed from one or both FSUs from the intact model in long and short-term simulations.

Table 5.18: ROM values (in deg) of the FE model with all ligaments (intact), with ligaments removed only on L4-L5 (Case 1), and with ligaments removed in both levels (Case 2), as a function of movement in long and short-term simulations. Between brackets are the per cent changes in relation to the intact model.

	Long-Term			**Short-Term**		
	Intact	Case 1	Case 2	Intact	Case 1	Case 2
E	0.57	0.57 (0%)	0.62 (8.14%)	1.60	3.51 (118.1%)	3.55 (120.5%)
F	1.93	1.93 (0.09%)	4.87 (152.6%)	2.01	2.04 (0.99%)	5.01 (148.1%)
AR	2.39	2.39 (0%)	3.32 (38.9%)	3.94	5.03 (27.8%)	5.95 (51.3%)
LB	1.68	1.68 (0%)	2.09 (24.4%)	2.07	2.61 (25.9%)	3.04 (46.4%)

In the long-term, if ligaments were only removed from the intervened level (L4-L5), ROM values remained the same as in the intact model. This was expected due to spinal fusion and given that the motion of the bottom FSU was practically zero. In the case of ligament removal from both levels, there was an evident increase in ROM compared with the intact model because L3-L4 level was not restricted by any ligament and could move freely. The lowest ROM increase occurred for extension (8.14%) given that this movement is more restricted by posterior processes. The motion in L4-L5 FSU remained close to zero.

In this case, it is possible to conclude that ligaments in the intervened level were sort of obsolete. Nonetheless, this was a long-term analysis, in which spinal fusion had already occurred. If one considers a short-term analysis, the outcomes were different since fusion had not yet occurred. With ligament removal, ROM increased compared with the intact model. This ROM variation was even more evident in the case of ligament removal from both levels since, in this case, both L3-L4 and L4-L5 FSUs were contributing to increase mobility. The increase in L4-L5 level was, however, bigger than the one of L3-L4 for all loading directions due to the looser interaction between cage and vertebrae. If ligaments were only removed from the bottom FSU, only this level contributed to the global ROM increase. However, the increase in flexion was very small (0.99%), possibly due to posterior fixation restriction. In L3-L4 FSU, ROM was the same as in the intact model since ligaments were present to restrict its movement.

In conclusion, although in long-term ligaments do not contribute to spinal stability due to complete spinal fusion, in the short-term these structures play a restricting role, limiting cage movements and helping to keep it in place.

Guo et al. [78] also studied the OLIF procedure intending to explore the stability of different posterior fixation systems. As mentioned in Chapter 3, results showed that the SA model could not provide sufficient stability, presenting the largest ROM and maximum cage stress amongst all models. These outcomes are aligned with the present work. Moreover, it was concluded that the bilateral pedicle screw device provided the best biomechanical stability, being associated with the minimum ROM and cage and screw stresses. This was also verified for the current simulations, although intersegmental mobility did not vary significantly between models with uni- and bilateral fixation. The work of Godzik et al. [6] supports this finding. They performed standard non-destructive flexibility tests to evaluate stability in cadaveric lumbar specimens with uni- or bilateral pedicle screw systems, in the presence or absence of interbody implants. Between models with interbody support and different pedicle screw fixation, no marked differences in ROM were found for all directions of motion.

Similarly, Chen et al. [79] investigated the influence of bilateral versus unilateral posterior fixation on the biomechanics of the lumbar spine, using FE models subjected to a TLIF approach. Their results indicated that models with left unilateral fixation are subjected to a higher motion when compared with bilateral devices. However, this was only verified for extension, RLB, and RAR. Conversely, in the present work, the decrease in ROM from unilateral to bilateral models was confirmed for all loading directions. Nonetheless, as the surgical approach between both studies is not exactly the same (TLIF approach in Chen et al. versus OLIF approach in the current work), a direct comparison cannot be made. Regarding load-sharing, all TLIF models with left unilateral fixation led to increased AF and screw stresses, when compared with models with bilateral fixation. This increase occurred especially in extension, RAR, RLB, and LAR (this last one only in the case of stress acting on AF). Based on current results, the increase in screw stress in the LUPF model was more evident in extension and flexion. In the remaining movements, there was a decrease in stress. Regarding AF stress, there were also some differences, namely in RLB, for which the load was higher in BPF than LUPF. Chen et al. determined then that the use of unilateral pedicle screw fixation in TLIF surgery is only advised if accompanied by a contralateral facet screw.

5.3.3 Degenerated Instrumented Models

Besides the instrumented models with healthy adjacent IVD, it is also relevant to evaluate models in which the adjacent IVD is degenerated, and understand its implications by comparison with the healthy equivalents. In the present work, only an adjacent mild degeneration was studied.

In both long and short-term analyses, ROM trends were the same in the degenerated or healthy instrumented models; namely, there was a decrease in ROM with the introduction of instrumentation, which was even more pronounced in the model with bilateral fixation. However, ROM reductions from the intact to instrumented models were less enhanced in the degenerated case (Mild-Cage) when compared with the healthy model (H-Cage). In the case of AR, there was a 40% ROM decrease in relation to 55% in the healthy model in long-term simulations.

Comparing ROM absolute values between the degenerated models and their healthy equivalents, there was a ROM increase in extension for all instrumented models with adjacent IVD mildly degenerated. This ROM increase from the healthy equivalents was maximum in the BPF model (41.2% in LT and 16.8% in ST), followed by the unilateral constructs (36.3% and 39.3% in LT, and 8.79% and 9.89% in ST, for LUPF and RUPF, respectively), and finally by the SA model (33.5% in LT and 4.18% in ST). Table 5.19 shows the ROM values of the healthy and degenerated instrumented models for each loading direction in the long-term.

Table 5.19: ROM values (in deg) of the healthy and degenerated instrumented models as a function of movement in long-term simulations. Between brackets are the per cent changes of the degenerated models in relation to the healthy equivalents.

	SA		**RUPF**		**LUPF**		**BPF**	
	H-Cage	Mild-Cage	H-Cage	Mild-Cage	H-Cage	Mild-Cage	H-Cage	Mild-Cage
E	0.50	0.66 (33.5%)	0.41	0.57 (39.3%)	0.42	0.58 (36.3%)	0.38	0.54 (41.2%)
F	1.98	1.97 (-0.49%)	1.94	1.93 (-0.69%)	1.95	1.94 (-0.71%)	1.93	1.91 (-0.70%)
RAR	1.36	2.39 (76.3%)	1.35	2.39 (76.5%)	1.36	2.39 (76.2%)	1.35	2.39 (76.6%)
LLB	1.17	1.66 (42.0%)	1.19	1.68 (41.4%)	1.18	1.67 (41.5%)	1.17	1.67 (41.9%)
RLB	1.13	1.64 (45.1%)	1.10	1.61 (46.7%)	1.10	1.62 (46.4%)	1.09	1.61 (46.8%)
LAR	4.22	3.63 (-14.0%)	4.21	3.62 (-13.9%)	4.22	3.63 (-14.1%)	4.21	3.62 (-14.0%)

In terms of flexion, ROM values slightly decreased from the healthy to the degenerated SA model (0.49% in LT and 0.46% in ST) and decreased further in the models with posterior fixation (around 0.70% in LT and 0.80% in ST). Between the models with different fixation systems, there were no significant differences in ROM variation from the healthy to the degenerated case. In LAR, a similar situation occurred, with a decrease in ROM from the healthy to the degenerated SA model. However, this decrease was more significant than in flexion (14.0% in LT and around 10% in ST) and it remained nearly constant throughout the different instrumented models.

Finally, regarding RAR and LB (in both directions), there was an increase in ROM from the healthy to the degenerated intact model. This trend was maintained in the instrumented models, but with a higher ROM difference. Between the different instrumented models there were no significant differences in ROM variation.

In summary, the spine became less stable in the presence of an adjacent mildly degenerated IVD for all movements, except flexion and LAR. However, ROM values in the intervened L4-L5 level remained approximately the same for healthy and equivalent degenerated models. Variations between healthy and degenerated instrumented models were higher in the long-term.

Regarding load distribution, the degenerated instrumented models also followed the trends of the healthy equivalents. The load supported by the cage was always higher in the SA model, decreasing

with the introduction of posterior fixation. The stress values acting on the cage were very similar between the healthy and respective degenerated models, except for extension, in which the load supported by the cage was considerably higher in the healthy model (12.67 MPa compared to 8.873 MPa in the Mild-Cage SA model). Table 5.20 presents the stress values supported by the cage in the healthy and degenerated instrumented models in long-term simulations. Posterior fixation stresses were very similar between H-Cage and Mild-Cage models. Both cage and posterior fixation stresses in the degenerated models were within the range of safe use regarding instrumentation failure.

Table 5.20: Cage stress values (in MPa) in the healthy and degenerated instrumented models as a function of movement in long-term simulations. Between brackets are the per cent changes of the degenerated models in relation to the healthy equivalents.

	SA		**RUPF**		**LUPF**		**BPF**	
	H-Cage	Mild-Cage	H-Cage	Mild-Cage	H-Cage	Mild-Cage	H-Cage	Mild-Cage
E	12.67	8.873 (-30.0%)	6.520	6.527 (0.11%)	5.792	5.382 (-7.08%)	3.992	3.892 (-2.51%)
F	6.627	6.670 (0.65%)	5.030	5.013 (-0.34%)	5.375	5.382 (0.13%)	4.138	4.144 (0.15%)
RAR	4.061	4.054 (-0.17%)	3.457	3.567 (3.18%)	3.604	3.590 (-0.39%)	3.039	3.066 (0.89%)
LLB	5.681	5.687 (0.11%)	5.614	5.635 (0.37%)	4.473	4.554 (1.81%)	4.248	4.305 (1.34%)
RLB	5.693	5.713 (0.35%)	4.582	4.641 (1.29%)	5.672	5.696 (0.42%)	4.192	4.223 (0.74%)
LAR	4.313	4.100 (-4.93%)	3.093	3.128 (1.31%)	3.945	3.776 (-4.28%)	2.934	2.845 (-3.03%)

Table 5.21: Stress values (in MPa) supported by L3-L4 IVD in the healthy and degenerated instrumented models as a function of movement in long-term simulations. Between brackets are the per cent changes of the degenerated models in relation to the healthy equivalents.

	SA		**RUPF**		**LUPF**		**BPF**	
	H-Cage	Mild-Cage	H-Cage	Mild-Cage	H-Cage	Mild-Cage	H-Cage	Mild-Cage
E	0.2141	0.1230 (-42.6%)	0.2428	0.1142 (-53.0%)	0.2639	0.1008 (-61.8%)	0.2283	0.1172 (-48.6%)
F	0.4116	0.1380 (-66.5%)	0.2670	0.1219 (-54.3%)	0.4821	0.1326 (-72.5%)	0.3138	0.1248 (-60.2%)
RAR	0.3074	0.1803 (-41.3%)	0.3083	0.1824 (-40.8%)	0.3237	0.1849 (-42.9%)	0.2981	0.1737 (-41.7%)
LLB	0.4780	0.3276 (-31.5%)	0.5284	0.3332 (-36.9%)	0.4550	0.3284 (-27.8%)	0.3825	0.3164 (-17.3%)
RLB	0.4232	0.3128 (-26.1%)	0.4177	0.3131 (-25.0%)	0.4133	0.3130 (-24.3%)	0.4257	0.3145 (-26.1%)
LAR	0.0979	0.1131 (15.5%)	0.0988	0.1139 (15.2%)	0.1115	0.1195 (7.16%)	0.0783	0.1119 (43.0%)

In the case of the adjacent IVD, some load trends were also maintained in the mildly degenerated models. Table 5.21 shows the stress values acting on L3-L4 IVD in the healthy and degenerated instrumented models as a function of loading direction in the long-term. Similar trends were observed in short-term simulations. With the introduction of bilateral fixation, load was removed from the IVD, leading to a reduction in stress values from SA to BPF models for all movements. However, load variations were significantly less pronounced throughout instrumented models in the degenerated case when compared to the healthy equivalents, possibly because the loads in the degenerated models were significantly lower than the ones in the healthy models (except for LAR). Figure 5.11 exemplifies this load decrease in the case of flexion in LUPF model. The stress values acting on the adjacent degenerated IVD were considerably smaller than the ones acting on the healthy IVD.

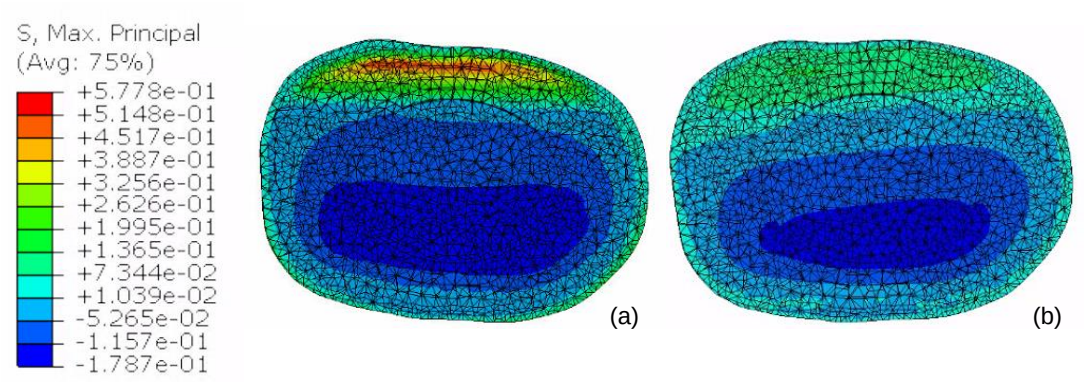

Figure 5.11: Stress values acting on L3-L4 IVD in the (a) healthy and (b) degenerated LUPF models during flexion.

5.3.4 Adjacent Disc Degeneration

ADD is a serious spinal condition since it affects the long-term success of interbody fusion surgery, possibly resulting in the recurrence of LBP and radiculopathy. In some patients, there may be a need for second surgeries to address new symptoms. It is estimated that, after lumbar fusion surgery, up to 20% of patients may experience recurrence of symptoms due to ADD [74]. Although the definite mechanisms of this condition are not yet fully clarified, previous studies have identified increases in ROM and IDP as the most probable causes [107]. In the case of lumbar spinal fusion, it is important to understand whether ADD is promoted by implant insertion and segmental fusion, or if there were already signs of ADD before surgery due to IVD degeneration. Tables 5.22 and 5.23 present the stress and ROM values of the L3-L4 level in degenerated and instrumented models, respectively. Between brackets in Table 5.23 are the per cent changes in relation to the previous model with the same stage of L3-L4 IVD degeneration, since the focus is on changes at the adjacent level due to L4-L5 degeneration.

If the intact degenerated models are considered, there was a decrease in ROM in the top FSU as the degeneration in L4-L5 IVD progressed. For example, from Mild-Mild to Mild-Mod, there was a reduction of almost 35% in mobility at the L3-L4 level. The same trends were verified for the stress acting on the IVD.

Table 5.22: ROM (in deg) and stress (in MPa) at the L3-L4 level in intact degenerated models as a function of movement. Between brackets are the per cent changes in relation to the previous model with the same stage of L3-L4 IVD degeneration.

		H-H	H-Mild	Mild-Mild	H-Mod	Mild-Mod
ROM	E	0.3104	0.3007 (-3.12%)	0.4676	0.3067 (1.98%)	0.3104 (-33.6%)
	F	1.8688	1.8627 (-0.33%)	1.8531	1.8678 (0.28%)	1.8688 (0.85%)
	AR	1.3159	1.3085 (-0.56%)	2.3491	1.3082 (-0.03%)	1.3159 (-44.0%)
	LB	1.1086	1.0935 (-1.36%)	1.6047	1.1041 (0.96%)	1.1086 (-30.9%)
Stress	E	0.2350	0.2324 (-1.11%)	0.1097	0.2340 (0.69%)	0.1102 (0.47%)
	F	0.3719	0.3705 (-0.38%)	0.1387	0.3734 (0.79%)	0.1397 (0.67.%)
	AR	0.3320	0.3319 (-0.02%)	0.1883	0.3318 (-0.05%)	0.1882 (-0.04%)
	LB	0.4026	0.4019 (-0.18%)	0.3175	0.4033 (0.36%)	0.3179 (0.14%)

Table 5.23: ROM (in deg) and stress (in MPa) at the L3-L4 level in instrumented models as a function of movement in long-term simulations. Between brackets are the per cent changes in relation to the SA model (or intact model in the case of SA).

		Intact	SA	RUPF	LUPF	BPF
ROM	E	0.3067	0.3699 (20.6%)	0.3330 (-9.98%)	0.3402 (-8.02%)	0.3190 (-13.8%)
	F	1.8678	1.8822 (0.77%)	1.8718 (-0.55%)	1.8752 (-0.37%)	1.8672 (-0.80%)
	AR	1.3082	1.3137 (0.42%)	1.3150 (0.10%)	1.3166 (0.22%)	1.3154 (0.13%)
	LB	1.1041	1.1482 (4.00%)	1.1537 (0.48%)	1.1526 (0.38%)	1.1469 (-0.11%)
Stress	E	0.2340	0.2141 (-8.52%)	0.2428 (13.4%)	0.2639 (23.3%)	0.2283 (6.64%)
	F	0.3734	0.4116 (10.2%)	0.2670 (-35.1%)	0.4821 (17.1%)	0.3138 (-23.8%)
	AR	0.3318	0.3074 (-7.34)	0.3083 (0.28%)	0.3237 (5.30%)	0.2981 (-3.02%)
	LB	0.4033	0.4780 (18.5%)	0.5284 (10.5%)	0.4550 (-4.80%)	0.3825 (-20.0%)

Regarding instrumented models, there was a significant increase in ROM and adjacent stress when the interbody cage was introduced. In general, the stresses acting on the IVD and ROM values of the top FSU were higher in instrumented models than in degenerated intact models, even if the most advanced stage of degeneration was considered. Therefore, the OLIF procedure presented a higher contribution to ADD than L4-L5 IVD degeneration. The stiffness of the construct and sagittal alignment may be risk factors [108]. The introduction of bilateral fixation may help lessen this contribution since, compared with the remaining instrumented models, the mobility and stresses supported by L3-L4 IVD were decreased.

These outcomes are aligned with the literature. Although some papers suggest that ADD is a result of the natural progression of degeneration and not affected by lumbar fusion [109], the majority show that lumbar fusion plays, in fact, a key role in the development of ADD and that adjacent ROM and IDP increase in this situation [74], [75], [110].

5.4 Discussion Summary

In the second part of this work, an L3-L5 FE model with morphological degeneration was developed and evaluated in terms of its biomechanical performance. ROM values increased in the first

stages of degeneration, following the enhanced elastic response of AF fibres, and then started decreasing as degeneration and IVD stiffness became more pronounced. The only exception occurred for the flexion movement, in which ROM remained the same as in the healthy model for the early stages of degeneration, possibly as a result of the model's morphological changes. In terms of stresses acting on the IVDs, these were lower when the IVDs were mildly degenerated, and increased with advancing degeneration due to IVD stiffening. The loads supported by L3-L4 IVD were in general higher than the ones acting on L4-L5 IVD, possibly due to the closest proximity between L3-L4 IVD and the point of application of the load.

With the introduction of ligament degeneration, similar results to the ones obtained in Part I were verified. FCL was the most restrictive ligament in flexion and AR, and ALL played the most significant role in extension. These findings were more pronounced as the percentage of degeneration increased. ISL and LF also presented small contributions to restrict flexion. Comparing the results from Parts I and II, ROM variations with ligament degeneration were more noticeable in the case WMD, thus showing that increased IVD degeneration, including IVD height reduction, results in increased ligament degeneration. This finding contributes to the assumption that ligament degeneration follows IVD degeneration.

An interbody cage and posterior instrumentation were posteriorly introduced in the model WMD to study the OLIF procedure and determine the most advantageous type of fixation for clinical practice. The SA model did not ensure solid fixation, and additional posterior fixation (pedicle screws, in this particular case) was required to distribute the load across the different structures and relieve the stress acting on the cage, avoiding implant migration or subsidence [78]. With interbody fusion, the probability of upper adjacent degeneration increased since ROM and the stress acting on the AF also increased at the L3-L4 level. The influence of the OLIF procedure on L3-L4 IVD degeneration was more severe than that resulting from L4-L5 progressive degeneration.

Both in long and short-term simulations there was increased stability with the use of posterior fixation: ROM decreased from the SA model to the models with unilateral constructs, and even further with bilateral fixation. However, ROM absolute values were significantly lower in the long-term since complete spinal fusion was achieved in this case. It is therefore important to confirm if short-term ROM values are within the range of acceptable physiological values, or if the motion is too exaggerated and may become an opposing force to the process of osseointegration. Actually, movements of bending and torsion of the spine are not allowed during the first weeks after surgery, and movements of low magnitude should be exerted during the recovery period [20], [111]. This is a way of limiting spinal mobility and stimulating the process of osseointegration. In this work, a higher moment was used, equal to the one applied in healthy spines, to enable comparison between short and long-term simulations. Following the decrease in ROM, the introduction of posterior fixation also allowed to reduce the stress acting on the cage and the adjacent IVD, particularly when bilateral fixation was used. In the case of L3-L4 IVD, bilateral fixation helped reduced the stress to values lower than the intact model, which may be beneficial to oppose the progression of degeneration on the adjacent level.

Therefore, to choose between unilateral and bilateral posterior fixation devices, different aspects must be taken into consideration. On one hand, unilateral devices involve less damage to the

paravertebral muscles, no tissue dissection on the contralateral side, and less perioperative bleeding. Therefore, there is a decrease in postoperative complications and pain, quicker patient recovery, and low instrument expenses. On the other hand, with bilateral fixation, there is increased morbidity, with higher risk of vascular or neurologic injury, but also increased spinal stability and lower stresses [78], [79]. Some studies have found unilateral instrumentation to be as effective as bilateral systems, with clinical studies indicating similar rates of fusion and implant failure for both constructs [6], [80], [112]–[114]. Other biomechanical and FE studies have shown bilateral fixation systems to provide greater spinal and implant stability [78], [79], [115]–[117]. Aoki et al. [118] examined 125 patients with lumbar DDD following a TLIF approach and found out that the incidence of cage migration was higher in patients with unilateral (8.3%) than with bilateral fixation (2.1%).

In the present work, from a biomechanical perspective, the bilateral construct was more favourable than the unilateral one since it provided greater stability and lower stresses acting on the adjacent IVD and instrumentation, avoiding cage subsidence, or migration, and ADD. However, from a clinical point of view, if the patient respects the recovery period and avoids excessive movements, there will probably be no significant differences in osseointegration and risk of screw failure between both constructs in the long-term. In this case, the unilateral fixation device would be the best option to minimise morbidity and associated costs [119]. There were no significant differences or trends to choose between right or left unilateral constructs, with both presenting similar levels of stability (similar ROM values). However, there was evidence that models with left unilateral constructs lead to higher stress values on the adjacent IVD, compared with right unilateral models, in which the stress is higher in the instrumentation. Therefore, right unilateral fixation devices may be a good option over left constructs to avoid IVD overload and the acceleration of adjacent degeneration. This finding supports clinical practice.

If degeneration is considered on the adjacent IVD, the spine became less stable for all loading directions, except flexion and LAR, and stress values acting on the IVD were smaller than the ones acting on a healthy IVD. Variations between healthy and degenerated instrumented models were higher in the long-term.

Regarding the role of ligaments, these structures present a restrictive behaviour in the short-term. They maintain the cage in place and avoid its migration, contributing to spinal fusion. In the long-term, since everything is completely osseointegrated, ligaments become obsolete. However, when possible, ligaments should be maintained in their original condition/position, as they can aid in the short-term fusion process.

Chapter 6

Conclusions and Future Work

6.1 Conclusions

This work provides a new perspective on how degeneration and interbody fusion influence spinal stability, taking advantage of the insights that numerical simulations can provide for multiple situations.

FCL and ALL were determined to be the most influential ligaments in spinal stability, but the importance of the last was diluted with degeneration. The compensation mechanisms identified here, when ligaments are removed and/or degeneration progresses, along with adjacent level degeneration, are very relevant factors to be accounted for in clinical practice and potentially for fusion surgery recommendations. Moreover, the procedure for ligament degeneration established in this work and the finding that ligament degeneration follows IVD degeneration may be useful for future FE studies.

Current results showed that morphological degeneration, namely IVD height reduction, together with changes in material properties lead to increasing ROM values in the early stages of degeneration (due to increased response from AF elastic fibres), which then decrease as degeneration progresses and the IVD stiffens. This behaviour was also verified in the model WOMD, thus not being triggered by morphological degeneration in particular. The main difference caused by morphological degeneration occurred for the flexion movement. In this case, in the first degeneration stage, ROM remained the same as in the healthy model because IVD height reduction prevented ROM from further increase. Absolute ROM values were lower in the model WMD for all loading directions due to increased IVD stiffness. The motion will be hence hampered when compared with a model with a lower degree of degeneration as the model WOMD. The trends in supported loads and ligament degeneration were the same in both models, but ROM variations were more pronounced in the model WMD. In flexion, the contribution of other ligaments, such as ISL and LF, also became more significant for motion restriction.

Regarding instrumented models, for the OLIF procedure, it was shown that a stand-alone cage is not sufficient to provide solid stability and supplementary fixation must be introduced. From a biomechanical perspective, bilateral fixation is the best option since maximum stability and lowest stresses are achieved with this fixation system. From a clinical perspective, unilateral fixation would be preferable due to its lowest morbidity. Models with left and right unilateral constructs presented similar ROM values, but the models with fixation on the left side resulted in higher stresses on the adjacent IVD. Therefore, right unilateral fixation may be a good option over left constructs to reduce IVD stress and degeneration, possibly because there is an additional support on the left side due to cage asymmetry. In all cases, ligaments help to keep the cage in place before spinal fusion occurs, but they lose function as osseointegration is achieved.

This work also showed that instrument placement has a stronger influence on the degeneration of the adjacent level than the degeneration of the pre-instrumented L4-L5 IVD. Therefore, interbody fusion is a major contributing factor to ADD progression.

6.2 Limitations and Future Work

In future studies, some factors should be improved since they may deepen the outcomes of the present work. In current simulations, ligaments were modelled as linear elastic, despite bilinear or non-linear approaches being available in the literature [8], [10], [60], [98], [120]. Nonetheless, given that currently there are no FE studies focused on spinal ligament degeneration, this can be considered a good first approach to the problem, avoiding imprecisions in material modelling, as already performed in previous studies [54], [55]. IVD and instrumentation modelling was also simplified. Regarding IVD, the visco- and poroelastic phenomena that past works have already mimicked were not included [61], [87], [121], hence, outcomes such as intradiscal pressure variation could not be accurately obtained. Additionally, the vertebral endplates were also not included in the models, as a simplification, but they should be considered in future studies given that changes in their structure and area are very connected with the progression of degeneration. In terms of instrumentation, the screw thread and the teeth on the cage surface were not represented, which may affect the outcomes, namely in the short-term simulations. Nevertheless, different interaction constraints were applied to approximate these structures.

Between instrumented models with unilateral fixation systems, there were no significant differences in terms of stability in the current results (only in terms of supported loads due to cage asymmetry). However, the developed models did not include representation of the musculature or surrounding organs. These structures may offer additional support to the intervened level, mostly from a given side, thus favouring the introduction of posterior fixation on the contralateral one. In this case, differences in stability between different models could be enhanced.

Lastly, the models in the present study are composed of only two motion segments, which is only an approximation of the lumbar spine and does not consider the full extent of the possible influence of adjacent levels. This type of model also forces the boundary conditions to be applied in L5, restricting the movement of this level, as opposed to what would happen if the BCs were applied in the sacrum of the full spine. Nonetheless, models of a few motion segments have already been considered in the literature to study degeneration [12], [69], [72], [73].

For future work, the order of ligament removal should be evaluated to determine whether it may or may not be neglected when analysing simulation outcomes. Although in this work simulations were performed in which ALL was the first and the last ligament to be removed and the obtained results were very similar, it is not guaranteed that the order of removal does not influence the outcomes, since the remaining ligaments may induce different effects. Therefore, it would be interesting to perform further simulations regarding ligament removal, first in a model without any ligaments other than the test ligament to be removed, and then in a model with all ligaments, in which the test ligament would be removed from the intact model. In this way, it would be possible to first evaluate the true removal effect of the individual test ligament, and then the possible compensation mechanisms that could be exerted

by all remaining ligaments. This approach becomes more consistent than removing ligaments in sets and in arbitrary stages, which can influence the obtained outcomes. Extension of the models to the full lumbar spine including new patient data, with different levels/types of degeneration, will also have to be explored.

Regarding degeneration of spinal structures, the next step would be the introduction of osteoporosis as this is also an age-related condition that will most likely affect spine behaviour and may be interconnected with IVD degeneration [93], [94]. Moreover, regarding the instrumented models, it would be interesting to study the impact of the lordotic angle on the obtained results since there is evidence that increased angles of the interbody cage act to reduce the maximum Von Mises stress at the adjacent level, whereas a decrease in lordotic angle may accelerate ADD [122].

References

[1] F. Balagué, B. Troussier, and J. J. Salminen, “Non-specific low back pain in children and adolescents: risk factors,” *Eur. Spine J.*, vol. 8, no. 6, pp. 429–438, Dec. 1999.

[2] J. Widmer, F. Cornaz, G. Scheibler, J. M. Spirig, J. G. Snedeker, and M. Farshad, “Biomechanical contribution of spinal structures to stability of the lumbar spine—novel biomechanical insights,” *Spine J.*, May 2020.

[3] M. M. Panjabi, “A hypothesis of chronic back pain: ligament subfailure injuries lead to muscle control dysfunction,” *Eur. Spine J.*, vol. 15, no. 5, pp. 668–676, May 2006.

[4] B. W. Koes, M. W. van Tulder, and S. Thomas, “Diagnosis and Treatment of Low Back Pain,” *J. Orthop. Trauma*, vol. 6, no. 3, p. 395, Sep. 1992.

[5] D. V. Patel, J. S. Yoo, S. S. Karmarkar, E. H. Lamoutte, and K. Singh, “Interbody options in lumbar fusion,” *J. Spine Surg.*, vol. 5, no. S1, pp. S19–S24, Jun. 2019.

[6] J. Godzik *et al.*, “Biomechanical Stability Afforded by Unilateral Versus Bilateral Pedicle Screw Fixation with and without Interbody Support Using Lateral Lumbar Interbody Fusion,” *World Neurosurg.*, vol. 113, pp. e439–e445, May 2018.

[7] W. M. Park, K. Kim, and Y. H. Kim, “Effects of degenerated intervertebral discs on intersegmental rotations, intradiscal pressures, and facet joint forces of the whole lumbar spine,” *Comput. Biol. Med.*, vol. 43, no. 9, pp. 1234–1240, Sep. 2013.

[8] E. Ibarz, Y. Más, J. Mateo, A. Lobo-Escolar, A. Herrera, and L. Gracia, “Instability of the lumbar spine due to disc degeneration. A finite element simulation,” *Adv. Biosci. Biotechnol.*, vol. 04, no. 04, pp. 548–556, 2013.

[9] A. Rohlmann, T. Zander, H. Schmidt, H.-J. Wilke, and G. Bergmann, “Analysis of the influence of disc degeneration on the mechanical behaviour of a lumbar motion segment using the finite element method,” *J. Biomech.*, vol. 39, no. 13, pp. 2484–2490, Jan. 2006.

[10] A. M. Ellingson, M. N. Shaw, H. Giambini, and K.-N. An, “Comparative role of disc degeneration and ligament failure on functional mechanics of the lumbar spine,” *Comput. Methods Biomech. Biomed. Engin.*, vol. 19, no. 9, pp. 1009–1018, Jul. 2016.

[11] F. Heuer, H. Schmidt, Z. Klezl, L. Claes, and H.-J. Wilke, “Stepwise reduction of functional spinal structures increase range of motion and change lordosis angle,” *J. Biomech.*, vol. 40, no. 2, pp. 271–280, Jan. 2007.

[12] T. Zander, A. Rohlmann, and G. Bergmann, “Analysis of Simulated Single Ligament Transection on the Mechanical Behaviour of a Lumbar Functional Spinal Unit / Rechnerische Analyse des Einflusses der Bänder auf das mechanische Verhalten eines Bewegungssegments der Lendenwirbelsäule,” *Biomed. Tech. Eng.*, vol. 49, no. 1–2, pp. 27–32, Jan. 2004.

[13] G. Tortora and B. Derrickson, *Introduction to the Human Body. The Essentials of Anatomy and Physiology*, 9th ed. John Wiley & Sons, 2012.

[14] F. H. Netter, *Atlas of Human Anatomy*, 7th ed. Elsevier, 2018.

[15] S. Standring, *Gray's Anatomy: The Anatomical Basis of Clinical Practice*, 41st ed. Elsevier, 2016.

[16] A. Castro, "Development of a biomimetic finite element model of the intervertebral disc diseases and regeneration," p. 235, 2013.

[17] N. Palastanga and R. W. Soames, *Anatomy and Human Movement: Structure and function*, 6th ed. Elsevier, 2012.

[18] M. Papadakis, "Pathophysiology and Biomechanics of the Aging Spine," *Open Orthop. J.*, vol. 5, no. 1, pp. 335–342, Sep. 2011.

[19] B. R. Whatley and X. Wen, "Intervertebral disc (IVD): Structure, degeneration, repair and regeneration," *Mater. Sci. Eng. C*, vol. 32, no. 2, pp. 61–77, Mar. 2012.

[20] A. A. White III and M. M. Panjabi, *Clinical Biomechanics of the Spine*, 2nd ed. 1990.

[21] R. L. Drake, A. W. Vogl, and A. W. M. Mitchell, *Gray`s Anatomy for Students*, 4th ed. Elsevier, 2020.

[22] G. D. O'Connell, S. Sen, and D. M. Elliott, "Human annulus fibrosus material properties from biaxial testing and constitutive modeling are altered with degeneration," *Biomech. Model. Mechanobiol.*, vol. 11, no. 3–4, pp. 493–503, Mar. 2012.

[23] V. M. Ravindra *et al.*, "Degenerative Lumbar Spine Disease: Estimating Global Incidence and Worldwide Volume," *Glob. Spine J.*, vol. 8, no. 8, pp. 784–794, Dec. 2018.

[24] S. Ganesan, A. S. Acharya, R. Chauhan, and S. Acharya, "Prevalence and Risk Factors for Low Back Pain in 1,355 Young Adults: A Cross-Sectional Study," *Asian Spine J.*, vol. 11, no. 4, pp. 610–617, Aug. 2017.

[25] S. Y. Lee, T.-H. Kim, J. K. Oh, S. J. Lee, and M. S. Park, "Lumbar Stenosis: A Recent Update by Review of Literature," *Asian Spine J.*, vol. 9, no. 5, p. 818, 2015.

[26] C. K. Lee and N. A. Langrana, "Lumbosacral Spinal Fusion A Biomechanical Study," *Spine (Phila. Pa. 1976).*, vol. 9, no. 6, pp. 574–581, Sep. 1984.

[27] R. J. Mobbs, K. Phan, G. Malham, K. Seex, and P. J. Rao, "Lumbar interbody fusion: techniques, indications and comparison of interbody fusion options including PLIF, TLIF, MI-TLIF, OLIF/ATP, LLIF and ALIF.," *J. spine Surg. (Hong Kong)*, vol. 1, no. 1, pp. 2–18, 2015.

[28] B. J. C. Freeman and J. Davenport, "Total disc replacement in the lumbar spine: a systematic review of the literature," *Eur. Spine J.*, vol. 15, no. S3, pp. 439–447, Aug. 2006.

[29] S. L. de Kunder, K. Rijkers, I. J. M. H. Caelers, R. A. de Bie, P. J. Koehler, and H. van Santbrink,

"Lumbar Interbody Fusion," *Spine (Phila. Pa. 1976).*, vol. 43, no. 16, pp. 1161–1168, Aug. 2018.

[30] R. A. Hibbs and L. F. Peltier, "A report of fifty-nine cases of scoliosis treated by the fusion operation," *Clin. Orthop. Relat. Res.*, Apr. 1988.

[31] F. H. Albee, "Transplantation of a Portion of the Tibia Into the Spine for Pott's Disease," *Clin. Orthop. Relat. Res.*, vol. 460, pp. 14–16, Jul. 2007.

[32] D. King, "Internal fixation for lumbosacral fusion," *J. Bone Jt. Surg.*, vol. 30, no. 3, pp. 560–578, Jul. 1948.

[33] H. H. Boucher, "A method of spinal fusion," *J. Bone Joint Surg. Br.*, vol. 41-B, no. 2, pp. 248–259, May 1959.

[34] M. B. Kabins and J. N. Weinstein, "The history of vertebral screw and pedicle screw fixation," *Iowa Orthop. J.*, vol. 11, p. 127, 1991.

[35] T. Oktenoglu *et al.*, "Pedicle screw-based posterior dynamic stabilisation of the lumbar spine: in vitro cadaver investigation and a finite element study," *Comput. Methods Biomech. Biomed. Engin.*, vol. 18, no. 11, pp. 1252–1261, Aug. 2015.

[36] A. Rohlmann, N. K. Burra, T. Zander, and G. Bergmann, "Comparison of the effects of bilateral posterior dynamic and rigid fixation devices on the loads in the lumbar spine: a finite element analysis," *Eur. Spine J.*, vol. 16, no. 8, pp. 1223–1231, Aug. 2007.

[37] K. Phan and R. J. Mobbs, "Evolution of Design of Interbody Cages for Anterior Lumbar Interbody Fusion," *Orthop. Surg.*, vol. 8, no. 3, pp. 270–277, Aug. 2016.

[38] H. Wang, W. Chen, J. Jiang, F. Lu, X. Ma, and X. Xia, "Analysis of the correlative factors in the selection of interbody fusion cage height in transforaminal lumbar interbody fusion," *BMC Musculoskelet. Disord.*, vol. 17, no. 1, p. 9, Dec. 2016.

[39] DePuy Synthes, "Oracle Cage System - Surgical Tecnhique."

[40] M. van Dijk, T. H. Smit, S. Sugihara, E. H. Burger, and P. I. Wuisman, "The Effect of Cage Stiffness on the Rate of Lumbar Interbody Fusion," *Spine (Phila. Pa. 1976).*, vol. 27, no. 7, pp. 682–688, Apr. 2002.

[41] R. A. Gittens, R. Olivares-Navarrete, Z. Schwartz, and B. D. Boyan, "Implant osseointegration and the role of microroughness and nanostructures: Lessons for spine implants," *Acta Biomater.*, vol. 10, no. 8, pp. 3363–3371, Aug. 2014.

[42] M. J. Fagan, S. Julian, and A. M. Mohsen, "Finite element analysis in spine research," *Proc. Inst. Mech. Eng. Part H J. Eng. Med.*, vol. 216, no. 5, pp. 281–298, May 2002.

[43] W. A. M. Brekelmans, H. W. Poort, and T. J. J. H. Slooff, "A New Method to Analyse the Mechanical Behaviour of Skeletal Parts," *Acta Orthop. Scand.*, vol. 43, no. 5, pp. 301–317, Jan. 1972.

[44] T. Belytschko, R. F. Kulak, A. B. Schultz, and J. O. Galante, “Finite element stress analysis of an intervertebral disc,” *J. Biomech.*, vol. 7, no. 3, pp. 277–285, May 1974.

[45] R. F. Kulak, T. B. Belytschko, A. B. Schultz, and J. O. Galante, “Nonlinear behavior of the human intervertebral disc under axial load,” *J. Biomech.*, vol. 9, no. 6, pp. 377–386, Jan. 1976.

[46] N. S. Hakim and A. I. King, “A computer-aided technique for the generation of a 3-D finite element model of a vertebra,” *Comput. Biol. Med.*, vol. 8, no. 3, pp. 187–196, 1978.

[47] N. S. Hakim and A. I. King, “A three dimensional finite element dynamic response analysis of a vertebra with experimental verification,” *J. Biomech.*, vol. 12, no. 4, pp. 277–292, Jan. 1979.

[48] K. J. Bozic, J. H. Keyak, H. B. Skinner, U. H. Bueff, and D. S. Bradford, “Three-Dimensional Finite Element Modeling of a Cervical Vertebra,” *J. Spinal Disord.*, vol. 7, no. 2, pp. 102–110, Apr. 1994.

[49] S. A. Shirazi-Adl, S. C. Shrivastava, and A. M. Ahmed, “Stress Analysis of the Lumbar Disc-Body Unit in Compression A Three-Dimensional Nonlinear Finite Element Study,” *Spine (Phila. Pa. 1976).*, vol. 9, no. 2, pp. 120–134, Mar. 1984.

[50] B. R. Simon, J. S. S. Wu, M. W. Carlton, J. H. Evans, and L. E. Kazarian, “Structural Models for Human Spinal Motion Segments Based on a Poroelastic View of the Intervertebral Disk,” *J. Biomech. Eng.*, vol. 107, no. 4, pp. 327–335, Nov. 1985.

[51] J. P. Laible, D. S. Pflaster, M. H. Krag, B. R. Simon, and L. D. Haugh, “A Poroelastic-Swelling Finite Element Model With Application to the Intervertebral Disc,” *Spine (Phila. Pa. 1976).*, vol. 18, no. 5, pp. 659–670, Apr. 1993.

[52] J. L. Wang, M. Parnianpour, A. Shirazi-Adl, A. E. Engin, S. Li, and A. Patwardhan, “Development and validation of a viscoelastic finite element model of an L2/L3 motion segment,” *Theor. Appl. Fract. Mech.*, vol. 28, no. 1, pp. 81–93, 1997.

[53] C. Breau, A. Shirazi-Adl, and J. de Guise, “Reconstruction of a human ligamentous lumbar spine using CT images — A three-dimensional finite element mesh generation,” *Ann. Biomed. Eng.*, vol. 19, no. 3, pp. 291–302, May 1991.

[54] E. Demir, P. Eltes, A. P. G. Castro, D. Lacroix, and İ. Toktaş, “Finite element modelling of hybrid stabilization systems for the human lumbar spine,” *Proc. Inst. Mech. Eng. Part H J. Eng. Med.*, vol. 234, no. 12, pp. 1409–1420, Dec. 2020.

[55] S.-H. Chen, C.-L. Tai, C.-Y. Lin, P.-H. Hsieh, and W.-P. Chen, “Biomechanical comparison of a new stand-alone anterior lumbar interbody fusion cage with established fixation techniques – a three-dimensional finite element analysis,” *BMC Musculoskelet. Disord.*, vol. 9, no. 1, p. 88, Dec. 2008.

[56] V. K. Goel, B. T. Monroe, L. G. Gilbertson, and P. Brinckmann, “Interlaminar Shear Stresses and Laminae Separation in a Disc,” *Spine (Phila. Pa. 1976).*, vol. 20, no. 6, pp. 689–698, Mar. 1995.

[57] A. Shirazi-Adl, A. M. Ahmed, and S. C. Shrivastava, “Mechanical Response of a Lumbar Motion Segment in Axial Torque Alone and Combined with Compression,” *Spine (Phila. Pa. 1976).*, vol. 11, no. 9, pp. 914–927, Nov. 1986.

[58] S. Naserkhaki, J. L. Jaremko, S. Adeeb, and M. El-Rich, “On the load-sharing along the ligamentous lumbosacral spine in flexed and extended postures: Finite element study,” *J. Biomech.*, vol. 49, no. 6, pp. 974–982, Apr. 2016.

[59] A. Rohlmann, L. Bauer, T. Zander, G. Bergmann, and H.-J. Wilke, “Determination of trunk muscle forces for flexion and extension by using a validated finite element model of the lumbar spine and measured in vivo data,” *J. Biomech.*, vol. 39, no. 6, pp. 981–989, Jan. 2006.

[60] L. M. Ruberté, R. N. Natarajan, and G. B. Andersson, “Influence of single-level lumbar degenerative disc disease on the behavior of the adjacent segments—A finite element model study,” *J. Biomech.*, vol. 42, no. 3, pp. 341–348, Feb. 2009.

[61] F. Galbusera, H. Schmidt, C. Neidlinger-Wilke, A. Gottschalk, and H.-J. Wilke, “The mechanical response of the lumbar spine to different combinations of disc degenerative changes investigated using randomized poroelastic finite element models,” *Eur. Spine J.*, vol. 20, no. 4, pp. 563–571, Apr. 2011.

[62] A. L. Nachemson and J. H. Evans, “Some mechanical properties of the third human lumbar interlaminar ligament (ligamentum flavum),” *J. Biomech.*, vol. 1, no. 3, pp. 211–220, Aug. 1968.

[63] P. Neumann, L. A. Ekström, T. S. Keller, L. Perry, and T. H. Hansson, “Aging, vertebral density, and disc degeneration alter the tensile stress-strain characteristics of the human anterior longitudinal ligament,” *J. Orthop. Res.*, vol. 12, no. 1, pp. 103–112, Jan. 1994.

[64] G. Keorochana *et al.*, “Magnetic resonance imaging grading of interspinous ligament degeneration of the lumbar spine and its relation to aging, spinal degeneration, and segmental motion,” *J. Neurosurg. Spine*, vol. 13, no. 4, pp. 494–499, Oct. 2010.

[65] E. M. K. . Barros, C. J. Rodrigues, N. R. Rodrigues, R. P. Oliveira, T. E. P. Barros, and A. J. Rodrigues, “Aging of the elastic and collagen fibers in the human cervical interspinous ligaments,” *Spine J.*, vol. 2, no. 1, pp. 57–62, Jan. 2002.

[66] M. Yamada *et al.*, “Age-Related Changes of Elements and Relationships Among Elements in Human Tendons and Ligaments,” *Biol. Trace Elem. Res.*, vol. 98, no. 2, pp. 129–142, 2004.

[67] R. Gunzburg, W. C. Hutton, G. Crane, and R. D. Fraser, “Role of the Capsulo-Ligamentous Structures in Rotation and Combined Flexion-Rotation of the Lumbar Spine,” *J. Spinal Disord.*, vol. 5, no. 4, pp. 1–7, Mar. 1992.

[68] M. A. Adams and W. C. Hutton, “The Relevance of Torsion to the Mechanical Derangement of the Lumbar Spine,” *Spine (Phila. Pa. 1976).*, vol. 6, no. 3, pp. 241–248, May 1981.

[69] M. Sharma, N. A. Langrana, and J. Rodriguez, “Role of Ligaments and Facets in Lumbar Spinal

Stability," *Spine (Phila. Pa. 1976).*, vol. 20, no. 8, pp. 887–900, Apr. 1995.

[70] M. R. Gudavalli and J. J. Triano, "An analytical model of lumbar motion segment in flexion," *J. Manipulative Physiol. Ther.*, vol. 22, no. 4, pp. 201–208, May 1999.

[71] M. A. Adams, W. C. Hutton, and J. R. R. Stott, "The Resistance to Flexion of the Lumbar Intervertebral Joint," *Spine (Phila. Pa. 1976).*, vol. 5, no. 3, pp. 245–253, May 1980.

[72] S. Naserkhaki, N. Arjmand, A. Shirazi-Adl, F. Farahmand, and M. El-Rich, "Effects of eight different ligament property datasets on biomechanics of a lumbar L4-L5 finite element model," *J. Biomech.*, vol. 70, pp. 33–42, Mar. 2018.

[73] Y. Alapan, C. Demir, T. Kaner, R. Guclu, and S. İnceoğlu, "Instantaneous center of rotation behavior of the lumbar spine with ligament failure," *J. Neurosurg. Spine*, vol. 18, no. 6, pp. 617–626, Jun. 2013.

[74] S. Jiang and W. Li, "Biomechanical study of proximal adjacent segment degeneration after posterior lumbar interbody fusion and fixation: a finite element analysis," *J. Orthop. Surg. Res.*, vol. 14, no. 1, p. 135, Dec. 2019.

[75] S. Tang and B. J. Rebholz, "Does anterior lumbar interbody fusion promote adjacent degeneration in degenerative disc disease? A finite element study," *J. Orthop. Sci.*, vol. 16, no. 2, pp. 221–228, Mar. 2011.

[76] F. Galbusera, H. Schmidt, and H.-J. Wilke, "Lumbar interbody fusion: a parametric investigation of a novel cage design with and without posterior instrumentation," *Eur. Spine J.*, vol. 21, no. 3, pp. 455–462, Mar. 2012.

[77] A. C. Y. Loenen *et al.*, "Misaligned spinal rods can induce high internal forces consistent with those observed to cause screw pullout and disc degeneration," *Spine J.*, pp. 1–10, Sep. 2020.

[78] H. Guo *et al.*, "Stability Evaluation of Oblique Lumbar Interbody Fusion Constructs with Various Fixation Options: A Finite Element Analysis Based on Three-Dimensional Scanning Models," *World Neurosurg.*, vol. 138, pp. e530–e538, Jun. 2020.

[79] S.-H. Chen, S.-C. Lin, W.-C. Tsai, C.-W. Wang, and S.-H. Chao, "Biomechanical comparison of unilateral and bilateral pedicle screws fixation for transforaminal lumbar interbody fusion after decompressive surgery -- a finite element analysis," *BMC Musculoskelet. Disord.*, vol. 13, no. 1, p. 72, Dec. 2012.

[80] D. Chen *et al.*, "Unilateral versus Bilateral Pedicle Screw Fixation Combined with Transforaminal Lumbar Interbody Fusion for the Treatment of Low Lumbar Degenerative Disc Diseases: Analysis of Clinical and Radiographic Results," *World Neurosurg.*, vol. 115, pp. e516–e522, Jul. 2018.

[81] T. Zander, A. Rohlmann, C. Klöckner, and G. Bergmann, "Comparison of the mechanical behavior of the lumbar spine following mono- and bisegmental stabilization," *Clin. Biomech.*, vol.

17, no. 6, pp. 439–445, Jul. 2002.

[82] V. Carvalho, “Finite element modelling of innovative interspinous process spacers for the lumbar spine Biomedical Engineering,” Instituto Superior Técnico, 2019.

[83] B. Yu, C. Zhang, C. Qin, and H. Yuan, “FE modeling and analysis of L4-L5 lumbar segment under physiological loadings,” *Technol. Heal. Care*, vol. 23, no. s2, pp. S383–S396, Jun. 2015.

[84] R. Eberlein, G. A. Holzapfel, and M. Fröhlich, “Multi-segment FEA of the human lumbar spine including the heterogeneity of the annulus fibrosus,” *Comput. Mech.*, vol. 34, no. 2, pp. 147–163, Jul. 2004.

[85] C.-S. Chen, C.-K. Feng, C.-K. Cheng, M.-J. Tzeng, C.-L. Liu, and W.-J. Chen, “Biomechanical Analysis of the Disc Adjacent to Posterolateral Fusion with Laminectomy in Lumbar Spine,” *J. Spinal Disord. Tech.*, vol. 18, no. 1, pp. 58–65, Feb. 2005.

[86] S. Saleem, H. M. Aslam, M. A. K. Rehmani, A. Raees, A. A. Alvi, and J. Ashraf, “Lumbar Disc Degenerative Disease: Disc Degeneration Symptoms and Magnetic Resonance Image Findings,” *Asian Spine J.*, vol. 7, no. 4, p. 322, 2013.

[87] A. P. G. Castro, W. Wilson, J. M. Huyghe, K. Ito, and J. L. Alves, “Intervertebral disc creep behavior assessment through an open source finite element solver,” *J. Biomech.*, vol. 47, no. 1, pp. 297–301, Jan. 2014.

[88] M. M. Panjabi, V. K. Goel, and K. Takata, “Physiologic Strains in the Lumbar Spinal Ligaments,” *Spine (Phila. Pa. 1976).*, vol. 7, no. 3, pp. 192–203, May 1982.

[89] W. C. Whiting and R. F. Zernicke, *Biomechanics of Musculoskeletal Injury*. Human Kinetics Publishers, 2008.

[90] A. Polikeit, L. P. Nolte, and S. J. Ferguson, “Simulated influence of osteoporosis and disc degeneration on the load transfer in a lumbar functional spinal unit,” *J. Biomech.*, vol. 37, no. 7, pp. 1061–1069, Jul. 2004.

[91] L. R. Amundsen, *Geriatric Rehabilitation Manual - Effects of age on joints and ligaments*. Elsevier Health Sciences, 2007.

[92] F. Galbusera *et al.*, “Material Models and Properties in the Finite Element Analysis of Knee Ligaments: A Literature Review,” *Front. Bioeng. Biotechnol.*, vol. 2, no. NOV, pp. 1–11, Nov. 2014.

[93] M. A. Adams and P. Dolan, “Recent advances in lumbar spinal mechanics and their clinical significance,” *Clin. Biomech.*, vol. 10, no. 1, pp. 3–19, Jan. 1995.

[94] R. Korez, B. Ibragimov, B. Likar, F. Pernus, and T. Vrtovec, “A Framework for Automated Spine and Vertebrae Interpolation-Based Detection and Model-Based Segmentation,” *IEEE Trans. Med. Imaging*, vol. 34, no. 8, pp. 1649–1662, Aug. 2015.

[95] P. A. Yushkevich *et al.*, “User-guided 3D active contour segmentation of anatomical structures: Significantly improved efficiency and reliability,” *Neuroimage*, vol. 31, no. 3, pp. 1116–1128, 2006.

[96] P. Cignoni, M. Callieri, M. Corsini, M. Dellepiane, F. Ganovelli, and G. Ranzuglia, “MeshLab: An open-source mesh processing tool,” *6th Eurographics Ital. Chapter Conf. 2008 - Proc.*, pp. 129–136, 2008.

[97] B. Weisse, A. K. Aiyangar, C. Affolter, R. Gander, G. P. Terrasi, and H. Ploeg, “Determination of the translational and rotational stiffnesses of an L4–L5 functional spinal unit using a specimen-specific finite element model,” *J. Mech. Behav. Biomed. Mater.*, vol. 13, pp. 45–61, Sep. 2012.

[98] S. Naserkhaki, J. L. Jaremko, and M. El-Rich, “Effects of inter-individual lumbar spine geometry variation on load-sharing: Geometrically personalized Finite Element study,” *J. Biomech.*, vol. 49, no. 13, pp. 2909–2917, Sep. 2016.

[99] Medtronic, “Oblique Lateral Interbody Fusion For L2 to L5 Surgical Technique.”

[100] J. Real, “Biomechanical Analysis of Fixation Devices for Lumbar Interbody Fusion,” Instituto Superior Técnico, 2019.

[101] F. Ghezelbash, H. Schmidt, A. Shirazi-Adl, and M. El-Rich, “Internal load-sharing in the human passive lumbar spine: Review of in vitro and finite element model studies,” *J. Biomech.*, vol. 102, p. 109441, Mar. 2020.

[102] M. Mimura, M. M. Panjabi, T. R. Oxland, J. J. Crisco, I. Yamamoto, and A. Vasavada, “Disc Degeneration Affects the Multidirectional Flexibility of the Lumbar Spine,” *Spine (Phila. Pa. 1976).*, vol. 19, no. 12, pp. 1371–1380, Jun. 1994.

[103] N. Tanaka, H. S. An, T.-H. Lim, A. Fujiwara, C.-H. Jeon, and V. M. Haughton, “The relationship between disc degeneration and flexibility of the lumbar spine,” *Spine J.*, vol. 1, no. 1, pp. 47–56, Jan. 2001.

[104] A. Fujiwara *et al.*, “The Effect of Disc Degeneration and Facet Joint Osteoarthritis on the Segmental Flexibility of the Lumbar Spine,” *Spine (Phila. Pa. 1976).*, vol. 25, no. 23, pp. 3036–3044, Dec. 2000.

[105] W. Wu, P. Geng, G. Li, D. Zhao, H. Zhang, and J. Zhao, “Influence of Layer Thickness and Raster Angle on the Mechanical Properties of 3D-Printed PEEK and a Comparative Mechanical Study between PEEK and ABS,” *Materials (Basel).*, vol. 8, no. 9, pp. 5834–5846, Sep. 2015.

[106] M. Niinomi, “Mechanical properties of biomedical titanium alloys,” *Mater. Sci. Eng. A*, vol. 243, no. 1–2, pp. 231–236, Mar. 1998.

[107] C. S. Lee *et al.*, “Risk factors for adjacent segment disease after lumbar fusion,” *Eur. Spine J.*, vol. 18, no. 11, pp. 1637–1643, 2009.

[108] M.-A. Rousseau and J.-Y. Lazennec, “Degenerative disease supra- and infra-jacent to fused lumbar and lumbo-sacral levels,” *Orthop. Traumatol. Surg. Res.*, vol. 102, no. 1, pp. S1–S8, Feb. 2016.

[109] E. K. Wai, E. R. G. Santos, R. A. Morcom, and R. D. Fraser, “Magnetic Resonance Imaging 20 Years After Anterior Lumbar Interbody Fusion,” *Spine (Phila. Pa. 1976).*, vol. 31, no. 17, pp. 1952–1956, Aug. 2006.

[110] C.-S. Chen, C.-K. Cheng, C.-L. Liu, and W.-H. Lo, “Stress analysis of the disc adjacent to interbody fusion in lumbar spine,” *Med. Eng. Phys.*, vol. 23, no. 7, pp. 485–493, Sep. 2001.

[111] Johns Hopkins Outpatient Center, “The Road To Recovery After Lumbar Spine Surgery,” Baltimore, 2016.

[112] M. Fernández-Fairen, P. Sala, H. Ramírez, and J. Gil, “A Prospective Randomized Study of Unilateral Versus Bilateral Instrumented Posterolateral Lumbar Fusion in Degenerative Spondylolisthesis,” *Spine (Phila. Pa. 1976).*, vol. 32, no. 4, pp. 395–401, Feb. 2007.

[113] J. Li, W. Wang, R. Zuo, and Y. Zhou, “Biomechanical Stability Before and After Graft Fusion with Unilateral and Bilateral Pedicle Screw Fixation: Finite Element Study,” *World Neurosurg.*, vol. 123, pp. e228–e234, Mar. 2019.

[114] W. Ding, Y. Chen, H. Liu, J. Wang, and Z. Zheng, “Comparison of unilateral versus bilateral pedicle screw fixation in lumbar interbody fusion: a meta-analysis,” *Eur. Spine J.*, vol. 23, no. 2, pp. 395–403, Feb. 2014.

[115] D. V. Ambati, E. K. Wright, R. A. Lehman, D. G. Kang, S. C. Wagner, and A. E. Dmitriev, “Bilateral pedicle screw fixation provides superior biomechanical stability in transforaminal lumbar interbody fusion: a finite element study,” *Spine J.*, vol. 15, no. 8, pp. 1812–1822, Aug. 2015.

[116] P. Schleicher *et al.*, “Biomechanical evaluation of different asymmetrical posterior stabilization methods for minimally invasive transforaminal lumbar interbody fusion,” *J. Neurosurg. Spine*, vol. 9, no. 4, pp. 363–371, Oct. 2008.

[117] Y. Kasai, T. Inaba, T. Kato, Y. Matsumura, K. Akeda, and A. Uchida, “Biomechanical study of the lumbar spine using a unilateral pedicle screw fixation system,” *J. Clin. Neurosci.*, vol. 17, no. 3, pp. 364–367, Mar. 2010.

[118] Y. Aoki *et al.*, “Examining risk factors for posterior migration of fusion cages following transforaminal lumbar interbody fusion: a possible limitation of unilateral pedicle screw fixation,” *J. Neurosurg. Spine*, vol. 13, no. 3, pp. 381–387, Sep. 2010.

[119] H. Xue, Y. Tu, and M. Cai, “Comparison of unilateral versus bilateral instrumented transforaminal lumbar interbody fusion in degenerative lumbar diseases,” *Spine J.*, vol. 12, no. 3, pp. 209–215, Mar. 2012.

[120] N. Damm, R. Rockenfeller, and K. Gruber, “Lumbar spinal ligament characteristics extracted

from stepwise reduction experiments allow for preciser modeling than literature data," *Biomech. Model. Mechanobiol.*, vol. 19, no. 3, pp. 893–910, Jun. 2020.

[121] T. Toumanidou and J. Noailly, "Musculoskeletal Modeling of the Lumbar Spine to Explore Functional Interactions between Back Muscle Loads and Intervertebral Disk Multiphysics," *Front. Bioeng. Biotechnol.*, vol. 3, no. AUG, pp. 1–13, Aug. 2015.

[122] F.-Y. Tsuang, J.-C. Tsai, and D.-M. Lai, "Effect of lordosis on adjacent levels after lumbar interbody fusion, before and after removal of the spinal fixator: a finite element analysis," *BMC Musculoskelet. Disord.*, vol. 20, no. 1, p. 470, Dec. 2019.

Appendix I

Table I.1: Segmental ROM per cent changes (%) measured on L3-L4 and L4-L5 levels for each movement with ligament removal and H-Mild IVD degeneration.

			Superficial ligaments	FCL	PLL	ALL
AR	Case 1	L3-L4	0.00	-1.28	-0.06	0.00
		L4-L5	0.00	10.43	0.26	0.00
	Case 2	L3-L4	0.00	2.25	-0.04	0.00
		L4-L5	0.00	10.18	0.25	0.00
F	Case 1	L3-L4	0.07	0.45	-0.03	0.00
		L4-L5	7.86	20.99	0.07	0.00
	Case 2	L3-L4	13.19	34.89	0.53	-0.57
		L4-L5	4.81	3.01	-0.19	-0.36
E	Case 1	L3-L4	0.00	0.00	0.00	-0.29
		L4-L5	0.00	0.00	0.00	9.04
	Case 2	L3-L4	0.00	0.00	4.71	1.95
		L4-L5	0.00	0.00	-0.11	8.84
LB	Case 1	L3-L4	0.00	0.05	0.00	0.08
		L4-L5	0.00	1.79	0.00	2.66
	Case 2	L3-L4	0.18	5.77	7.54	0.27
		L4-L5	0.00	0.81	-0.34	2.58

Table I.2: Segmental ROM per cent changes (%) measured on L3-L4 and L4-L5 levels for each movement with ligament removal and Mild-Mild IVD degeneration.

			Superficial ligaments	FCL	PLL	ALL
AR	Case 1	L3-L4	0.00	1.70	0.04	0.00
		L4-L5	0.00	9.72	0.24	0.00
	Case 2	L3-L4	0.09	17.68	0.05	0.00
		L4-L5	-0.01	8.12	0.22	0.00
F	Case 1	L3-L4	0.01	-0.04	0.00	0.00
		L4-L5	6.52	19.82	0.08	0.00
	Case 2	L3-L4	17.30	31.20	0.48	0.00
		L4-L5	0.24	-10.96	-0.39	0.00
E	Case 1	L3-L4	0.00	0.00	0.00	-0.63
		L4-L5	0.00	0.00	0.00	9.15
	Case 2	L3-L4	0.00	0.00	0.00	3.17
		L4-L5	0.00	0.00	0.00	8.97
LB	Case 1	L3-L4	0.00	-0.01	0.00	-0.12
		L4-L5	0.01	1.79	0.00	2.40
	Case 2	L3-L4	0.26	1.44	0.00	4.15
		L4-L5	-0.04	1.45	0.00	1.96

Table I.3: Segmental ROM per cent changes (%) measured on L3-L4 and L4-L5 levels for each movement with ligament removal and Mild-Mod IVD degeneration.

			Superficial ligaments	FCL	PLL	ALL
AR	Case 1	L3-L4	0.00	1.67	0.05	-0.01
		L4-L5	0.00	8.67	0.17	0.00
	Case 2	L3-L4	0.09	17.67	0.05	0.00
		L4-L5	0.00	7.51	0.17	0.00
F	Case 1	L3-L4	0.03	0.05	0.00	0.00
		L4-L5	6.62	16.84	0.09	0.00
	Case 2	L3-L4	17.31	44.44	0.53	0.00
		L4-L5	0.38	-11.80	-0.37	0.00
E	Case 1	L3-L4	0.00	0.00	0.00	-0.63
		L4-L5	0.00	0.00	0.00	8.13
	Case 2	L3-L4	0.00	0.00	0.00	3.14
		L4-L5	0.00	0.00	0.00	8.01
LB	Case 1	L3-L4	0.00	-0.01	0.00	-0.32
		L4-L5	0.00	0.56	0.00	4.01
	Case 2	L3-L4	0.27	1.38	0.00	4.07
		L4-L5	-0.05	0.25	0.00	3.65